

2022

## Optimisation of process parameters in abrasive waterjet contour cutting of AISI 304L

Jennifer M. Llanto  
*Edith Cowan University*

Follow this and additional works at: <https://ro.ecu.edu.au/theses>



Part of the [Engineering Commons](#)

---

### Recommended Citation

Llanto, J. M. (2022). *Optimisation of process parameters in abrasive waterjet contour cutting of AISI 304L*. Edith Cowan University. Retrieved from <https://ro.ecu.edu.au/theses/2502>

This Thesis is posted at Research Online.  
<https://ro.ecu.edu.au/theses/2502>

# Edith Cowan University

## Copyright Warning

You may print or download ONE copy of this document for the purpose of your own research or study.

The University does not authorize you to copy, communicate or otherwise make available electronically to any other person any copyright material contained on this site.

You are reminded of the following:

- Copyright owners are entitled to take legal action against persons who infringe their copyright.
- A reproduction of material that is protected by copyright may be a copyright infringement. Where the reproduction of such material is done without attribution of authorship, with false attribution of authorship or the authorship is treated in a derogatory manner, this may be a breach of the author's moral rights contained in Part IX of the Copyright Act 1968 (Cth).
- Courts have the power to impose a wide range of civil and criminal sanctions for infringement of copyright, infringement of moral rights and other offences under the Copyright Act 1968 (Cth). Higher penalties may apply, and higher damages may be awarded, for offences and infringements involving the conversion of material into digital or electronic form.



---

# Optimisation of process parameters in abrasive waterjet contour cutting of AISI 304L

---

**Master of Engineering  
Science**

**By:**

**Jennifer Milaor Llanto**

**Supervisors:**

**Dr. Majid Tolouei Rad**

**Dr. Ana Vafadarshamasbi**

**JANUARY 25, 2022**

**EDITH COWAN UNIVERSITY**

**270 Joondalup Dr, Joondalup WA 6027**

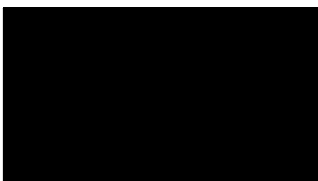
# AUTHOR DECLARATION

I solemnly declare that the entire composition of this thesis is an end result of my own work. Moreover, I sincerely declare that this thesis does not, to the best of my knowledge and belief:

- (i) Incorporate without acknowledgment any material previously submitted for a degree or diploma in any institution of higher education.
- (ii) Contain any material previously published or written by another person except where due reference is made in the text; or
- (iii) Contain any defamatory material.
- (iv) I also grant permission for the Library at Edith Cowan University to make duplicate copies of my thesis as required

Name: Jennifer Milaor Llanto

Signed ...



.....

Date ..... 25<sup>th</sup> of January 2022

.....



## ACKNOWLEDGEMENTS

I am expressing my deepest gratitude to my principal supervisor, **Dr. Majid Tolouei-Rad** for the guidance, advice and support throughout the course of this study. I am conveying my sincere appreciation to my associate supervisor, **Dr. Ana Vafadar** for her exemplary contributions and relevant recommendations towards my research work. The completion of this work would not have been possible without their support and substantial contributions. Their passion for research and trust conferred upon me, have motivated me throughout my research journey. I have significantly improved my research and academic knowledge because of their help and guidance. I wish to express my thanks to my fellow research student, **Muhammad Aamir** for technical support, advices and suggestions. Also, I am extending my genuine recognitions to laboratory technicians, **Adrian Davis** and **Zhuo Guanliang** for their support to my ECU workshop activities and to **Michael Stein** for his assistance in my writing structure and proficiency.

Special thanks to Edith Cowan University and the school of engineering, ECU for providing advanced facilities and requirements to fulfill this work.

Substantially, I am expressing my heartfelt gratefulness to my husband **Nicasio Dexter Llanto Jr.** and Milaor family, for inspiring and providing unconditional support to me enable to fulfill my dream.

Above all, glorify to our Almighty GOD for the gift of health, wisdom and blessed life to fulfill this MSc with his graces.

# Table of Contents

AUTHOR DECLARATION .....	i
ACKNOWLEDGEMENTS .....	ii
List of figures .....	vi
List of tables .....	viii
List of abbreviations and nomenclature .....	x
Abstract .....	xi
Chapter 1 Introduction.....	1
1.1 Background .....	1
1.2 Significance of the research work .....	2
1.3 Research work objectives .....	2
1.4 Thesis outline.....	3
1.5 List of publications included as part of the thesis .....	4
Chapter 2 Literature review .....	5
2.1 Introduction .....	5
2.1.1 Abrasive waterjet machining system .....	6
2.1.2 Abrasive waterjet erosion mechanism.....	7
2.1.3 AWJM process and advantages .....	7
2.1.4 Abrasive waterjet machining application.....	9
2.2 Abrasive waterjet cutting application limitations and challenges .....	11
2.3 Abrasive waterjet cutting process parameters and influences .....	13
2.3.1 Abrasive waterjet cutting input process parameters functions and influences .....	14
2.3.2 Abrasive waterjet cutting output process parameters .....	21
2.4 Abrasive waterjet cutting process improvements and optimisation.....	22
2.4.1 AWJ cutting process parameters improvements .....	22
2.4.2 AWJM cutting process parameters optimisation.....	25
2.5 Conclusions and potential future scope of study .....	28
2.5.1 Conclusions .....	28
2.5.2 Potential future scope of study .....	29

Chapter 3 Impacts of traverse speed and material thickness on AWJ contour cutting of AISI 304L.....	30
3.1 Introduction .....	30
3.2 Materials and methods.....	33
3.3 Results and discussions.....	37
3.3.1 Kerf top width and bottom results.....	37
3.3.2 Analysis of kerf taper angle .....	42
3.3.3 Material removal rate results and analysis .....	42
3.3.4 Statistical analysis .....	46
3.4 Conclusions .....	47
Chapter 4 Analysis and optimisation of process parameters AWJ contour cutting of AISI 304L .....	48
4.1 Introduction .....	48
4.2. Materials and methods.....	53
4.2.1 Workpiece and contour cutting profiles.....	53
4.2.2 AWJ machining setup and parameters .....	55
4.2.3 Design of experiment.....	57
4.3 Results and discussions.....	59
4.3.1 Effects of input parameters on surface roughness and material removal rate.....	59
4.4 Optimisation with taguchi S/N ratio .....	67
4. Confirmation test.....	72
5. Conclusions .....	72
Chapter 5 Multi-objective optimisation on abrasive waterjet contour cutting of AISI 304L	74
5.1 Introduction .....	74
5.2. Methodology.....	76
5.2.1 Material and experiment design.....	78
5.2.2 Modelling and multi-objective optimisation.....	81
5.3 Results and discussion .....	83
5.3.1 Regression models and analysis for surface roughness.....	83

5.3.2 Regression models and analysis for material removal rate .....	88
5.3.3 Regression models and analysis for kerf taper angle .....	92
5.4 Response surface methodology multi-objective optimisation .....	96
5.5 Conclusions .....	101
Chapter 6 Conclusion and potential future work .....	102
6.1 Conclusions .....	102
6.2 Potential future work .....	103
APPENDIX A Data for impacts of traverse speed and material thickness in AWJ contour cutting tests .....	105
APPENDIX B Data for single-objective optimisation of AWJ contour cutting process parameters .....	107
APPENDIX C Data for multi-objective optimisation of AWJ contour cutting process parameters .....	110
BIBLIOGRAPHY .....	112

## List of figures

Figure 2.1. AWJM mechanism and components [12].	6
Figure 2.2. Statistics of (a) various workpieces employed in AWJM applications and (b) material type from 2017 to 2020 publications reviewed in this work.	9
Figure 2.3. Machinability of frequently employed materials in AWJ cutting applications [73].	10
Figure 2.4. Cause and effect diagram of AWJM process parameters [16,84,85].	14
Figure 2.5. Nozzle system [96].	18
Figure 2.6. Survey of identified most influential AWJ cutting input process parameters reviewed publications from 2017 to 2020 [30-71].	21
Figure 3.1. Statistics of impacts of traverse speed in (a) material removal rate and (b) kerf taper angle AWJ straight line cutting of various metals [50,82,83,85,98,123,124].	32
Figure 3.2. Experimental set-up (a) schematic diagram of the nozzle system and (b) AWJ cutting head and material positioning.	35
Figure 3.3. Scheme of AWJM kerf geometries.	37
Figure 3.4. Sample images of kerf width of arcs and straight profiles.	40
Figure 3.5. Percentage of variation between top and bottom kerf widths for AISI 304L with material thickness of (a) 4 mm, (b) 8 mm, and (c) 12 mm.	41
Figure 3.6. Impacts of material thickness and traverse speed on kerf taper angle in AWJ profile cutting of AISI304L.	44
Figure 3.7. Impacts of material thickness and traverse speed towards material removal rate in AWJ profile cutting of AISI304L.	45
Figure 3.8. ANOVA results of KTA and MRR for AWJ contour cutting of AISI 304L with varied thickness.	46
Figure 4.1. Schematic representation of AWJM cutting.	49
Figure 4.2. AWJM contour cutting path for (a) taguchi $L_{27}$ tests [32]. (b) confirmation test.	55
Figure 4.3. AWJM contour cutting experiment and analysis setup.	57
Figure 4.4. Topography of AISI 304L cut surface with 4 mm thickness using varied traverse speed.	59
Figure 4.5. Topography of AISI 304L cut surface with 8 mm thickness using varied traverse speed.	59
Figure 4.6. Topography of AISI 304L cut surface with 12 mm thickness using varied traverse speed.	60
Figure 4.7. Topography of AISI 304L cut surface with 4 mm thickness using varied waterjet pressure.	60

Figure 4.8. Topography of AISI 304L cut surface with 8 mm thickness using varied waterjet pressure.....	60
Figure 4.9. Topography of AISI 304L cut surface with 12 mm thickness using varied waterjet pressure.....	61
Figure 4.10. Topography of AISI 304L cut surface with 4 mm thickness using varied abrasive mass flow rate.....	61
Figure 4.11. Topography of AISI 304L cut surface with 8 mm thickness using varied abrasive mass flow rate.....	61
Figure 4.12. Topography of AISI 304L cut surface with 12 mm thickness using varied abrasive mass flow rate.....	62
Figure 4.13. Main effect plot of means of surface roughness against input parameters.....	70
Figure 4.14. Main effect plot of means for material removal rate against input parameters...	72
Figure 5.1. Multi-objective optimisation process flow chart. ....	77
Figure 5.2. AWJM setup and process parameters.....	79
Figure 5.3. AWJ contour cutting profiles. ....	80
Figure 5.4. Residual plots for surface roughness.....	87
Figure 5.5. Percentage contribution of variables for surface roughness. ....	87
Figure 5.6. Residual plots for material removal rate. ....	91
Figure 5.7. Percentage contribution of variables for material removal rate.....	91
Figure 5.8. Residual plots for kerf taper angle. ....	95
Figure 5.9. Percentage contribution of variables for kerf taper angle.....	95
Figure 5.10. Response optimisation plot. ....	100

## List of tables

Table 2.1. Comparison of non-conventional cutting technologies [3,15-17,22-26].	8
Table 2.2. AWJM materials and areas of application [54,74-76].	11
Table 2.3. AWJ cutting defects amongst various metallic materials [21,67,80-82].	13
Table 2.4. Quality defects in AWJ cutting of metallic with different thickness [6,23,66,81].	13
Table 2.5. Abrasive material categories along with their properties and industrial applications [9,72,91,92].	16
Table 2.6. Abrasive mesh size and grade [9,72,92,96].	17
Table 2.7. Output process parameters analytic equations.	22
Table 2.8. Impacts of the most influencing process parameters in AWJ cutting output parameters.	24
Table 2.9. Several studies (2018 to 2020) in AWJ cutting carried out through the taguchi method.	25
Table 2.10. A list of several studies (2017 to 2020) with a diverse optimisation technique in AWJ cutting process.	26
Table 3.1. Chemical and mechanical properties of AISI 304L in wt%.	34
Table 3.2. Abrasive waterjet machine MAXIEM 1515 (OMAX Corp., Kent, WA, USA) specifications.	34
Table 3.3. AWJ cutting profiles and path.	35
Table 3.4. Variable input parameters values.	36
Table 3.5. Constant input parameters values.	36
Table 4.1. Chemical composition in wt% of AISI 304L [145].	54
Table 4.2. Mechanical properties of AISI 304L [145,158].	54
Table 4.3. Machine specifications and cutting input parameters.	56
Table 4.4. $L_{27}$ Orthogonal array of taguchi.	58
Table 4.5. $L_{27}$ Orthogonal array of taguchi for surface roughness results.	63
Table 4.6. $L_{27}$ Orthogonal array of taguchi for material removal rate results.	65
Table 4.7. Analysis of variance of surface roughness.	66
Table 4.8. Analysis of variance of material removal rate.	67
Table 4.9. Optimum parameters for surface roughness.	67
Table 4.10. Optimum parameters for material removal rate.	70
Table 5.1. Chemical and mechanical composition of AISI 304L [158].	78
Table 5.2. Levels of input process parameters.	80
Table 5.3. Output parameters for varied profiles.	80
Table 5.4. Taguchi $L_9$ orthogonal array.	81
Table 5.5. Summary of multi-linear regression coefficients for $R_a$ .	84

Table 5.6. Predicted $R_a$ values of regression models for $t = 4$ mm. ....	84
Table 5.7. Predicted $R_a$ values of regression models for $t = 8$ mm. ....	85
Table 5.8. Predicted $R_a$ values of regression models for $t = 12$ mm. ....	85
Table 5.9. Summary of linear regression coefficients for MRR. ....	88
Table 5.10. Predicted MRR values of regression model for $t = 4$ mm. ....	89
Table 5.11. Predicted MRR values of regression model for $t = 8$ mm. ....	89
Table 5.12. Predicted MRR values of regression model for $t = 12$ mm. ....	89
Table 5.13. Summary of linear regression coefficients for KTA. ....	92
Table 5.14. Predicted KTA values of regression model for $t = 4$ mm. ....	93
Table 5.15. Predicted KTA values of regression model for $t = 8$ mm. ....	93
Table 5.16. Predicted KTA values of regression model for $t = 12$ mm. ....	93
Table 5.17. Solutions for RSM multi-objective optimisation. ....	98



## List of abbreviations and nomenclature

AA	Aluminum alloy
AFR	Abrasive mass flow rate
AISI	Austenitic stainless steel
AL	Aluminum
AM	Abrasive material type
ANOVA	Analysis of variance
AS	Abrasive size
AWJ	Abrasive waterjet
AWJM	Abrasive waterjet machining
DOC	Depth of cut
ECDM	Electro chemical discharge machine
EDM	Electro discharge machine
HAZ	Heat affected zone
JIA	Jet impact angle
KBW	Kerf bottom width
KTA	Kerf taper angle
MRR	Material removal rate
LBM	Laser beam machine
MMC	Metal matrix composite
ND	Nozzle diameter
OD	Orifice diameter
P	Waterjet pressure
SOD	Standoff distance
Ti6AL-4V	Titanium alloy
TS	Traverse speed
$R_a$	Surface roughness
h	Thickness of the material
l	inclined length of workpiece
ht	Depth of cut
Vf	Traverse speed
W	Kerf width
$W_t$	Kerf top width
$W_b$	Kerf bottom width
t	Material thickness
y	Profile height in a defined point

## Abstract

This research work presents an optimisation of abrasive waterjet contour cutting process parameters with the objectives of maximising material removal rate, whilst minimising taper angle and surface roughness. This thesis contains an in-depth review of the systems behind abrasive waterjet machining and recent progress trends regarding its applications. The impacts of input parameters are investigated including traverse speed, waterjet pressure and abrasive mass flow rate against selected responses in abrasive waterjet contour cutting of austenitic stainless steel 304L. Experimental data is utilised to generate regression models in predicting responses, where the results are statistically evaluated to assess the percentage contribution of each parameter in the performance of contour cutting. Techniques, such as Taguchi and Response Surface Methodology, are employed to perform a single and multi-objective optimisation. Abrasive waterjets demonstrate similar responses in cutting curvature and straight line profiles during contour cutting. The study reveals that an increasing level of waterjet pressure and abrasive mass flow rate results in lower surface roughness, lower kerf taper angle and higher rate of material removal. Similarly, a lower rate of traverse speed achieves minimum surface roughness and kerf taper angle, whereas increasing its rate attains the maximum value of material removal rate.

# Chapter 1 Introduction

## 1.1 Background

Non-traditional technologies are commonly utilised when available conventional machining processes are unable to obtain required quality and productivity targets. Amongst advanced non-conventional technologies, the abrasive waterjet machine is broadly applied for contour cutting operations.

Abrasive waterjet machining, abbreviated to AWJM throughout this study, is an advanced mechanical non-conventional technology that is widely applied in machining difficult-to-cut materials such as metals, non-metals composites and natural materials [1]. The reason behind AWJM's broad utilisation is due to its competitive advantages, such as lack of heat formed on the cutting area, capability in machining hard-to-cut materials of various thickness, better surface integrity, proficiency in cutting complicated shapes, as well as its better dimensional accuracy due to minor distortion [2]. Moreover, AWJM has become recognized as sustainable and environmentally friendly, as it does not generate any hazardous chemical and vapour, that are harmful to humans or the environment [3]. However, problems have emerged with the AWJM technique, such as quality defects and low productivity, which have emerged since its first applications. Kerf geometric inaccuracies, high occurrences of surface roughness and low removal rate are common defects and issues that have been noted with abrasive waterjet contour cutting, most specifically in ductile materials such as stainless steel [4-6]. In this work, austenitic stainless steel 304L, abbreviated to AISI 304L throughout this study, has been used to investigate abrasive waterjet machining material responses and behaviours. Austenitic stainless steel 304L is difficult-to-cut due to its high machinability level and high alloying content [7]. The machining of this material creates challenges such as geometric inaccuracies and the requirement of cooling applications (steel reference). Abrasive waterjet machining is considered an effective method for cutting stainless steel due to its absence of the heated affected zone (HAZ).

Abrasive waterjet operations are integrated with several process parameters that directly impact on the machine's performances. Moreover, abrasive waterjet contour cutting with proper process parameter settings remains a challenging procedure for manufacturers. Therefore, it is essential to form a progressive and comprehensive study of these process parameters as a means of determining its effective usage.

Providing a solution to these critical issues has been the main purpose of this research, where proper utilisation of AWJM has resolved these aforementioned challenges. The fundamentals of cutting performance are associated with quality and productivity, where the basis of quality

of cut relates to kerf geometric accuracy and surface roughness, while material removal rate is a factor affecting productivity.

## **1.2 Significance of the research work**

This research project creates an opportunity to provide manufacturing industries a process control solution for precise cutting and improved productivity in machining. To date, AWJM progress and improvements have been implemented primarily in relation to cutting straight line profiles, with only limited knowledge regarding the machining of complex shapes, such as curves with differing radii. Hence, contour cutting consisting of straight and curvature profiles have been frequently applied in manufacturing industries. This work will support developments and strategies for efficient utilisation of abrasive waterjet contour cutting.

## **1.3 Research work objectives**

Low productivity and cutting defects such as kerf geometry inaccuracy, roughness in the cut surface and poor material removal are some of the challenges that stainless steel fabrication industries have recently faced. These issues directly affect product quality, productivity, and production costs [8]. Accordingly, in order to ensure achievement of quality and productivity targets, it is essential to select suitable values for influencing process parameters in abrasive waterjet contour cutting. Therefore, following are the specific objectives of this research work:

1. To provide an in-depth comprehension of abrasive waterjet fundamental mechanisms and a substantial understanding of its process parameters for machining of metallic and difficult-to-cut materials, particularly AISI 304L.
2. To perform experimental analysis of abrasive waterjet contour cutting applied on AISI 304L. This research will investigate the effects of input process parameters, such as traverse speed and material thickness, in cutting responses such as kerf taper angle and material removal rate.
3. To conduct a single-objective optimisation in determining the optimal settings and input parameters i.e., traverse speed, waterjet pressure and abrasive mass flow rate, resulting in either minimum surface roughness or maximum material removal rate.
4. To generate a regression model and perform a multi-objective optimisation that considers the following objectives: to minimise surface roughness and kerf taper angle and maximise material removal rate.

## 1.4 Thesis outline

In order to achieve these set objectives, this research proposal has been organised into six chapters, as detailed below.

Chapter 1 presents the significance, objectives and scope of this research work, highlighted with a brief background of abrasive waterjet machining applications.

Chapter 2 outlines the working mechanisms, advantages, limitations, challenges and applications of AWJM. First and foremost, in fulfilling the overall objectives of this work, an in-depth knowledge of the systems behind abrasive waterjet machining is required. Process parameters and their effects on the performance of abrasive waterjet machining are extensively discussed. Previous optimisation works, experiments and modeling with AWJM are also reviewed in this chapter. This review is a significant reference in analysing the influences of the process parameters for attaining improvements in abrasive waterjet contour cutting performance. This chapter has been published as a review paper in the *“Applied Science, in a special issue: Advanced Manufacturing of Metals”*, an official journal of MDPI.

Chapter 3 details the experimental study performed after gaining proficient knowledge in abrasive waterjet operations. This chapter details the impacts of traverse speed and material thickness towards achieving lower kerf taper angle and higher material removal rate in abrasive waterjet contouring of AISI 304L. It has been published as a research article in the *“Applied Science, in a special issue: Advanced Manufacturing of Metals”*, an official journal of MDPI. Aside from traverse speed and material thickness, other machining input parameters such as waterjet pressure and abrasive mass flow rate, provide significant contributions towards abrasive waterjet machining performance.

Chapter 4 illustrates further experimental analysis using the Taguchi method. Moreover, a single-objective optimisation was performed with the objectives of either minimising surface roughness or maximising material removal rate. Accordingly, Taguchi’s S/N ratio method was applied in determining the optimum value of traverse speed, waterjet pressure and abrasive mass flow rate in abrasive waterjet contour cutting of AISI 304L, with the aim of achieving high surface integrity and efficiency, in terms of surface roughness and material removal rate. This chapter has been published as a research article in the *“Metals, in a special issue: Optimisation and analysis of metal cutting processes”*, an official journal of MDPI.

Chapter 5 demonstrates the multi-objective optimisation in AWJM of AISI 304L. The experimental data obtained was subsequently used to generate regression models. These were utilised for prediction of response values and multi-objective optimisation. In this chapter, response surface methodology was employed to determine the optimum values of the process parameters towards multi-objectives of minimising surface roughness, kerf taper angle and maximising material removal rate. This chapter still under review for international journal publication.

Finally, Chapter 6 summarises the key findings and conclusions and states the achievements and contributions completed in this research work. This section also covers potential future work regarding abrasive waterjet contour cutting of AISI 304L.

### 1.5 List of publications included as part of the thesis

The following list of published and submitted articles are embedded as part or chapters of this thesis:

1. **Llanto, J. M.**, Tolouei-Rad, M., Vafadar, A., & Aamir, M. (2021). Recent Progress Trend on Abrasive Waterjet Cutting of Metallic Materials: A Review. *Applied Sciences*, *11*(8), 3344. Link: <https://www.mdpi.com/2076-3417/11/8/3344>
2. **Llanto, J. M.**, Tolouei-Rad, M., Vafadar, A., & Aamir, M. (2021). Impacts of Traverse Speed and Material Thickness on Abrasive Waterjet Contour Cutting of Austenitic Stainless Steel AISI 304L. *Applied Sciences*, *11*(11), 4925. Link: <https://www.mdpi.com/2076-3417/11/11/4925>
3. **Llanto, J. M.**, Vafadar, A., Aamir, M., & Tolouei-Rad, M. (2021). Analysis and Optimisation of Process Parameters in Abrasive Waterjet Contour Cutting of AISI 304L. *Metals*, *11*(9), 1362. Link: <https://www.mdpi.com/2075-4701/11/9/1362>
4. **Llanto, J. M.**, Vafadar, A., & Tolouei-Rad, M. Multi-objective optimisation in abrasive waterjet contour cutting of AISI 304L. This is under review for publication in an international journal.

## Chapter 2 Literature review

This chapter has been published as a review paper in the *“Applied Science, in a special issue: Advanced Manufacturing of Metals”*, an official journal of MDPI, as listed in section 1.5. In order to maintain uniformity in the presentation of the thesis, the format was changed but the contents are the same. This chapter provides a comprehensive review of recent developments, mechanisms, process parameter functions and improvements in abrasive waterjet machine applications, particularly with cutting operations in fabrication industries. It presents the overall stance of the recent trends and progress in abrasive waterjet machining which is significant to the thesis. This chapter facilitates in identifying the research gaps and opportunities for development as considered by this research work. This aids as an appropriate reference to the thesis relating with the abrasive waterjet cutting process parameters.

Sections 2.1 to 2.5.2 of Thesis have been published  
as the following article.



Review

# Recent Progress Trend on Abrasive Waterjet Cutting of Metallic Materials: A Review

Jennifer Milaor Llanto \* , Majid Tolouei-Rad, Ana Vafadar  and Muhammad Aamir 

School of Engineering, Edith Cowan University, Joondalup, WA 6027, Australia; m.rad@ecu.edu.au (M.T.-R.); a.vafadarshamasbi@ecu.edu.au (A.V.); m.aamir@ecu.edu.au (M.A.)

\* Correspondence: j.llanto@ecu.edu.au

**Abstract:** Abrasive water jet machining has been extensively used for cutting various materials. In particular, it has been applied for difficult-to-cut materials, mostly metals, which are used in various manufacturing processes in the fabrication industry. Due to its vast applications, in-depth comprehension of the systems behind its cutting process is required to determine its effective usage. This paper presents a review of the progress in the recent trends regarding abrasive waterjet cutting application to extend the understanding of the significance of cutting process parameters. This review aims to append a substantial understanding of the recent improvement of abrasive waterjet machine process applications, and its future research and development regarding precise cutting operations in metal fabrication sectors. To date, abrasive waterjet fundamental mechanisms, process parameter improvements and optimization reports have all been highlighted. This review can be a relevant reference for future researchers in investigating the precise machining of metallic materials or characteristic developments in the identification of the significant process parameters for achieving better results in abrasive waterjet cutting operations.

**Keywords:** abrasive waterjet; machining; metal cutting; process parameters; optimization



**Citation:** Llanto, J.M.; Tolouei-Rad, M.; Vafadar, A.; Aamir, M. Recent Progress Trend on Abrasive Waterjet Cutting of Metallic Materials: A Review. *Appl. Sci.* **2021**, *11*, 3344. <https://doi.org/10.3390/app11083344>

Academic Editor: Andrea Spagnoli

Received: 19 March 2021  
Accepted: 5 April 2021  
Published: 8 April 2021

**Publisher's Note:** MDPI stays neutral with regard to jurisdictional claims in published maps and institutional affiliations.



**Copyright:** © 2021 by the authors. Licensee MDPI, Basel, Switzerland. This article is an open access article distributed under the terms and conditions of the Creative Commons Attribution (CC BY) license (<https://creativecommons.org/licenses/by/4.0/>).

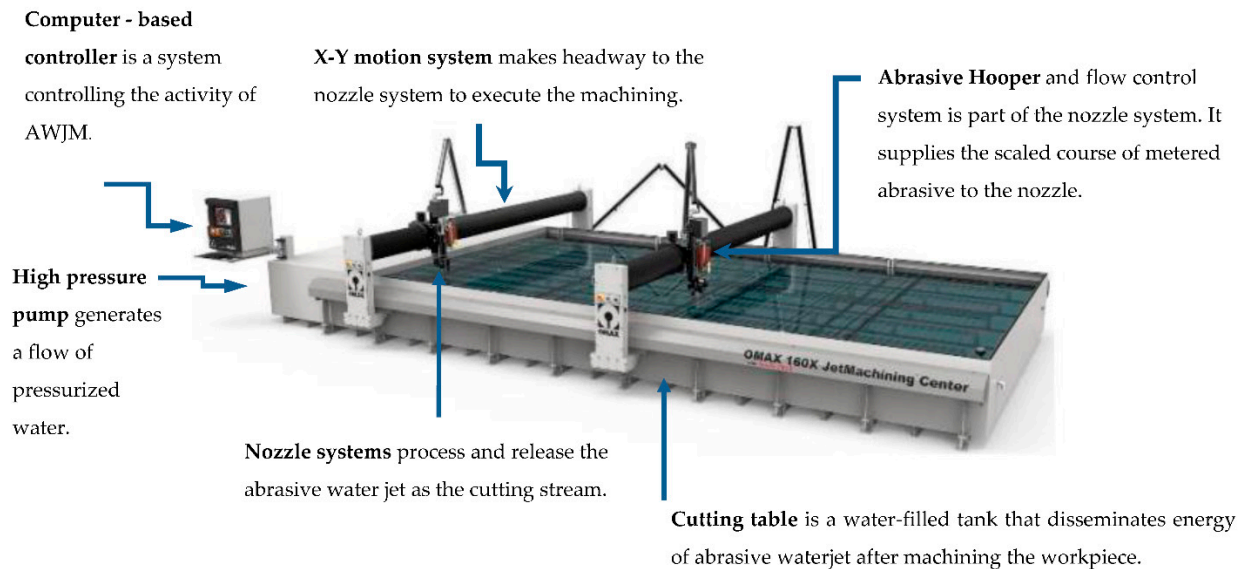
## 1. Introduction

Cutting is the process of applying a force to penetrate or separate a workpiece [1]. With current advances in technologies, there has been a rapidly increasing demand for quality cut parts with complex geometries in the fabrication industry. Abrasive waterjet machining (AWJM) is an advanced technology that can be used for cutting processes. AWJM was developed from plain waterjet machines, wherein in 1980 abrasives were first added to plain waterjets to cut industrial material [2]. AWJM allows for versatility in machining an extensive range of materials, from the easiest to the most strenuous to cut. AWJM is recognized as an implicit solution for machining metallic and heat-sensitive materials without leaving a heat-affected zone (HAZ) or any residual stresses during the machining process [3]. Among the various advanced machining technologies, AWJM has exhibited significant emergence in manufacturing industries due to its extensive operations and exceptional quality of cut of intricate profiles with a minimum cutting force on the workpiece and yield of better dimensional accuracy due to insignificant distortion [4]. However, AWJM with proper process parameter settings remains a challenging procedure for manufacturers. Therefore, an enhanced understanding of AWJM mechanisms and modelling is needed to ensure more effective applications.

This review aims to address gaps in existing studies by foregrounding the leading features of the abrasive waterjet (AWJ) cutting of metallic materials and providing significant, up-to-date research from the theoretical and experimental analysis. This paper is structured to present AWJM mechanism advantages and applications, and identifies limitations and current challenges faced by AWJ cutting, as well its process parameter functions and influences. Accordingly, recent process parameter improvements and optimizations are reviewed.

### 1.1. Abrasive Waterjet Machining System

In the AWJM system, materials are removed using erosion processes. Erosion is a type of wear with the manifestation of accelerating and the continuous collision of abrasive particles in a high velocity in liquid form [4]. An example of a typical AWJM is shown in Figure 1 [5]. The underlying operating structure of AWJM includes a high-pressure pump system, a cutting head, a table and a computer-based controller [6].



**Figure 1.** AWJM mechanism and components [5].

The computer-based controller is incorporated into the AWJM system, functioning independently, which enables to download varied types of diagram programs. This comprises tools that are distinct to AWJM, such as manual or automatic cut in/out tools, tools for the generation of cutting paths, collision prediction and resolution, tool assignment for surface quality, etc. [7]. Mixing the granular abrasive with a high-pressure waterjet stream makes the AWJM capable of machining. A high-pressure pump drives the pressurized water in the nozzle system. This system includes an abrasive hopper, orifice, mixing chamber and focusing tube. The water travels with a high level of velocity and is forced out of the orifice in a very thin stream structure [8]. A hopper that includes a plastic tube holds abrasive particles and dispenses them to the cutting head, where particles are then drawn into a waterjet stream in the mixing chamber. The high-speed waterjet, set alongside abrasive particles, is compounded and accelerated to create an abrasive waterjet. The focusing tube directs the abrasive waterjet to its focal point when cutting a working piece [9].

### 1.2. Abrasive Waterjet Erosion Mechanism

The AWJM process of removing material from a target workpiece emerges through an erosive venture of abrasive particles travelling with high velocity [10]. Material removal rates in AWJM transpire across two primary models, such as cutting and deformation/ploughing deformation wear mechanism [4]. Erosion mechanisms vary depending on workpiece material and properties [11]. A workpiece can be categorized as ductile, brittle or composite. In ductile materials, erosion can occur using two procedures, i.e., repeated plastic deformation and cutting action. In general, ductile erosion is applicable to metals and other similar materials that are capable of a significant plastic deformation process [12]. For the brittle materials erosion process, removal of material occurs through crack propagation and chipping, resulting in contact stresses caused during the impact of abrasive particles, which is then defined as the cracking method [13]. In the case of

composite materials, abrasives penetrate the material and produce breakages that initiate the formation of cracks, which in turn results in delamination [14].

### 1.3. AWJM Process and Advantages

The cutting process is a core method in the manufacturing industry. AWJM is highly capable of machining from hard to soft materials at a very low machining force, which avoids the destruction of the target workpiece's properties [3]. Abrasive waterjet machining is a non-conventional cold processing technology used for material processing with significant advantages [1,15], which has been the reasoning behind the rapidly progressing application of AWJM, particularly in metallic materials [6]. The reduction of temperature is carried through the presence of cooling water due to the presence of cooling water, which renders AWJM [6].

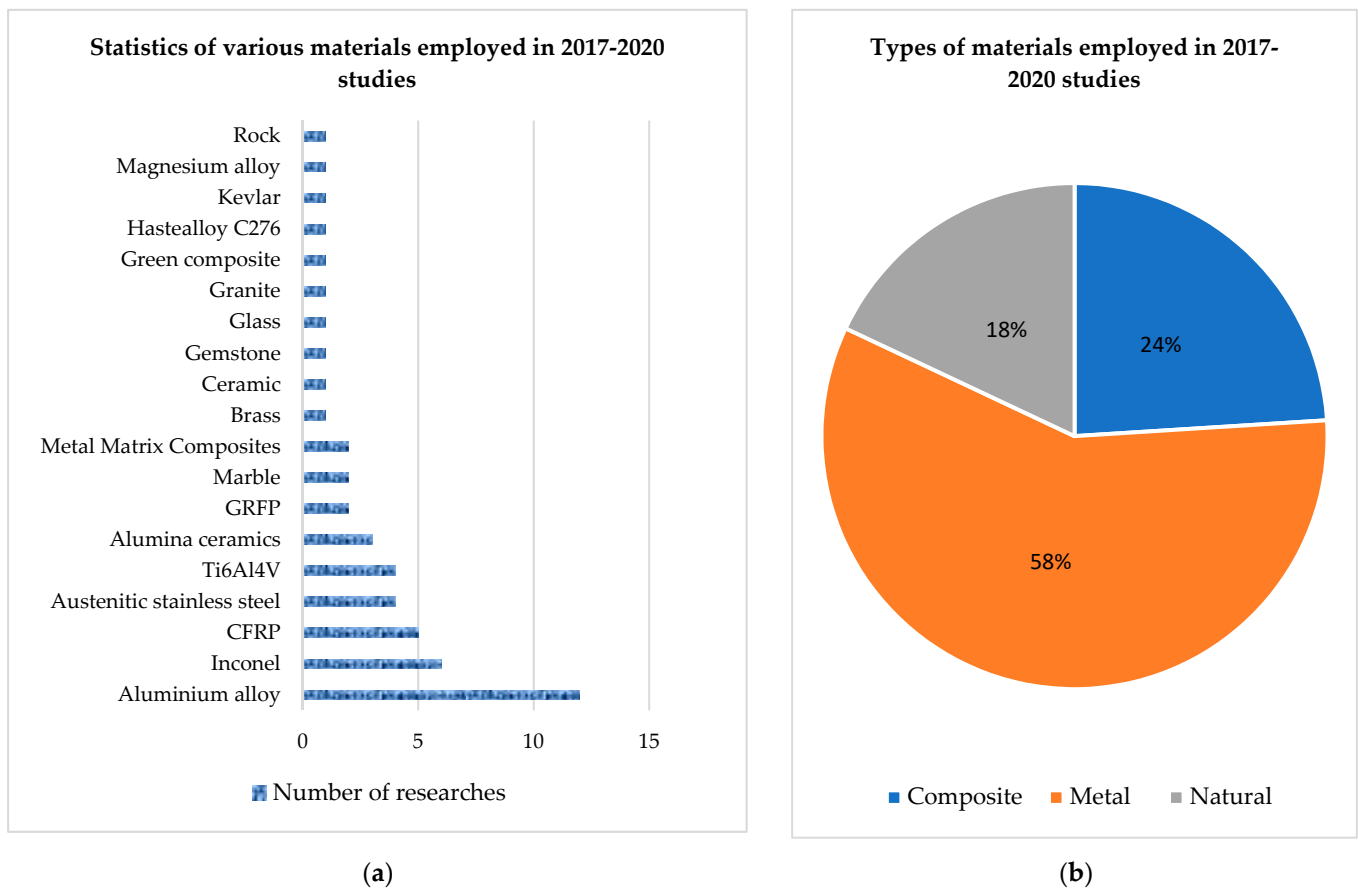
Table 1 illustrates AWJM's superiority compared to other non-conventional machines based on experimental studies on various workpieces [8–10,16–21]. It substantiates AWJM compared to other technologies, indicating versatility in cutting diverse material with a wide range of thickness, absence of tool wear and flexibility in cutting intricate geometries. Other machines such as EDM and ECDM involve the use of high-intensity energy to cut hard metals and materials that are difficult to machine [8–10]. However, the usage of high thermal heating sources causes craters, cracks, thermal damages, and destructively tensile residual stresses; hence, materials that are low conductors of heat are very applicable [10]. In AWJM applications, the absence of thermal distortion is achieved due to its cold cutting process since the material temperature will not exceed 70 °C [22]. EDM and ECDM generate hazardous solid, liquid, and gaseous products resulting in sludge containing metal ions, acids, nitrate, oils and even traces of heavy metal ions due to anodic electrochemical dissolution, which are very harmful to humans and the environment [17]. AWJM is also considered environmentally friendly and sustainable as it does not omit any hazardous vapor; hence, AWJM generates waste such as abrasives that adversely affect the environment. Sustainable manufacturing aims to achieve an efficient operation at the same time, reducing the environmental effect [17]. Recycling and reusing these abrasives make AWJM more economical, effective, and environmentally friendly [22–24]. The discussed competitive advantages of AWJM have been the rational reason behind its expanding utilization and continuous progression.

**Table 1.** Comparison of non-conventional cutting technologies [8–10,16–21].

Cutting Activity	AWJM	LBM	EDM	ECDM
Heated affected zone (HAZ)	No	Yes	Yes	Yes
Material Distortion	No	Yes	No	Yes
Tool Wear	No	No	Yes	Yes
Material Removal Rate (mm <sup>3</sup> /s)	Medium-slow (approx. ≤ 2)	Fast (approx. 2–3) for non-reflective materials only	Medium (approx.1–2)	Medium (approx.1–2)
Type of material	metals, composites, natural, electrically, non-conductive, non-reflective	metals, composites, natural, electrically, non-conductive, non-reflective surface	Only electrically conductive such as metals and composites	Only electrically conductive such as metals and composites
Material thickness (mm)	Ranging ≤ 304.8	Ranging ≤ 20	Ranging ≤ 304.8	Ranging ≤ 304.8
Type of shapes	Complex and complicated shapes	Complex and complicated shapes	Simple	Simple
Burr formation	Minimal	High	High	Minimal
Hazardous vapour	None	fumes, gases	CO & CH <sub>4</sub>	NaOH/NaNO <sub>3</sub>

#### 1.4. Abrasive Waterjet Machining Application

In the past and recent years, AWJM has gained high interest amongst researchers, as it is a versatile tool that is used in almost all manufacturing processes and materials. Figure 2 presents the statistics of various workpieces utilized in AWJM applications, as established from several reviewed publications [25–66]. The first chart (a) shows a generated summary of various workpieces that have been employed in AWJM applications, while the second chart (b) represents created synopsis material types for enhanced analysis based on several research studies used from the year 2017 to 2020.

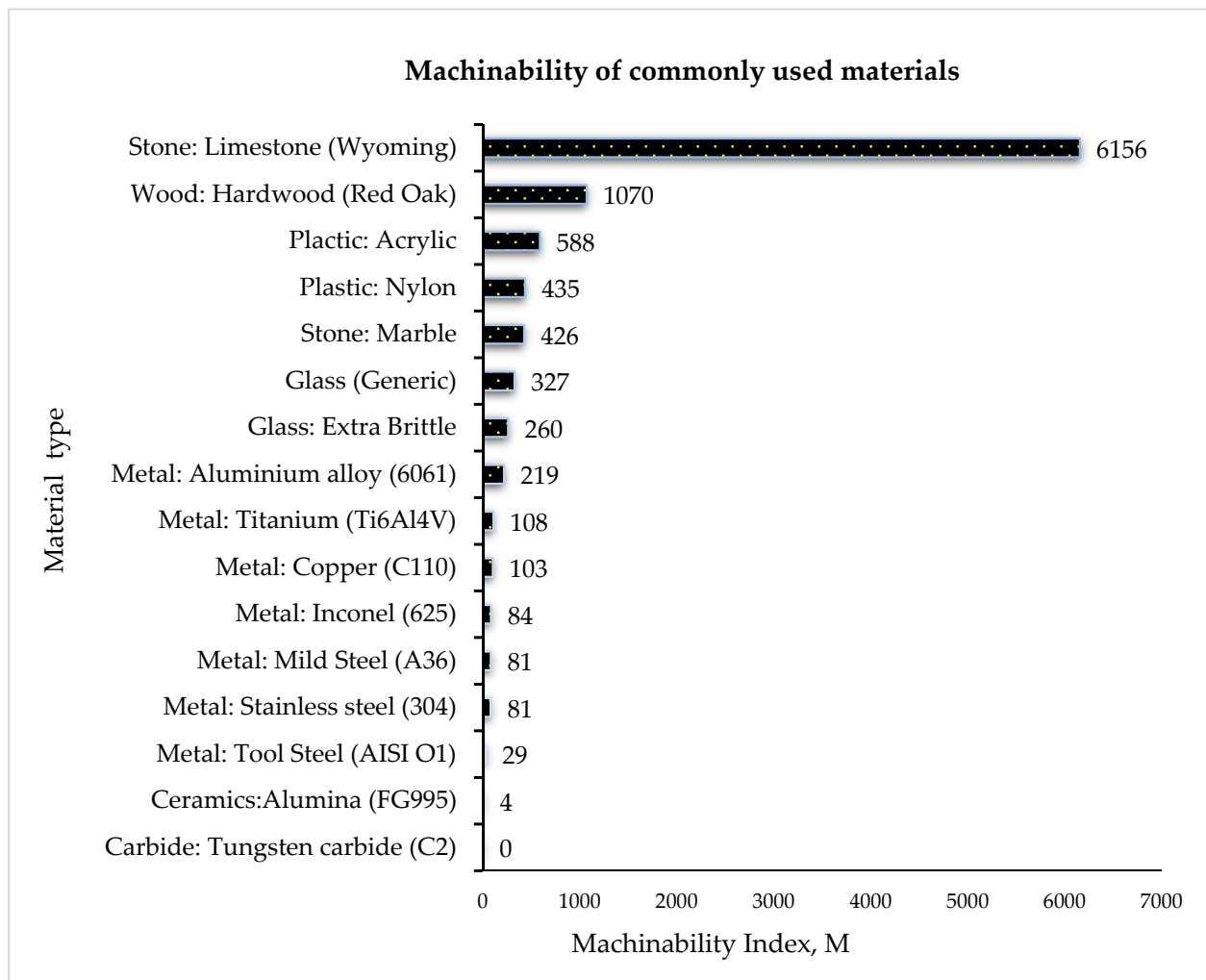


**Figure 2.** Statistics of (a) various workpieces employed in AWJM applications and (b) material type from 2017 to 2020 publications reviewed in this work.

A number of studies in metal, composite, and natural materials discovered similar quality defects such as surface roughness, striation marks and kerf geometry inaccuracies [25–66]. As shown in Figure 2a, aluminum alloy, which is a metallic material, has captured the highest value of twelve (12) research studies, whilst natural material, rock, has gained the least attention amongst these selected recent researches in AWJM application. As illustrated in Figure 2b, metal materials have received the highest attention, attaining 58% of the population of these selected latest studies in AWJM performance. These are difficult-to-cut materials that possess drawbacks related to their high alloying content (i.e., chromium and nickel), low thermal conductivity, high ductility, and low machinability level [67]. It was noted that the mentioned quality issues and defects are highly influenced by their material properties [68,69].

Varied types of materials possess divergent machinability due to their different mechanical and chemical properties, and a number of metallic materials identified as one of the most hard-to-cut materials [28]. Figure 3 illustrates the typical machinability of several

employed materials in abrasive waterjet (AWJ) cutting applications [69]. The machinability index indicates the speed of the machining process.



**Figure 3.** Machinability of frequently employed materials in AWJ cutting applications [69].

Cutting machinability can be estimated by several indices such as the forces merging while cutting, cutting speed, surface quality of cut material, etc. [69]. Moreover, a higher machinability index denotes a faster cutting speed which has been established based on extensive cutting tests [69]. Figure 3 also demonstrates that tungsten carbide denotes the lowest level of machinability, subsequently followed by ceramics and metals such as stainless steel, Inconel and titanium; in this regard, these workpieces are the most difficult-to-machine materials.

AWJM has also been recognized to be an effective technology in cutting non-conducting material with a low machinability index. Research to date has explored differing operating mechanisms of AWJM for various industrial conditions and applications. Table 2 enumerates AWJM applications in different industry sectors with regards to specific material usage [49,70–72], which shows that AWJM applications cover a vast range of industrial domains.

**Table 2.** AWJM materials and areas of application [49,70–72].

Materials		Industrial Application
Type	Workpiece	
Natural	Concrete, cement, ceramics, graphite, stone or rock.	Mining, manufacturing and processing of ceramics and graphite, building, construction, housing, and tile industry.
Metals	Titanium, aluminium, stainless steel, and alloys.	Automotive, marine, aerospace, architecture and civil, medical, food industry, automotive, electronics industry.
Composites	Wire glass, laminated glass, optic glass, composites, and magnetic materials.	Aerospace, automotive, electronics industry, Glass, decorations, promotional, optical fiber, and the medical industry.

After expounding the machining mechanism and benchmarking performance against other non-conventional technologies, in addition to enumerating the advantages and applications of AWJM, it is essential to discern the technology's current conditions, limitations and process drawbacks that affect its technological effectiveness. A very high noise (approximately 80 to 100 Db) is produced by AWJM during the machining process, and acquisition costs are driven by the high-pressure pump, high volume of required water quality, and purity [3,6,15,24]. Therefore, recent states of AWJM applications, boundaries, and challenges, particularly in cutting operations, are further discussed in the succeeding sections of this review.

## 2. Abrasive Waterjet Cutting Application Limitations and Challenges

AWJM is extensively used for cutting operations; hence, there is a necessity for enhancing its performance. AWJ cutting processes still face challenges in quality and productivity performance, mostly metallic material identified as one of the hard-to-cut material due to its low machinability. There have been reported cutting defects when using an abrasive waterjet machine. Damage may also vary depending on the material to be machined [73]. The issue of material response to AWJM in terms of its behavior, i.e., burr formation, high surface roughness, striation marks, distorted kerf geometry, and delamination, has been studied since the beginning of AWJM applications in the 1980s [74,75]. Table 3 shows common AWJ cutting issues that have been restudied by researchers, particularly metallic materials.

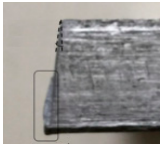
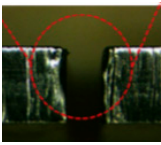
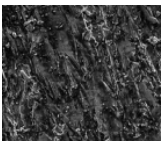
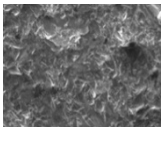
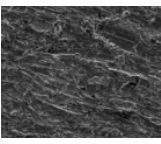
Table 3 details that previous works have encountered similar customary defects inherent in this machine's application for difficult-to-cut materials, particularly metals [15,62,76–78]. Several studies have shown that AWJ cutting has been broadly applied to metallic materials with varied thicknesses. The AWJ cutting process has also been revealed to contain similar defects, such as kerf taper, roughness and cracking of cutting metals regardless of the thickness. A summary of recent studies applying AWJ cutting of metals with varied thicknesses is itemized in Table 4.

As shown in Table 4, the kerf taper angle and surface roughness are major quality issues identified in the AWJ cutting of metallic materials with varied thickness. Accordingly, a machinability study performed by Khan et al. [79] detailed the AWJM performance in cutting low alloy steel of different thicknesses (5, 10, 15, 20 mm). Their experiments revealed that the material thickness impacts machine performance, such as the material removal rate, surface roughness, and kerf wall inclination. Hence, it is necessary to investigate the influence of material thickness for precise AWJM, as cutting operations involve various thicknesses of product formation in fabrication industries.

The aforementioned issues are challenges to AWJ cutting performance. However, these issues have been recently reinvestigated and it was concluded that AWJM performance relies on its process parameters. Therefore, it is necessary to have a continuous comprehensive study of process parameters to improve AWJ cutting performance, which is discussed in the succeeding section.



**Table 3.** AWJ cutting defects amongst various metallic materials [15,62,76–78].

Defects	Material	Images	Key Findings and References
Cutting residue, striation and roughness	AISI 304		Miao et al. [76] have found quality defects such as cutting residue, kerf taper and striation in cutting AISI 304 using abrasive waterjet machine. These defects are caused by the decreasing energy of the jet.
Kerf taper angle	AISI 1090		Mohamad et.al. [62] have identified the kerf taper angle as an intrinsic characteristic of AWJ cutting of AISI 1090 mild steel. They determined that variation in the kerf top width wider and kerf bottom geometries resulted in a higher kerf taper angle.
Surface Roughness	Ti-6Al-4V		Gnanavelbabu et al. [77] applied AWJ cutting of Ti-6Al-4V and observed roughness and striations marks in cut surfaces. They discovered that the cut surface finish differs depending in the depth from surface entry of the abrasive jet.
Material removal rate, Kerf taper angle	Inconel 600		Uthayakumar et al. [78] have known quality defects, such as kerf geometric inaccuracy and a low material removal rate in cutting super nickel alloy using abrasive waterjet machine. They established a high occurrence of inaccurate kerf geometries using a high level of water pressure and increasing the traverse speed.
Depth of Cut	SS304		Supriya et al. [15] have determined that one of the challenges faced with cutting stainless steel is achieving a high depth of cut due to its low machinability. They concluded that using abrasive waterjet machine with a high level of pressure settings have increased the depth of cut.

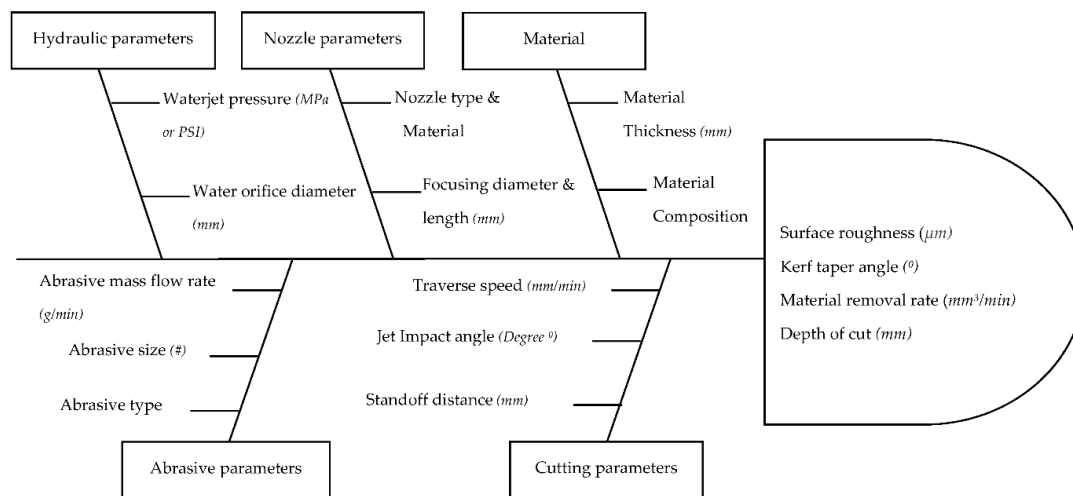
**Table 4.** Quality defects in AWJ cutting of metallic with different thickness [18,61,77,80].

Year & Author	Metallic Material	Thickness	Defects
Gnanavelbabu et al. 2018 [77]	Ti6Al4V	5 mm	KTA, MRR, Ra
Wang et al. 2019 [61]	AA 6061-T6	5, 10, 25, 50 mm	KTA
Yuvaraj et al. 2017 [80]	AISI D2 Steel	60 mm	Ra
Akkurt et al. 2018 [18]	SS 304	20 mm	Ra

### 3. Abrasive Waterjet Cutting Process Parameters and Influences

The abrasive waterjet (AWJ) cutting process incorporates several independent process parameters that directly affect the machine's performances. As illustrated in the cause-and-effect diagram of the AWJM process parameters given in Figure 4, the input process parameters are categorized as follows (1) hydraulic, (2) nozzle, (3) material, (4) abrasive, and (5) cutting. The input process parameters primarily affect the machining performance or output parameters of AWJM application. Learning the specific functions of these influential

variables will be fundamental towards development and improvement initiatives of quality and efficiency of the entire cutting process.



**Figure 4.** Cause-and-effect diagram of AWJM process parameters [9,81].

### 3.1. Abrasive Waterjet Cutting Input Process Parameters Functions and Influences

The AWJ cutting input process parameters are comprised of specific functions governing the execution of various machining operations.

#### 3.1.1. Hydraulic System

The hydraulic system is the waterjet pressure denoted by (P) and measured in MPa or PSI. A continuous flow of pressurized water generated from the AWJM water pressure pump drives the cutting head controlled by an accumulator and pressure tubing [3,6].

**Impacts of waterjet pressure:** Waterjet pressure affects the distribution of water and jet abrasive particles during material erosion processes. Naresh Babu, M. et al. [82] have recommended that high-level pressure, with a value of 399 MPa, can acquire superior surface quality in cutting brass-360. Additionally, Akkurt et al. [83] have utilized an ultra-high-pressure (UHP) waterjet cutting system in evaluating deformation on materials with the same composition but different thicknesses such as Al-6061 aluminum alloy, brass-353, AISI 1030, and AISI 304 steel materials. Their experiment showed that a very high waterjet pressure negatively affects the surface roughness as the thickness of the material decreases. A high-level water pressure produces high velocity, resulting in a stronger impact of abrasive particles [49]. Ultra-high-pressure (UHP) AWJM pumps provide water pressure to the cutting head at continued pressures from 40,000 psi (276 MPa) to 87,000 psi (600 MPa) and have progressed its industrial application since its commercialization due to its wide range of application, i.e., 2D shape cutting, surface grinding, weight reduction of space-borne mirrors, and various machining tasks tasks [84]. Pashmforoush et al. [85] have observed that geometrical tolerances were obtained by increasing waterjet pressure to a value of 300 MPa when cutting Hardox 400 steel. The achieved results denote that by the increase of jet pressure, the surface quality improves and the geometrical errors are reduced. This is similar to Khan et al. [79] as they have concluded that a jet pressure of 240 MPa can yield a high material removal rate for AWJ cutting of EN24 Steel 14. These previous works established that waterjet pressure is directly proportional to the depth of jet penetration and the material removal rate.













#### 3.1.2. Abrasive System

The abrasive system is composed of abrasive material type, size, shape, and flow rate. The abrasive mass flow rate is the stream of its particles alongside waterjet pressure, which is typically measured in g/min [6].



**Impacts of abrasive type:** Abrasives are categorized into natural, zirconia alumina, glass, steel, and copper. These types have inherent diverse characteristics such as the level of hardness and grit shape. In particular, Percec et al. [64] have conducted an experiment in cutting titanium using different abrasives, i.e., garnet, olivine, and crushed glass abrasives. Based on his experiments, garnet gave the highest material removal or cut penetration. Later, they carried out a comparative investigation between garnet and corundum abrasive. They concluded that corundum abrasive applications could be suggested within certain economic circumstances due to the decreased lifespan of focusing tubes [86]. Furthermore, it has been established that AWJ cutting performance is vastly affected by the density, shape, and hardness of abrasives. Table 5 exhibits categories of abrasive materials utilized in various industries, in conjunction with their details and properties.

**Table 5.** Abrasive material categories along with their properties and industrial applications [1,68,87,88].

Category Details	A. Glass		B. Natural	
Abrasive types				
	Glass beads	Garnet	Ceramic beads	Black corundum
Hardness	MOHS 5–6		MOHS 7–8	
Shape	Round		Irregular sharp—edged	
Application	Grinding, polishing, drilling, cutting, tumbling media, sharpening, and metal cleaning			
Industrial use	Automotive, metal fabrication, machinery, electronic, construction, metallurgy, petrochemical			
Category Details	C. Zirconia Alumina			
Abrasive types				
	Black Silicon carbide	Green Silicon carbide	White fused alumina	Brown fused alumina
Hardness	MOHS 9			
Shape	Round		Irregular sharp—edged	
Application	Drilling, lapping, grinding, or polishing			
Industrial use	Automotive, metal fabrication, optics, household applications, construction, metallurgy			
Category Details	D. Steel Grit, Shot, Cut Wire and Copper Slag			
Abrasive types				
	Steel grit	Steel shot	SS Cut wire	Copper slag
Hardness	MOHS 7–9 or HRC (Hardness Rockwell C) 40–60			
Shape	Irregular rounded			
Application	Cleaning, surface preparation, stone cutting, shot peening			
Industrial use	Automotive, construction, metallurgy, petrochemical industry			

AWJM has capabilities in machining hard-to-cut materials because of its abrasive particles. Table 5 showed a representation of each abrasive category characteristic, such as particle shape, hardness, application, and industrial usage. The zirconia alumina group of abrasives indicates dominance in hardness.

Hlavacova et al. [89] have linearly machined high-carbon steel DIN norm No.1.2436 (CSN EN 19437) plate 61–mm-thick using seven different abrasives: Australian garnet, Ukraine garnet, olivine, corundum, chromite, and zirconium sized from 200 to 300  $\mu\text{m}$ , and unsorted Australian garnet. They discovered that corundum, which was approximately equal to garnet, increased cutting speed at 20%. Garnet has a comparatively low wear of focusing tubes when utilized [90]. A survey reported that 90% of users employ garnet as an abrasive type during AWJM applications [4]. Other reasons behind the high usage of garnet are attributed to its competitive price of approximately 0.48 €/Kg [24]. However, the economic concern should be weighed against abrasive performance. Hence, the abrasive type is governed by the hardness of the workpiece [17]. Therefore, a harder workpiece requires a harder abrasive particle. In general, abrasive hardness directly exerts MRR and the depth of cut on the material; accordingly, a harder abrasive indicates higher MRR and DOC, leading to a higher machining efficiency.

Impacts of abrasive size: Abrasives come with varied sizes or mesh corresponding to their specific conditions or grades. The particle grain mass and volume directly impinge on kinetic energy, which influences AWJM output parameters [91]. Various mesh numbers with the corresponding mesh size and grade are summarized in Table 6.

**Table 6.** Abrasive mesh size and grade [1,68,88,92].

Mesh Number #	Mesh in Microns $\mu\text{m}$	Grade
40–60	250–400	Coarse
80–100	180–210	Medium coarse
120–150	90–105	Medium fine
180–220	70–88	Fine
240 upwards	$\leq 60$	Very fine

The selection of an appropriate abrasive size and type depends on the hardness of the workpiece [92]. Thamizhvalavan et al. [93] have investigated the machining hybrid metal matrix which consists of Al 6063 reinforced with boron carbide ( $\text{B}_4\text{C}$ ) and zirconium silicate ( $\text{ZrSiO}_4$ ) in the form of particulates in the proportion of 5%  $\text{B}_4\text{C}$  and 5%  $\text{ZrSiO}_4$  using different type and mesh size of abrasives. They used aluminum oxide ( $\text{Al}_2\text{O}_3$ ) and garnet with varied mesh size numbers of 60, 80 and 100. They concluded that a higher rate of material removal was achieved by using an abrasive type aluminum oxide ( $\text{Al}_2\text{O}_3$ ) with a mesh size number of 80. Abrasives with all varied sizes showed the formation of striations in cut surfaces [93]. Moreover, Yuvaraj et al. [35] have analysed the effects of applying varying mesh sizes of garnet, including size 80, 100, and 120 in cutting AA5083—H32, where garnet with size number 80 produced a higher depth of cut, low kerf taper angle and surface roughness. Notwithstanding these studies, the abrasive mesh number is directly proportional to MRR, and a higher mesh size leads to higher roughness which results in a lower quality of cut surface.

Impacts of abrasive mass flow rate: In AWJ cutting operation, increasing the abrasive mass flow rate increases the erosion efficiency, containing a higher number of abrasives which relatively increases the depth of cut and decreases surface roughness value [36]. An increased rate of waterjet pressure denotes a parallel performance with abrasive flow rate [92]. Babu et al. [94] have presented a study of AWJ cutting process parameters performance in minimizing the surface roughness and kerf angle of AISI 1018 mild steel. They have observed that increasing the level of waterjet pressure, alongside with abrasive mass flow rate reduced the kerf taper angle and surface roughness. This achieved the minimum kerf geometries and less striation surface. Pawar et al. [44] have applied a moderate rate of abrasive mass flow. Mainly, a higher AFR directly leads to a higher

MRR and DOC of machined material; however, it provides a conditional opposite effect in surface roughness and kerf taper angle, depending on the type of material.

### 3.1.3. Nozzle System

The nozzle system comprises the material type, nozzle diameter (ND), and orifice diameter (OD). The orifice ranges from 0.13 to 0.76 mm [95]. It is accountable for transforming water pressure into velocity; moreover, potential energy is converted into kinetic that is being transmitted to abrasive particles. The nozzle focuses the abrasive waterjet and leads it to the workpiece [6]. An illustration of a nozzle system working scheme is shown in Figure 5.

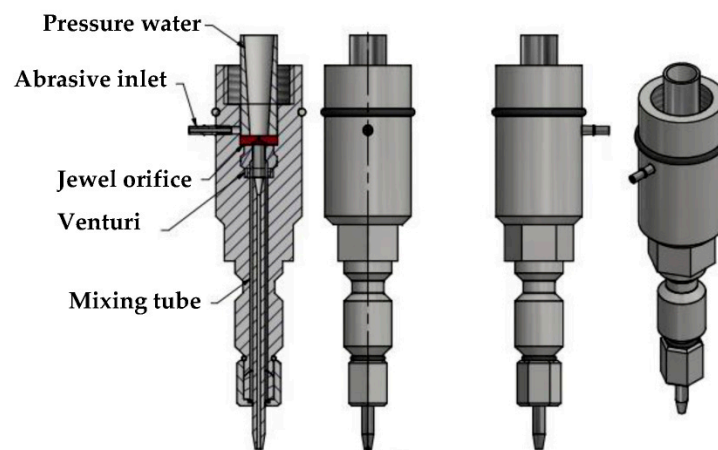


Figure 5. Nozzle system [92].

As illustrated in Figure 5, the waterjet pressure water travels at a high velocity and generates a Venturi effect or vacuum in the mixing chamber located beneath the orifice. A metered portion of abrasive particles enters through the abrasive inlet and is forced down with the waterjet stream in the mixing chamber [96]. The abrasive particles are mixed with the waterjet, creating an abrasive water jet. The nozzle is a vulnerable component of an abrasive waterjet machine and is commonly composed of silicon carbide, tungsten carbide cobalt, boron carbide, composite, and ceramic materials. Varied materials possess diverse properties that enable a nozzle to lengthen its utilization and wear [96]. In comparison to metals, ceramic nozzles ( $\text{SiC}$ ,  $\text{Al}_2\text{O}_3$ ,  $\text{ZrO}_2$ ,  $\text{B}_4\text{C}$  and  $\text{Si}_2\text{N}_4$ ) are universally used in line with mechanical properties, maximum hardness, a high melting point, and lesser resistance to heat shock. Furthermore, they can work 30 times longer than other carbon steel nozzles [91].

Impacts of nozzle and orifice diameter: Variation in the nozzle diameter and orifice leads to machining inconsistency due to the ascending airflow rate, jet deviating, and path size, hence impacting the material removal rate, surface roughness, and geometric accuracy in the broad-spectrum [6]. Furthermore, Kmec et al. [36] have investigated cutting austenitic steel AISI 304, which has recently been the most prevalent type of anti-corrosion material in various industrial applications. They used different abrasive nozzle diameter sizes including 0.76 mm and 1.02 mm. They conclude that the minimum surface roughness was achieved by using the smallest nozzle diameter of 0.76 mm. Additionally, Mogul et al. [27] have studied surface roughness in cutting Titanium Ti6AL4V using an abrasive waterjet machine, where variations in the diameter ratio of the focusing nozzle and orifice were adopted. A different approach of ratio 3:1 nozzle and orifice diameter were employed in their experiments. The results indicate that increasing the waterjet orifice and focusing the nozzle diameter can minimize the surface roughness of the cut material. Later, Nandakumar, et al. [97] has examined the nozzle head oscillating method in AWJ cutting of aluminum hybrid composites. They concluded that a lower degree level of oscillation angle decreased the Kerf taper angle and surface roughness. Substantially, these previous

researches indicate that the nozzle diameter and orifice influences the material removal rate, surface roughness, and geometric accuracy in a broad-spectrum.

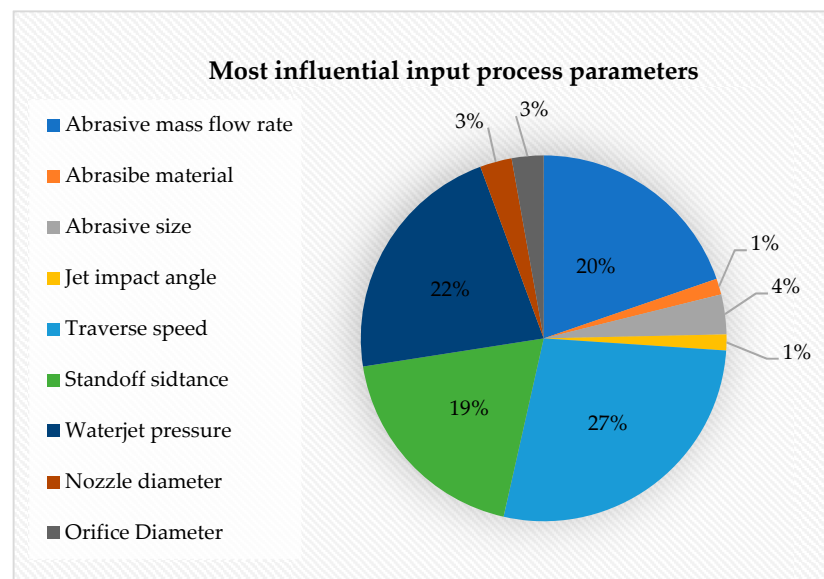
#### 3.1.4. Cutting System

These are the traverse speed, stand-off distance and jet impact angle. The traverse speed corresponds to the turning of a tank during machining, measured in mm/min. The standoff distance is the height from the endpoint of the nozzle up to the top surface of the target material, where it is indicated in mm. The jet impact angle is the angling of the jet towards a cutting level surface [6]. Recently, a relevant increase in productivity was obtained by utilizing AWJM with multiple cutting heads. There are two traverse systems that can be utilized simultaneously and independently to machine larger and multiple parts [5].

**Impacts of traverse speed:** Traverse speed variation has a significant effect on AWJM output parameters. Sasikumar et al. [98] reported that minimizing the kerf angle and surface roughness in AWJ cutting of hybrid aluminum 7075 metal matrix composites can be obtained by applying a low level of traverse speed and a high level of pressure. Their results are consistent with Gnanavelbabu et al. [77], who explored minimizing the kerf taper angle in cutting AA6061 using a low level of traverse speed. Ishfaq et al. [99] have distinguished that traverse speed was the most significant and impacting parameter for the material removal rate in AWJ cutting of stainless-clad steel workpieces. Additionally, the feed rate was revealed to be the most influential parameter in controlling the responses on surface roughness and kerf-angle in abrasive waterjet cutting of AISI 1018 with 5 mm thickness [94]. Moreover, Karmiris-Obratański et al. [100] explored AWJM multiple passes and achieved a higher depth of cut by utilizing a higher number of passes and higher-level traverse speed; hence, under particular conditions, the application of multiple passes can provide better results as compared with single pass machining. On the basis of these studies, the traverse speed is directly proportional to the material removal rate but inversely relative to the depth of cut, surface roughness, and kerf taper.

**Impacts of stand-off distance:** A higher distance from the nozzle exit and workpiece top surface results in decreasing velocity of the particles, which denotes a lower material removal rate, roughness, and kerf taper angle [92]. Kechagias et al. [81] have examined that decreased kerf width and roughness of cut parts can be obtained by applying a near standoff distance, a lower rate of traverse speed, and a smaller nozzle diameter at a higher material thickness when cutting steel sheets using an abrasive waterjet machine (TRIP 800 HR-FH and TRIP 700 CR-FH). In summary, it has been found that a combination of a high-level standoff distance and high-rate traverse speed lowers the contact time of abrasive particles within the cutting process.

**Impacts of jet impact angle:** Varying the jet impingement angle leads to different impacts in AWJM output parameters depending on the hardness scale of a workpiece [101]. For instance, Yuvaraj et al. [35] have proposed the importance of managing the jet impact angle to intensify AWJ cutting output responses. They reported that varying the impingement of the jet angle, along with using a different abrasive mesh size can affect the kerf width, taper ratio, and cut surface roughness when cutting AA5083-H32. An oblique jet angle of 70° was shown to lead to lesser kerf taper ratio, roughness and striations. Furthermore, Kumar et al. [80] have conducted an experiment using a different metal, D2 Steel, and concluded that a jet impact angle of 70° sustained better cut surface integrity. A larger degree of jet impingement angle results in a higher material removal rate, particularly in hard-to-cut materials; thus, an acute jet impact angle provides a precise cutting performance predominantly in soft materials [91]. In this paper, Figure 6 illustrates the statistics of the identified influential AWJM input process parameters within a range of publications from 2017–2020 [25–66]. Figure 6 illustrates the weighted distribution of the AWJ cutting input process parameters identified to be significant in AWJ cutting performance.



**Figure 6.** Survey of identified most influential AWJ cutting input process parameters reviewed publications from 2017 to 2020 [25–66].

Among these research findings, 27% proved that traverse speed is the most influential input parameter in the AWJ cutting process, followed by waterjet pressure, abrasive mass flow rate and standoff distance with a percentage contribution of 22, 20, and 19%, respectively. There is a limited number of studies that considered the abrasive size, nozzle and orifice diameter, abrasive material and jet impact angle; hence, the impacts of these input parameters cannot be justified because of gaining less attention from researchers and having low usage in several experimental investigations. This can be considered as a potential area for future development and studies.

### 3.2. Abrasive Waterjet Cutting Output Process Parameters

The output process parameters of the AWJM include the material removal rate, depth of cut, kerf taper angle, kerf width, and surface roughness. These output parameters have been identified as quality attributes and are correlated with quality performance [102]. The depth of cut refers to the level of penetration of the workpiece. The material removal rate is determined by the quantity of removed material from a workpiece per unit time and is computed by the volume of removed material or from the difference in weight prior to and after machining. Furthermore, the material removal rate is a denotation of the machining rate performance. The kerf taper is the tapering angle resulting from AWJM and is the measurement by the ratio of the sum of kerf top width and kerf bottom and thickness of the workpiece. The taper width is the measurement of the top and bottom cut width of the target workpiece. The surface roughness is the scale of smoothness of the machined surface, denoting the precision of executed cutting processes. AWJ cutting processes involve several types of parametric variables that can impact machining performance. For this reason, it is necessary to use comprehensive equations or formulas when governing machining performance. Table 7 enumerates equations for determining output parameters.

Suitable values for the proper selection of process parameters must be determined and should be optimized for further development, which is discussed in the next section.



**Table 7.** Output process parameters analytic equation.

Output Process Parameter	Analytic Equations	Unit of Measurement	Equation Number and Reference
Depth of cut ( $ht$ )	$ht = L \sin 25^\circ$	mm	Equation (1) [103]
Material removal rate (MRR)	$MRR = ht.W.vt$	$\text{mm}^3/\text{min}$	Equation (2) [77]
Kerf taper angle (KTA)	$KTA \theta = \arctan \frac{W_t - W_b}{2h}$	Degree ( $^\circ$ )	Equation (3) [77]
Surface roughness ( $R_a$ )	$R_a = \frac{1}{l} \int_0^l y(x) dx$	$\mu\text{m}$	Equation (4) [104]

#### 4. Abrasive Waterjet Cutting Process Parameters Improvements and Optimization

Manufacturing industries are becoming more technically and economically attentive with advancements in the worldwide economy [105]. This demand produces a need for process parameter improvements and optimization.

##### 4.1. AWJ Cutting Process Parameters Improvements

Abrasive waterjet cutting process parameters are factors that impact the effectiveness of machining performance. Defects such as the surface quality, kerf geometric inaccuracies and low material removal rate are directly correlated to transverse speed, standoff distance, waterjet pressure, and abrasive mass flow rate as well as material properties and material thickness. Therefore, nominating suitable values for these factors should be managed appropriately. Functional relations between these responses and input parameters of AWJ cutting were obtained and studied by many experimental results of numerous authors. Table 8 details a number of experimental investigations from recently published research, providing evaluations of correlations between input and output process parameters of AWJM, particularly in cutting operations. Based on the studies summarized in Table 8, water pressure at a high level provided a higher depth of cut and higher material removal rate [33,58]. A lower value of transverse speed ranging from 60 to 90 mm/min was favorable in achieving a lower surface roughness, and a higher material removal rate and depth of cut [30,33,78,106].

Table 8. Impacts of the most influencing process parameters in AWJ cutting output parameters.

Output Parameters and Materials		Input Parameters											Key Findings and References	
		Water Pressure, MPa			Traverse Speed, mm/min			Stand of Distance, mm			Abrasive Mass Flow Rate, g/min			
		Range												
		100–200	201–300	301–400	60–90	91–120	121–150	1–3	4–6	7–9	100–250	251–400	401–550	
DOC	AA2014			✓		✓		✓					✓	They obtained a high value of DOC at 29.70 mm by increasing the value of $p$ , which is recognised as the most influencing factor in AWJ cutting [58].
	AZ91			✓	✓									They found that increasing water pressure and decreasing traverse speed values can achieve a maximum value of 12.57 mm DOC in AWJ cutting of magnesium alloy [33]
MRR	Ti-6Al-4V		✓			✓						✓		They determined that high-level of AFR at 340 g/min, TS at 120 mm/min and moderate P at 275 MPa obtained a maximum MRR with a value 345.8 mm <sup>3</sup> /min in abrasive waterjet machining [77].
	Inconel 600		✓		✓									They achieved a maximum value 350 mm <sup>3</sup> /min of MRR by utilizing a moderate value of parameters i.e., P at 280 MPa and TS at 40–60 mm/min [78].
MRR	Inconel 617		✓		✓			✓					✓	They discovered that a lower or near SOD with an increasing value of AFR and TR was favourable in achieving a maximum value of MRR [107].
	Brass		✓		✓						✓			They concluded that P provides the utmost impact in minimizing $R_a$ . A low rate of P at 200 MPa with a medium rate of TS at 100 mm/min obtained a minimum $R_a$ value of 1.45 $\mu$ m [30].
KTA	AISI 1018			✓		✓		✓			✓			They attained a minimum value of KTA by decreasing feed rate and it has been identified to be the most significant parameter controlling the AWJ cutting responses [94].

As presented in Table 8, a value of abrasive mass flow rate ranging to 100 to 250 g/min achieved the minimum value of surface roughness and kerf taper angle [30,106]. Thus, it has been found that a nearer standoff distance provides a better AWJ cutting performance [58,106].

#### 4.2. AWJ Cutting Process Parameters Optimisation

Generally, optimization is utilized to achieve the minimum probable costs of cutting operations with a proper combination of process parameters considering indexes such as quality, productivity, and cost. Recently, an effective optimization technique, the Taguchi method, has become increasingly successful in optimizing some AWJM applications [108]. Several studies using the Taguchi method in their experimental work are shown in Table 9, mitigating the effectiveness of this technique.

**Table 9.** Several studies (2018 to 2020) in AWJ cutting carried out through the Taguchi method.

Material	Input Parameter	Output Parameter	Key Findings and References
Metal Matrix Composites	SOD, TS, AFR	R <sub>a</sub>	Maneiah et al. [25] used Taguchi-L9 orthogonal array in their experimental investigations. The results showed that the essential parameters in reducing R <sub>a</sub> were TS and AFR.
Ti6AL4V	P, TS, AFR, ND, OD	R <sub>a</sub> , DOC	Mogul et al. [27] worked in the prediction of cutting depth by using the Taguchi method. It was proven that TS was the most influencing parameter for a higher depth of cut.
Inconel 625	P, AFR, SOD	KTA	Jeykrishnan et al. [29] employed Taguchi's technique in this study, and it was observed that P played a significant role in lower kerf taper angle.
Brass	P, TS, AFR	R <sub>a</sub> , MRR	By utilizing Taguchi's L9 orthogonal array, Marichamy et al. [30] proved the feasibility of utilising an abrasive waterjet machine in cutting brass material. They concluded that increasing P, TS, and AFR can minimise R <sub>a</sub> and maximise MRR.
AZ91 Magnesium alloy	P, TS	DOC	Niranjan et al. [33] examined influence of process parameters in the depth of cut through the Taguchi experimental design of the L9 orthogonal array. The result showed that a higher DOC could be obtained with high P and low TS.
Ti-6Al-4V and Inconel 825	P, SOD, AFR	R <sub>a</sub>	Rajamanickam et al. [34] achieved a higher MRR for Ti-6Al-4V at a value of 3.132 gm/min and 3.246 gm/min for Inconel 825 by utilising an experimental Taguchi approach.

Taguchi is a technique applied for improving quality performance depending merely on process parameters. Taguchi's orthogonal array is useful in establishing impacts created by these cutting parameters with two or more mixed levels, which lessens the number of required experimental trials [109]. Aside from the Taguchi methodology, there are several other tools applied to quantify the correlation between AWJM input and output parameters. Table 10 enlisted several noteworthy research studies that have been published, which



focused on different experimental and simulation studies to achieve the optimum degree of these process parameters.

**Table 10.** A list of several studies (2017 to 2020) with a diverse optimization technique in AWJ cutting process.

Material	Input Parameter	Output Parameter	Optimisation Techniques	Key Findings and References
AA5083-H32	P, JIA, AS	R <sub>a</sub> , KTA, KTW, KBW	Fuzzy TOPSIS method	Yuvaraj et al. [35] employed an optimisation technique to select optimal values of input parameters, specifically, P of 150 MPa, AS of #80, and JIA of 70°. They concluded that oblique JIA improved the cutting performance of abrasive waterjet machine.
Inconel 718	P, SOD, AFR	R <sub>a</sub> , MRR, KTA	Vlsekriterijumska Optimizacija I Kompromisno Resenje in Serbian (VIKOR) method	Samson et al. [37] distinguished the optimised parameter combinations of 180 MPa P, 0.42 kg/min of AFR and 2 mm SOD. They concluded that the lower standoff distance was favourable, as it increased the material removal rate.
Inconel 718	P, TS, AFR, AM	R <sub>a</sub>	Response surface methodology—Box Behnken Method (RSM-BBM)	Kumar et al. [42] obtained a surface roughness within the range of 2.75 to 4.94 µm with the optimal level of P at 40,757 psi, AFR at 1.25 lb/min, SOD at 0.6 mm and TS at 20 mm/min. They discovered that TS and AFR were the most important parameters in the machining of Inconel 718.
Al7075/TiB2	P, TS, AFR, AS, SOD, OD	R <sub>a</sub> , MRR, KTA	Taguchi DEAR (Data Envelopment Analysis Based Ranking) Methodology	Manoj et al. [43] discovered that waterjet pressure has the highest influence in AWJ cutting responses such as MRR, Ra and KTA. The optimal process parameters combination achieved are P of (280 MPa), TS of 345 mm/min and SOD of 4 mm.
AA631-T6	TS, SOD, AFR	R <sub>a</sub> , MRR, KTA	Jaya algorithm (JA)	Rao et al. [110] utilised single-objective (SAO) and multi-objective (MOJA) to achieve better cutting performance. The maximum value of MRR obtained by the MO-Jaya algorithm was 6769.6 µm <sup>3</sup> /µs, and the minimum value of Ra obtained by the MO-Jaya algorithm was 2.7002 µm.
Inconel 617	SOD, P, TS, AFR	MRR, Geometric accuracy	Weighted principal components analysis (WPCA)	Nair et al. [107] studied MRR and geometric accuracy considering SOD, P, TS, AFR as input parameters. They determined optimal factors and observed that waterjet pressure was a less significant factor as the minimum setting was adequate enough to execute the machining process.
AA 6061	P, TS, AFR, SOD, ND	R <sub>a</sub> , MRR, KTA	Grey wolf optimizer (GWO)	Chakraborty et al. [47] attained the optimum parametric settings, which were P of 310 MPa, TS of 0.05 mm/s, AFR of 11.5 g/s, and nozzle tilted in 115°, by using the GWO method. This combination resulted in an MRR of 6769.597 µm <sup>3</sup> /µs.
Ti-6Al-4V	P, TS, SOD, AFR	DOC	Artificial Neural Network (ANN)	Selvan et al. [72] concluded that SOD and TS are inversely proportional to DOC.

Yuvaraj and Kumar [35] applied the fuzzy TOPSIS (Technique for Order Preference by Similarities to Ideal Solution) method as an optimization technique to attain better AWJ cutting performance with AA5083-H32. They considered the pressure, jet impact angle, and abrasive size as input parameters to achieve minimum values of surface roughness, kerf taper angle, and kerf width. Furthermore, they also used an additional algorithm method, the Grey-fuzzy method, to optimize AWJM process parameters for different materials like glass fiber reinforced polymer [35].

Samson et al. [37] have obtained optimal values of AWJM process parameters for machining Inconel 718, utilizing the Vlsekriterijumska Optimizacija Kompromisno Resenje in Serbian (VIKOR) method. The researchers advanced the VIKOR method by employing an analytic hierarchy process (AHP) to convey the weight of the comparative significance

of the aspects. This involved a multi-criterion decision-making (MCDM) system suitable for selecting feasible or almost ideal solutions from a set of presented alternatives [111]. The results showed that low pressure, abrasive mass flow rate, and standoff distance can minimize the kerf taper angle and roughness and maximize the material removal rate.

A hybrid response surface and Box–Behnken methodology (RSM-BBD), Kumar et al. [42] have shown the influence of pressure, traverse speed, abrasive mass flow rate, and abrasive particle in determining a tolerable level of roughness for cutting Inconel 718 and in formulating a mathematical model for predicting results. Confirmation experiments have validated the precision of these developed models.

Manoj et al. [43] have employed a Taguchi-DEAR methodology to evaluate AWJ cutting process parameters—i.e., waterjet pressure, traverse speed and standoff distance for TiB<sub>2</sub> particles in reinforced Al7075 composite materials. They anticipated higher levels of material removal rate and lower levels of surface roughness and taper angle. A customary of results of investigation were plotted to determine combinations of suitable process parameters based on a multi-response performance index (MRPI).

Rao et al. [110] considered the traverse speed, standoff distance, and abrasive mass flow rate as input parameters of an AWJ cutting process of AA631-T6. The results of material removal, roughness, and taper angle were considered against the application of the Jaya algorithm (JO). This optimization algorithm can be used to solve constrained and unconstrained conditions, to achieve an optimum alternative and avoid the worst ones [112].

Nair and Kumanan [107] used weighted principal components analysis (WPCA) to optimize AWJM process parameters in machining Inconel 617. The measured performance indicators included the material removal rate (MRR) and geometric accuracy. The WPCA method uses internal test and training samples to calculate the ‘weighted’ covariance matrix. The theoretical basis of WPCA is determined through a ‘weighted’ covariance matrix. Moreover, WPCA highlights training samples similar to the test sample and lessens the impact of other training samples [113].

Chakraborty and Mitra [47] have carried out the grey wolf optimizer (GWO) technique for AWJ cutting of AA6061, considering multiple objectives including material removal rate, surface roughness, overcut and taper. The GWO algorithm is a non-dominated set of Pareto solutions whose optimization imitates the hunting activities of grey wolves. A distinct advantage of GWO is that it identifies the best possible solution and stores this through the aid of social hierarchy.

Selvan et al. [72] developed mathematical equations using the regression investigation method (RIM) artificial neural network (ANN) procedures to select the optimum parameters. ANN is a computer-aided program mimicking the way the human brain manages information, collecting information by identifying outlines and interactions in data, acquired through experience other than from programming [39]. They observed that the developed model using ANN can predict AWJ cutting responses with at least 90% accuracy. This can be further used in predicting the output for different parameter conditions such as waterjet pressure, traverse speed, standoff distance, and abrasive mass flow rate for AWJ cutting of various materials.

This review section outlined several optimization techniques of AWJ cutting operations in diverse experimental conditions with the objective of attaining higher productivity and better quality.

## 5. Conclusions and Potential Future Scope of Study

There has been an exponential increase in the demand for AWJM in various manufacturing industries, which is why further study of performance enhancement is necessary. This review presents an overview of recent developments and progress made in applications of AWJ cutting, which are valuable for future studies. Based on the above-mentioned reviews and discussions, the following conclusion and potential future scopes of study have been identified:

### 5.1. Conclusions

- The intensive review of the trend of recently published research studies has revealed that aluminium and other metal workpieces gained 53% of the attention in exploring AWJM application improvements. A total of 27% of recent studies have proved that traverse speed greatly impacts abrasive waterjet (AWJ) cutting performance, followed by abrasive mass flow rate and waterjet pressure with statistics of 22% and 20%, respectively. Garnet with a hardness scale of MOHS 7–8 and a mesh size of #80 at 180  $\mu\text{m}$  gained 90% utilisation in AWJM applications due to its better performance and competitive price.
- AWJ cutting of hard-to-cut workpieces such as metallic materials including tungsten carbide, tool steel, and Inconel alloys have demonstrated distinct characteristics such as the fast speed at a rate of 2 to 3  $\text{mm}^3/\text{s}$ , versatility in cutting with thickness ranging from  $\leq 304.8$  mm, the ability to machine complicated shapes, and environmentally sustainable qualities. These characteristics explain their wide range of current applications across various industries.
- Cutting metallic materials with low machinability, i.e., stainless steel, Inconel and titanium, can attain lower surface roughness, higher depth of cut and material removal rate at a waterjet pressure ranging from 201 to 300 MPa. A traverse speed ranging from 60 to 90 mm/min, abrasive mass flow rate of 401 to 500 g/min, and stand-off distance ranging from 1.0 to 3.0 mm were established to achieve a lower surface roughness, lower kerf taper angle, and higher material removal rate applicable to various metals. Different optimisation techniques such as weighted principal components analysis (WPCA), surface and Box–Behnken methodology (RSM-BBD) and grey wolf optimiser (GWO) were employed and proved to be notably efficient in defining the optimum values of process parameters.

### 5.2. Potential Further Study

- AWJ cutting has acquired high interest in improving process performance at specific input parameter conditions. Hence, limited studies considered other parameters such as the jet impact angle, abrasive, and nozzle sizes. A further study on the impacts of these mentioned input parameters in AWJ cutting of various materials with different thicknesses can be considered for future improvements.
- Based on a review of past literature, numerous research studies and experiments have been conducted to evaluate the difference between the straight-slit and linear cutting process of AWJMs. Nonetheless, limited reports present AWJM performance in contour cutting. Thus, the cuttings of complex and complicated geometries are more regularly applied in manufacturing industries rather than straight-slit or linear cutting. Undertaking an empirical and analytical study of the effects of the process parameters in AWJ contour cutting would be important to various manufacturing processes in the fabrication industry.
- A prolific number of works have been fulfilled in predicting and monitoring AWJ cutting performance and responses in terms of quality and productivity. Its effectiveness in machining cost and intelligent process controlling are two areas that can be studied further to determine future developments.

**Author Contributions:** Conceptualization: M.T.-R., J.M.L.; investigation and writing original draft: J.M.L.; review and supervision: M.T.-R. and A.V.; Editing and project administration: M.A. and J.M.L. All authors have read and agreed to the published version of the manuscript.

**Funding:** This research received no external funding.

**Institutional Review Board Statement:** Not applicable.

**Informed Consent Statement:** Not applicable.

**Data Availability Statement:** Not applicable.

**Acknowledgments:** The authors would like to thank the School of Engineering, Edith Cowan University, Australia, for providing and administering the needed requirements in accomplishing this research.

**Conflicts of Interest:** The authors declare no conflict of interest.

### Abbreviations

The following abbreviations and nomenclatures are used in this paper:

DOC	Depth of cut
ECDM	Electro chemical discharge machine
EDM	Electro discharge machine
HAZ	Heat affected zone
JIA	Jet impact angle
KBW	Kerf bottom width
KTA	Kerf taper angle
KTW	Kerf top width
KW	Kerf width
MRR	Material removal rate
LBM	Laser beam machine
MMC	Metal matrix composite
ND	Nozzle diameter
OD	Orifice diameter
P	Waterjet pressure
SOD	Standoff distance
Ti6AL-4V	Titanium alloy
TS	Traverse speed
$h$	Thickness of the material
$l$	inclined length of workpiece
$ht$	Depth of cut
$vt$	Traverse speed
$y$	profile height in a defined point
$W$	Kerf width
$W_t$	Kerf top width
$W_b$	Kerf bottom width.
$Ra$	Thickness of the material
$y$	profile height in a defined point
AA	Aluminum alloy
AFR	Abrasive mass flow rate
AL	Aluminum
AM	Abrasive material type
AS	Abrasive size
AWJ	Abrasive waterjet
AWJM	Abrasive waterjet machining

### References

1. Alsoufi, M.S. State-of-the-Art in Abrasive Water Jet Cutting Technology and the Promise for Micro-and Nano-Machining. *Int. J. Mech. Eng. Appl.* **2017**, *5*, 1–14. [[CrossRef](#)]
2. Gupta, K. Introduction to Abrasive Water Jet Machining. In *Abrasive Water Jet Machining of Engineering Materials*; Springer: Berlin/Heidelberg, Germany, 2020; pp. 1–11.
3. Liu, X.; Liang, Z.; Wen, G.; Yuan, X. Waterjet machining and research developments: A review. *Int. J. Adv. Manuf. Technol.* **2019**, *102*, 1257–1335. [[CrossRef](#)]
4. Natarajan, Y.; Murugesan, P.K.; Mohan, M.; Khan, S.A.L.A. Abrasive Water Jet Machining process: A state of art of review. *J. Manuf. Process.* **2020**, *49*, 271–322. [[CrossRef](#)]
5. Liu, H. “7M” Advantage of Abrasive Waterjet for Machining Advanced Materials. *J. Manuf. Mater. Process.* **2017**, *1*, 11. [[CrossRef](#)]
6. Saravanan, S.; Vijayan, V.; Suthahar, S.T.J.; Balan, A.V.; Sankar, S.; Ravichandran, M. A review on recent progresses in machining methods based on abrasive water jet machining. *Mater. Today Proc.* **2020**, *21*, 116–122. [[CrossRef](#)]
7. Liu, H.; Schubert, E. Micro abrasive-waterjet technology. In *Micromachining Techniques for Fabrication of Micro and Nano Structures*; InTechOpen: London, UK, 2012; pp. 205–233.

8. Singh, P.; Pramanik, A.; Basak, A.; Prakash, C.; Mishra, V. Developments of non-conventional drilling methods—A review. *Int. J. Adv. Manuf. Technol.* **2020**, *106*, 2133–2166. [[CrossRef](#)]
9. Sureban, R.; Kulkarni, V.N.; Gaitonde, V. Modern Optimization Techniques for Advanced Machining Processes—A Review. *Mater. Today Proc.* **2019**, *18*, 3034–3042. [[CrossRef](#)]
10. Nguyen, T.; Wang, J. A review on the erosion mechanisms in abrasive waterjet micromachining of brittle materials. *Int. J. Extrem. Manuf.* **2019**, *1*, 012006. [[CrossRef](#)]
11. Mieszala, M.; Torrubia, P.L.; Axinte, D.A.; Schwiedrzik, J.J.; Guo, Y.; Mischler, S.; Michler, J.; Philippe, L. Erosion mechanisms during abrasive waterjet machining: Model microstructures and single particle experiments. *J. Mater. Process. Technol.* **2017**, *247*, 92–102. [[CrossRef](#)]
12. Hlaváčová, I.M.; Sadílek, M.; Váňová, P.; Szumilo, Š.; Tyč, M. Influence of steel structure on machinability by abrasive water jet. *Materials* **2020**, *13*, 4424. [[CrossRef](#)]
13. Kowsari, K.; Nouraei, H.; James, D.; Spelt, J.; Papini, M. Abrasive slurry jet micro-machining of holes in brittle and ductile materials. *J. Mater. Process. Technol.* **2014**, *214*, 1909–1920. [[CrossRef](#)]
14. Ruiz-Garcia, R.; Ares, P.F.M.; Vazquez-Martinez, J.M.; Gomez, J.S. Influence of Abrasive Waterjet Parameters on the Cutting and Drilling of CFRP/UNS A97075 and UNS A97075/CFRP Stacks. *Materials* **2019**, *12*, 107. [[CrossRef](#)] [[PubMed](#)]
15. Supriya, S.; Srinivas, S. Machinability studies on stainless steel by abrasive water jet-Review. *Mater. Today Proc.* **2018**, *5*, 2871–2876. [[CrossRef](#)]
16. Rajurkar, K.P.; Sundaram, M.M.; Malshe, A.P. Review of Electrochemical and Electrodischarge Machining. *Procedia Cirp* **2013**, *6*, 13–26. [[CrossRef](#)]
17. Rajurkar, K.P.; Hadidi, H.; Pariti, J.; Reddy, G.C. Review of Sustainability Issues in Non-traditional Machining Processes. In Proceedings of the International Conference on Sustainable Materials Processing and Manufacturing (SMPM 2017), Kruger, South Africa, 23–25 January 2017; pp. 714–720. [[CrossRef](#)]
18. Akkurt, A. Surface properties of the cut face obtained by different cutting methods from AISI 304 stainless steel materials. *Indian J. Mater. Sci.* **2009**, *16*, 373–384.
19. Krajcarz, D. Comparison Metal Water Jet Cutting with Laser and Plasma Cutting. In Proceedings of the 24th Daaam International Symposium on Intelligent Manufacturing and Automation, Zadar, Croatia, 23–26 October 2013; Volume 69, pp. 838–843. [[CrossRef](#)]
20. Chaturvedi, C.; Rao, P.S. Some Technical Issues and Critical Assessment of Abrasive Water Jet Machining (AWJM) Process. *Int. J. Innov. Technol. Explor. Eng.* **2020**, *9*, 39520. [[CrossRef](#)]
21. Rakshit, R.; Das, A.K. A review on cutting of industrial ceramic materials. *Precis. Eng.* **2019**, *59*, 90–109. [[CrossRef](#)]
22. Kovacevic, R.; Mohan, R.; Beardsley, H.E. Monitoring of Thermal Energy Distribution in Abrasive Waterjet Cutting Using Infrared Thermography. *J. Manuf. Sci. Eng.* **1996**, *118*, 555–563. [[CrossRef](#)]
23. Babu, M.K.; Chetty, O.K. A study on recycling of abrasives in abrasive water jet machining. *Wear* **2003**, *254*, 763–773. [[CrossRef](#)]
24. Schramm, A.; Morczinek, F.; Götze, U.; Putz, M. Technical-economic evaluation of abrasive recycling in the suspension fine jet process chain. *Int. J. Adv. Manuf. Technol.* **2020**, *106*, 981–992. [[CrossRef](#)]
25. Maneiah, D.; Shunmugasundaram, M.; Reddy, A.R.; Begum, Z. Optimization of machining parameters for surface roughness during abrasive water jet machining of aluminium/magnesium hybrid metal matrix composites. *Mater. Today Proc.* **2020**, *27*, 1293–1298. [[CrossRef](#)]
26. Tripathi, D.R.; Vachhani, K.H.; Kumari, S.; Abhishek, K. Experimental investigation on material removal rate during abrasive water jet machining of GFRP composites. *Mater. Today Proc.* **2020**, *26*, 1389–1392. [[CrossRef](#)]
27. Mogul, Y.I.; Nasir, I.; Myler, P. Investigation and optimization for depth of cut and surface roughness for control depth milling in Titanium Ti6AL4V with abrasive water jet cutting. *Mater. Today Proc.* **2020**, *28*, 604–610. [[CrossRef](#)]
28. Naik, M.B.; Srikanth, D.; Rao, M.S. Abrasive Jet Machining on Soda lime Glass-An experimental investigation. *Int. J. Res. Publ.* **2020**, *44*, 887.
29. Jeykrishnan, J.; Ramnath, B.V.; Vignesh, S.S.; Sridharan, P.; Saravanan, B. Optimization of Process Parameters in Abrasive Water Jet Machining/Cutting (AWJM) of Nickel Alloy using Traditional Analysis to Minimize Kerf Taper Angle. *Mater. Today Proc.* **2019**, *16*, 392–397. [[CrossRef](#)]
30. Marichamy, S.; Ravichandran, M.; Stalin, B.; Babu, S.B. Optimization of abrasive water jet machining parameters for  $\alpha$ - $\beta$  brass using Taguchi methodology. *FME Trans.* **2019**, *47*, 116–121. [[CrossRef](#)]
31. Kumar, P.; Tank, B.; Kant, R. Experimental investigation on abrasive waterjet machining of fibre vinyl ester composite. *J. Manuf. Eng.* **2019**, *14*, 134–138. [[CrossRef](#)]
32. Srikanth, D.V.; Rao, M.S. Application of Taguchi & Response surface methodology in Optimization for machining of ceramics with abrasive jet machining. *Mater Today Proc.* **2015**, *2*, 3308–3317. [[CrossRef](#)]
33. Niranjana, C.; Srinivas, S.; Ramachandra, M. An experimental study on depth of cut of AZ91 Magnesium Alloy in abrasive water jet cutting. *Mater. Today Proc.* **2018**, *5*, 2884–2890. [[CrossRef](#)]
34. Rajamanickam, S.; Manjunathan, R.; Mariyappan, K.; Aravindh, S. Comparative analysis of MRR on abrasive water jet machining parameters over aerospace alloys: Inconel 825 & Ti-6Al-4V. *Int. J. Pure Appl. Math.* **2018**, *118*, 727–733.
35. Yuvaraj, N.; Kumar, M.P. Optimisation of abrasive water jet cutting process parameters for AA5083-H32 aluminium alloy using fuzzy TOPSIS method. *Int. J. Mach. Mach. Mater.* **2018**, *20*, 118–140.



36. Kmec, J.; Gombár, M.; Harničárová, M.; Valíček, J.; Kušnerová, M.; Kříž, J.; Kadnár, M.; Karková, M.; Vagaská, A. The Predictive Model of Surface Texture Generated by Abrasive Water Jet for Austenitic Steels. *Appl. Sci.* **2020**, *10*, 3159. [[CrossRef](#)]
37. Samson, R.M.; Rajak, S.; Kannan, T.D.B.; Sampreet, K. Optimization of Process Parameters in Abrasive Water Jet Machining of Inconel 718 Using VIKOR Method. *J. Inst. Eng.* **2020**, *101*, 579–585. [[CrossRef](#)]
38. Senthilkumar, T.; Muralikannan, R.; Kumar, S.S. Surface morphology and parametric optimization of AWJM parameters using GRA on aluminum HMMC. *Mater. Today Proc.* **2020**, *22*, 410–415. [[CrossRef](#)]
39. Madara, S.R.; Pillai, S.R. Modelling of surface roughness in abrasive waterjet cutting of Kevlar 49 composite using artificial neural network. *Mater. Today Proc.* **2020**. [[CrossRef](#)]
40. Jagadish; Bhowmik, S.; Ray, A. Prediction of surface roughness quality of green abrasive water jet machining: A soft computing approach. *J. Intell. Manuf.* **2019**, *30*, 2965–2979. [[CrossRef](#)]
41. Brucely, Y.; Jai Aultrin, K.S.; Jaison, D. Using Genetic Algorithm Optimizing the Cutting Parameters of AWJM Process for Aluminium 6061 Alloy. *Int. J. Recent Trends Eng. Res.* **2019**, *5*, 48–56. [[CrossRef](#)]
42. Kumar, A.; Singh, H.; Kumar, V. Study the parametric effect of abrasive water jet machining on surface roughness of Inconel 718 using RSM-BBD techniques. *Mater. Manuf. Process.* **2018**, *33*, 1483–1490. [[CrossRef](#)]
43. Manoj, M.; Jinu, G.R.; Muthuramalingam, T. Multi Response Optimization of AWJM Process Parameters on Machining TiB2 Particles Reinforced Al7075 Composite Using Taguchi-DEAR Methodology. *Silicon* **2018**, *10*, 2287–2293. [[CrossRef](#)]
44. Pawar, P.J.; Vidhate, U.S.; Khalkar, M.Y. Improving the quality characteristics of abrasive water jet machining of marble material using multi-objective artificial bee colony algorithm. *J. Comput. Des. Eng.* **2018**, *5*, 319–328. [[CrossRef](#)]
45. Rao, R.V.; Rai, D.P.; Balic, J. Multi-objective optimization of abrasive waterjet machining process using Jaya algorithm and PROMETHEE Method. *J. Intell. Manuf.* **2019**, *30*, 2101–2127. [[CrossRef](#)]
46. Nair, A.; Kumanan, S. Optimization of size and form characteristics using multi-objective grey analysis in abrasive water jet drilling of Inconel 617. *J. Braz. Soc. Mech. Sci.* **2018**, *40*, 121. [[CrossRef](#)]
47. Chakraborty, S.; Mitra, A. Parametric optimization of abrasive water-jet machining processes using grey wolf optimizer. *Mater. Manuf. Process.* **2018**, *33*, 1471–1482. [[CrossRef](#)]
48. Johari, N.F.; Zain, A.M.; Mustaffa, N.H.; Udin, A. Machining parameters optimization using hybrid firefly algorithm and particle swarm optimization. *J. Phys. Conf. Ser.* **2017**, *892*, 012005. [[CrossRef](#)]
49. Liu, S.; Zhou, F.; Li, H.; Chen, Y.; Wang, F.; Guo, C. Experimental Investigation of Hard Rock Breaking Using a Conical Pick Assisted by Abrasive Water Jet. *Rock Mech. Rock Eng.* **2020**, *53*, 4221–4230. [[CrossRef](#)]
50. Madara, S.R.; Selvan, C.P.; Sampath, S.; Pillai, S.R. Impact of process parameters on surface roughness of hastelloy using abrasive waterjet machining technology. *Int. J. Recent Technol. Eng.* **2019**, *7*, 419–425.
51. Balamurugan, K.; Uthayakumar, M.; Sankar, S.; Hareesh, U.; Warriar, K. Effect of abrasive waterjet machining on LaPO<sub>4</sub>/Y<sub>2</sub>O<sub>3</sub> ceramic matrix composite. *J. Aust. Ceram. Soc.* **2018**, *54*, 205–214. [[CrossRef](#)]
52. Krajcarz, D.; Bańkowski, D.; Młynarczyk, P. The Effect of Traverse Speed on Kerf Width in AWJ Cutting of Ceramic Tiles. *Procedia Eng.* **2017**, *192*, 469–473. [[CrossRef](#)]
53. Lima, C.E.d.A.; Lebrón, R.; de Souza, A.J.; Ferreira, N.F.; Neis, P.D. Study of influence of traverse speed and abrasive mass flowrate in abrasive water jet machining of gemstones. *Int. J. Adv. Manuf. Technol.* **2016**, *83*, 77–87. [[CrossRef](#)]
54. Kumar, R.S.; Gajendran, S.; Kesavan, R. Evaluation of Optimum Machining Parameters by AWJM for Granite through Multi Response Methods. *Mater. Today Proc.* **2020**, *22*, 3056–3066. [[CrossRef](#)]
55. Kalusuraman, G.; Kumaran, S.T.; Siva, I.; Kumar, S.A. Cutting performance of luffa cylindrica fiber-reinforced composite by abrasive water jet. *J. Test. Eval.* **2020**, *48*, 3417–3428. [[CrossRef](#)]
56. Kumar, R.S.; Gajendran, S.; Kesavan, R. Estimation of Optimal Process Parameters for Abrasive Water Jet Machining Of Marble Using Multi Response Techniques. *Mater. Today Proc.* **2018**, *5*, 11208–11218. [[CrossRef](#)]
57. Yu, Y.; Sun, T.X.; Yuan, Y.M.; Gao, H.; Wang, X.P. Experimental investigation into the effect of abrasive process parameters on the cutting performance for abrasive waterjet technology: A case study. *Int. J. Adv. Manuf. Tech.* **2020**, *107*, 2757–2765. [[CrossRef](#)]
58. Shibin, R.; Anandakrishnan, V.; Sathish, S.; Sujana, V.M. Investigation on the abrasive water jet machinability of AA2014 using SiC as abrasive. *Mater. Today Proc.* **2020**, *21*, 519–522. [[CrossRef](#)]
59. Yogeswaran, R.; Pitchipoo, P. Characterization and machining analysis of AA3003 honeycomb sandwich. *Mater. Today Proc.* **2020**, *28*, 4–7. [[CrossRef](#)]
60. Shukla, R.; Singh, D. Experimentation investigation of abrasive water jet machining parameters using Taguchi and Evolutionary optimization techniques. *Swarm Evol. Comput.* **2017**, *32*, 167–183. [[CrossRef](#)]
61. Wang, S.; Zhang, S.; Wu, Y.; Yang, F. Exploring kerf cut by abrasive waterjet. *Int. J. Adv. Manuf. Technol.* **2017**, *93*, 2013–2020. [[CrossRef](#)]
62. Mohamad, W.; Kasim, M.; Norazlina, M.; Hafiz, M.; Izamshah, R.; Mohamed, S. Effect of standoff distance on the kerf characteristic during abrasive water jet machining. *Results Eng.* **2020**, *6*, 100101. [[CrossRef](#)]
63. El-Hofy, M.; Helmy, M.; Escobar-Palafox, G.; Kerrigan, K.; Scaife, R.; El-Hofy, H. Abrasive water jet machining of multidirectional CFRP laminates. *Procedia CIRP* **2018**, *68*, 535–540. [[CrossRef](#)]
64. Percec, A. Experimental research into alternative abrasive material for the abrasive water-jet cutting of titanium. *Int. J. Adv. Manuf. Technol.* **2018**, *97*, 1529–1540. [[CrossRef](#)]

65. Li, M.; Huang, M.; Chen, Y.; Kai, W.; Yang, X. Experimental study on hole characteristics and surface integrity following abrasive waterjet drilling of Ti6Al4V/CFRP hybrid stacks. *Int. J. Adv. Manuf. Tech.* **2019**, *104*, 4779–4789. [[CrossRef](#)]
66. Tiwari, T.; Sourabh, S.; Nag, A.; Dixit, A.R.; Mandal, A.; Das, A.K.; Mandal, N.; Srivastava, A.K. Parametric investigation on abrasive waterjet machining of alumina ceramic using response surface methodology. *IOP Conf. Ser. Mater. Sci. Eng.* **2018**, *377*, 012005. [[CrossRef](#)]
67. Kaladhar, M.; Subbaiah, K.V.; Rao, C.S. Machining of austenitic stainless steels—a review. *Int. J. Mach. Mach. Mater.* **2012**, *12*, 178–192. [[CrossRef](#)]
68. Hashish, M. A Modeling Study of Metal Cutting With Abrasive Waterjets. *J. Eng. Mater. Technol.* **1984**, *106*, 88–100. [[CrossRef](#)]
69. Liu, H.-T.P. Advanced waterjet technology for machining curved and layered structures. *Curved Layer. Struct.* **2019**, *6*, 41–56. [[CrossRef](#)]
70. Sarayakupoğlu, T. Abrasive Water Jet (AWJ) Applications in the Aviation Industry. *Int. J. Mech. Prod. Eng. Res. Dev. (IJMPERD)* **2019**, *9*, 347–356. [[CrossRef](#)]
71. Aurich, J.C.; Kirsch, B.; Setti, D.; Axinte, D.; Beaucamp, A.; Butler-Smith, P.; Yamaguchi, H. Abrasive processes for micro parts and structures. *CIRP Ann.* **2019**, *68*, 653–676. [[CrossRef](#)]
72. Selvan, M.C.P.; Midhunchakkaravarthy, D.; Senanayake, R.; Pillai, S.R.; Madara, S.R. A mathematical modelling of Abrasive Waterjet Machining on Ti-6Al-4V using Artificial Neural Network. *Mater. Today Proc.* **2020**. [[CrossRef](#)]
73. Pahuja, R.; Ramulu, M. Machinability of randomly chopped discontinuous fiber composites: A comparative assessment of conventional and abrasive waterjet. In Proceedings of the 23rd International Conference on Waterjetting, Seattle, WA, USA, 13 November 2016; pp. 127–148.
74. Chen, M.; Zhang, S.; Zeng, J.; Chen, B.; Xue, J.; Ji, L. Correcting shape error on external corners caused by the cut-in/cut-out process in abrasive water jet cutting. *Int. J. Adv. Manuf. Technol.* **2019**, *103*, 849–859. [[CrossRef](#)]
75. Miao, X.; Qiang, Z.; Wu, M.; Song, L.; Ye, F. Research on quality improvement of the cross section cut by abrasive water jet based on secondary cutting. *Int. J. Adv. Manuf. Technol.* **2018**, *97*, 71–80. [[CrossRef](#)]
76. Miao, X.; Ye, F.; Wu, M.; Song, L.; Qiang, Z. The method of 3D nozzle tilt cutting of abrasive water jet. *Int. J. Adv. Manuf. Technol.* **2019**, *103*, 3109–3114. [[CrossRef](#)]
77. Gnanavelbabu, A.; Saravanan, P.; Rajkumar, K.; Karthikeyan, S. Experimental investigations on multiple responses in abrasive waterjet machining of Ti-6Al-4V alloy. *Mater. Today Proc.* **2018**, *5*, 13413–13421. [[CrossRef](#)]
78. Uthayakumar, M.; Khan, M.A.; Kumaran, S.T.; Slota, A.; Zajac, J. Machinability of nickel-based superalloy by abrasive water jet machining. *Mater. Manuf. Process.* **2016**, *31*, 1733–1739. [[CrossRef](#)]
79. Khan, M.A.; Gupta, K. Machinability Studies on Abrasive Water Jet Machining of Low Alloy Steel for Different Thickness. *IOP Conf. Ser. Mater. Sci. Eng.* **2020**, *709*, 044099. [[CrossRef](#)]
80. Yuvaraj, N.; Kumar, M.P. Surface integrity studies on abrasive water jet cutting of AISI D2 steel. *Mater. Manuf. Process.* **2017**, *32*, 162–170. [[CrossRef](#)]
81. Kechagias, J.; Petropoulos, G.; Vaxevanidis, N. Application of Taguchi design for quality characterization of abrasive water jet machining of TRIP sheet steels. *Int. J. Adv. Manuf. Technol.* **2012**, *62*, 635–643. [[CrossRef](#)]
82. Naresh Babu, M.; Muthukrishnan, N. Investigation on surface roughness in abrasive water-jet machining by the response surface method. *Mater. Manuf. Process.* **2014**, *29*, 1422–1428. [[CrossRef](#)]
83. Akkurt, A.; Kulekci, M.K.; Seker, U.; Ercan, F. Effect of feed rate on surface roughness in abrasive waterjet cutting applications. *J. Mater. Process. Technol.* **2004**, *147*, 389–396. [[CrossRef](#)]
84. Liu, H.; Schubert, E.; McNiel, D.; Soo, K. Applications of abrasive-fluidjets for precision machining of composites. In Proceedings of the International SAMPE Symposium and Exhibition (Proceedings), Seattle, WA, USA, 17–20 May 2010; pp. 17–20.
85. Pashmforoush, F.; Hassanpour Babajan, A.; Beyraghi Baranlou, R. Experimental Study of Geometric Tolerances and Surface Roughness in Abrasive Water Jet Machining Process of Hardox 400 Steel. *Modares Mech. Eng.* **2020**, *20*, 953–961.
86. Perec, A.; Pude, F.; Grigoryev, A.; Kaufeld, M.; Wegener, K. A study of wear on focusing tubes exposed to corundum-based abrasives in the waterjet cutting process. *Int. J. Adv. Manuf. Tech.* **2019**, *104*, 2415–2427. [[CrossRef](#)]
87. Liu, H.-T. Waterjet technology for machining fine features pertaining to micromachining. *J. Manuf. Process* **2010**, *12*, 8–18. [[CrossRef](#)]
88. Dong, Y.Z.; Liu, W.W.; Zhang, H.; Zhang, H.C. On-line recycling of abrasives in abrasive water jet cleaning. *CIRP Conf. Life Cycle Eng.* **2014**, *15*, 278–282. [[CrossRef](#)]
89. Hlavacova, I.; Geryk, V. Abrasives for water-jet cutting of high-strength and thick hard materials. *Int. J. Adv. Manuf. Technol.* **2017**, *90*, 1217–1224. [[CrossRef](#)]
90. Perec, A.; Pude, F.; Stirnimann, J.; Wegener, K. Feasibility Study on the Use of Fractal Analysis for Evaluating the Surface Quality Generated by Waterjet. *Teh. Vjesn.* **2015**, *22*, 879–883. [[CrossRef](#)]
91. Melentiev, R.; Fang, F. Recent advances and challenges of abrasive jet machining. *CIRP J. Manuf. Sci. Technol.* **2018**, *22*, 1–20. [[CrossRef](#)]
92. Hashish, M. Optimization Factors in Abrasive-Waterjet Machining. *J. Eng. Ind.* **1991**, *113*, 29–37. [[CrossRef](#)]
93. Thamizhvalavan, P.; Arivazhagan, S.; Yuvaraj, N.; Ramesh, B. Machinability study of abrasive aqua jet parameters on hybrid metal matrix composite. *Mater. Manuf. Process.* **2019**, *34*, 321–344. [[CrossRef](#)]
94. Babu, M.N.; Muthukrishnan, N. Exploration on Kerf-angle and surface roughness in abrasive waterjet machining using response surface method. *J. Inst. Eng.* **2018**, *99*, 645–656. [[CrossRef](#)]
95. Hashish, M. A Model for Abrasive-Waterjet (AWJ) Machining. *J. Eng. Mater. Technol.* **1989**, *111*, 154–162. [[CrossRef](#)]

96. Radovanovic, M. Multi-Objective Optimization of Abrasive Water Jet Cutting Using MOGA. *Procedia Manuf.* **2020**, *47*, 781–787. [[CrossRef](#)]
97. Nandakumar, N.; Sasikumar, K.; Sambathkumar, M.; Saravanan, N. Investigations on AWJ cutting process of hybrid aluminium 7075 metal matrix composites using nozzle oscillation technique. *Mater. Today Proc.* **2020**, *33*, 2798–2802. [[CrossRef](#)]
98. Sasikumar, K.; Arulshri, K.; Ponappa, K.; Uthayakumar, M. A study on kerf characteristics of hybrid aluminium 7075 metal matrix composites machined using abrasive water jet machining technology. *J. Eng. Manuf.* **2018**, *232*, 690–704. [[CrossRef](#)]
99. Ishfaq, K.; Ahmad Mufti, N.; Ahmed, N.; Pervaiz, S. Abrasive waterjet cutting of clad material: Kerf taper and MRR analysis. *Mater. Manuf. Process.* **2019**, *34*, 544–553. [[CrossRef](#)]
100. Karmiris-Obratański, P.; Karkalos, N.E.; Kudelski, R.; Papazoglou, E.L.; Markopoulos, A.P. On the Effect of Multiple Passes on Kerf Characteristics and Efficiency of Abrasive Waterjet Cutting. *Metals* **2021**, *11*, 74. [[CrossRef](#)]
101. Yuvaraj, N.; Kumar, M.P. Cutting of aluminium alloy with abrasive water jet and cryogenic assisted abrasive water jet: A comparative study of the surface integrity approach. *Wear* **2016**, *362*, 18–32. [[CrossRef](#)]
102. Mardi, K.B.; Dixit, A.; Mallick, A. Studies on non-traditional machining of metal matrix composites. *Mater. Today Proc.* **2017**, *4*, 8226–8239. [[CrossRef](#)]
103. Srinivas, S.; Babu, N.R. Penetration Ability of Abrasive Waterjets in Cutting of Aluminum-Silicon Carbide Particulate Metal Matrix Composites. *Mach. Sci. Technol.* **2012**, *16*, 337–354. [[CrossRef](#)]
104. Gostimirovic, M.; Pucovsky, V.; Sekulic, M.; Rodic, D.; Pejic, V. Evolutionary optimization of jet lag in the abrasive water jet machining. *Int. J. Adv. Manuf. Technol.* **2019**, *101*, 3131–3141. [[CrossRef](#)]
105. Hanif, M.I.; Aamir, M.; Ahmed, N.; Maqsood, S.; Muhammad, R.; Akhtar, R.; Hussain, I. Optimization of facing process by indigenously developed force dynamometer. *Int. J. Adv. Manuf. Technol.* **2019**, *100*, 1893–1905. [[CrossRef](#)]
106. Kumar, P.; Kant, R. Development of a predictive model for kerf taper angle in AWJM of Kevlar epoxy composite. *Mater. Today Proc.* **2020**, *28*, 1164–1169. [[CrossRef](#)]
107. Otto, K.N.; Antonsson, E.K. Extensions to the Taguchi Method of Product Design. *J. Mech. Des.* **1993**, *115*, 5–13. [[CrossRef](#)]
108. Aamir, M.; Tu, S.S.; Tolouei-Rad, M.; Giasin, K.; Vafadar, A. Optimization and Modeling of Process Parameters in Multi-Hole Simultaneous Drilling Using Taguchi Method and Fuzzy Logic Approach. *Materials* **2020**, *13*, 680. [[CrossRef](#)] [[PubMed](#)]
109. Rao, R.V.; Rai, D.P.; Balic, J. Optimization of Abrasive Waterjet Machining Process using Multi-objective Jaya Algorithm. *Mater. Today Proc.* **2018**, *5*, 4930–4938. [[CrossRef](#)]
110. Nair, A.; Kumanan, S. Multi-performance optimization of abrasive water jet machining of Inconel 617 using WPCA. *Mater. Manuf. Process.* **2017**, *32*, 693–699. [[CrossRef](#)]
111. Opricovic, S.; Tzeng, G.H. Extended VIKOR method in comparison with outranking methods. *Eur. J. Oper. Res.* **2007**, *178*, 514–529. [[CrossRef](#)]
112. Rao, R. Jaya: A simple and new optimization algorithm for solving constrained and unconstrained optimization problems. *Int. J. Ind. Eng. Comp.* **2016**, *7*, 19–34.
113. Fan, Z.; Liu, E.; Xu, B. Weighted principal component analysis. In *International Conference on Artificial Intelligence and Computational Intelligence*; Springer: Berlin/Heidelberg, Germany, 2011; pp. 569–574.



### **Chapter 3 Impacts of traverse speed and material thickness on AWJ contour cutting of AISI 304L**

This chapter has been published as a research article in the *“Applied Science, in a special issue: Advanced Manufacturing of Metals”*, an official journal of MDPI. The details embedded in this chapter are the same, except for formatting changes to maintain uniformity in the content of the thesis. Subsequently, after conducting a comprehensive study in abrasive waterjet mechanisms, this chapter presents an experimental investigation in contour cutting of different profiles. This chapter details an investigation on the impacts of traverse speed and material thickness in abrasive waterjet machining of AISI 304L with an aim of obtaining higher rate of material removal and lower kerf taper angle. Moreover, this chapter demonstrates a statistical analysis to evaluate the significance of traverse speed and material thickness towards material removal rate and kerf taper angle.

Sections 3.1 to 3.4 of Thesis have been published as the following article.

Article

# Impacts of Traverse Speed and Material Thickness on Abrasive Waterjet Contour Cutting of Austenitic Stainless Steel AISI 304L

Jennifer Milaor Llanto , Majid Tolouei-Rad, Ana Vafadar  and Muhammad Aamir 

School of Engineering, Edith Cowan University, Joondalup, WA 6027, Australia; m.rad@ecu.edu.au (M.T.-R.); a.vafadarshamasbi@ecu.edu.au (A.V.); m.aamir@ecu.edu.au (M.A.)

\* Correspondence: j.llanto@ecu.edu.au

**Abstract:** Abrasive water jet machining is a proficient alternative for cutting difficult-to-machine materials with complex geometries, such as austenitic stainless steel 304L (AISI304L). However, due to differences in machining responses for varied material conditions, the abrasive waterjet machining experiences challenges including kerf geometric inaccuracy and low material removal rate. In this study, an abrasive waterjet machining is employed to perform contour cutting of different profiles to investigate the impacts of traverse speed and material thickness in achieving lower kerf taper angle and higher material removal rate. Based on experimental investigation, a trend of decreasing the level of traverse speed and material thickness that results in minimum kerf taper angle values of  $0.825^\circ$  for machining curvature profile and  $0.916^\circ$  for line profiles has been observed. In addition, higher traverse speed and material thickness achieved higher material removal rate in cutting different curvature radii and lengths in line profiles with obtained values of  $769.50 \text{ mm}^3/\text{min}$  and  $751.5 \text{ mm}^3/\text{min}$ , accordingly. The analysis of variance revealed that material thickness had a significant impact on kerf taper angle and material removal rate, contributing within the range of 69–91% and 62–69%, respectively. In contrast, traverse speed was the least factor measuring within the range of 5–18% for kerf taper angle and 27–36% for material removal rate.

**Keywords:** abrasive waterjet machining; contour cutting; traverse speed; material thickness; austenitic stainless steel; kerf taper angle; material removal rate



**Citation:** Llanto, J.M.; Tolouei-Rad, M.; Vafadar, A.; Aamir, M. Impacts of Traverse Speed and Material Thickness on Abrasive Waterjet Contour Cutting of Austenitic Stainless Steel AISI 304L. *Appl. Sci.* **2021**, *11*, 4925. <https://doi.org/10.3390/app11114925>

Academic Editor: Mark Jackson

Received: 6 May 2021

Accepted: 25 May 2021

Published: 27 May 2021

**Publisher's Note:** MDPI stays neutral with regard to jurisdictional claims in published maps and institutional affiliations.



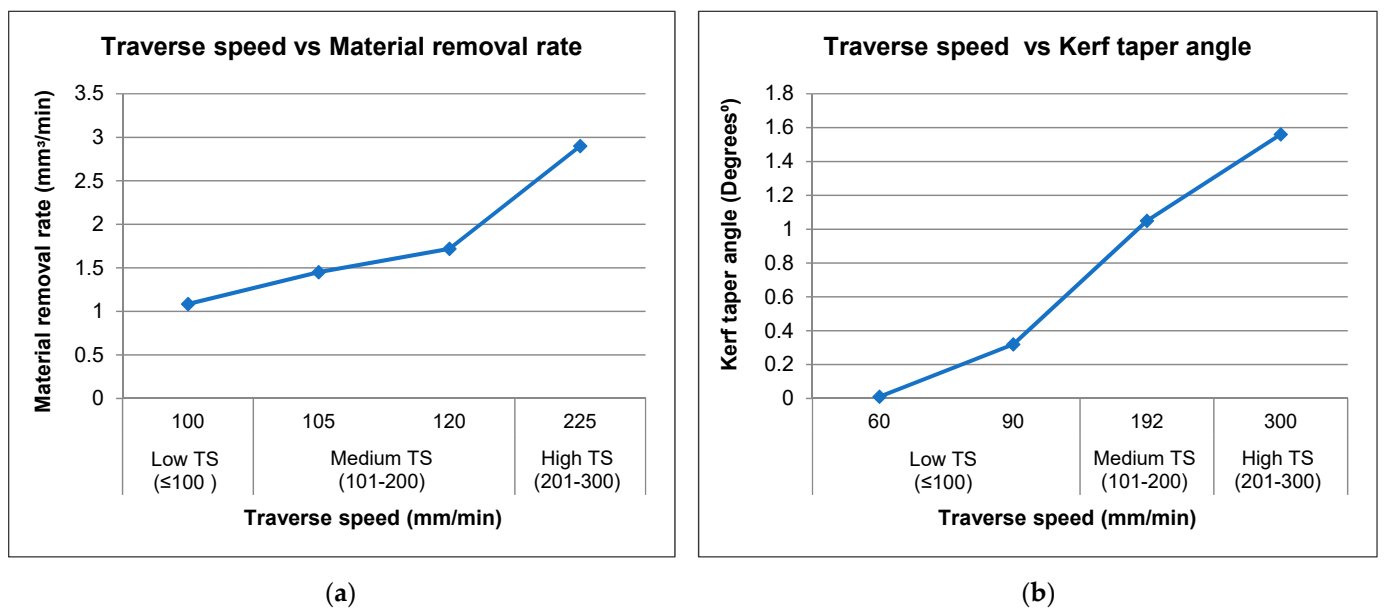
**Copyright:** © 2021 by the authors. Licensee MDPI, Basel, Switzerland. This article is an open access article distributed under the terms and conditions of the Creative Commons Attribution (CC BY) license (<https://creativecommons.org/licenses/by/4.0/>).

## 1. Introduction

Austenitic stainless steel 304L (AISI 304L) possesses excellent forming and welding characteristics, which has led to its broad application in industries such as automotive, shipbuilding and marine, material handling equipment, automotive parts, as well as construction materials [1]. AISI 304L is widely used in various thickness in the fabrication industry and in many cases requires contour machining to achieve complex and complicated profiles. However, AISI 304L is a difficult-to-cut material due to its high alloying content (i.e., chromium and nickel), low thermal conductivity, high ductility, and low machinability level [1]. Therefore, when cutting AISI 304L, it can be challenging to choose an alternative to achieve precise cutting without compromising metallurgical properties. Although various non-conventional technologies have been applied to cut stainless steel, such as a laser beam machines; this technology often has a high thermal distortion that alters metallurgical properties of the workpiece [2]. Abrasive waterjet machining (AWJM) is one of these advanced technologies that has been a popular method for cutting metallic and heat-sensitive materials due to several advantages, such as the absence of heat-affected zone (HAZ) and no changes in material properties [3]. AWJM can cut both hard and delicate materials with a wide range of thicknesses with a very low machining force, preventing the destruction of the properties of the target workpiece [4]. Moreover, whilst AWJM is also considered environmentally friendly and sustainable as it does not omit any

hazardous vapours; hence, AWJM produces waste abrasives that affect the environment. Accordingly, recycling or reusing of these abrasives has the potential to resolve ecological issues and concerns relating to AWJ application [5–7].

Abrasive waterjet machining is comprised of several input process parameters that ultimately determine the efficiency and quality of the machining processes. These parameters are generally categorised as hydraulic, abrasives, cutting and mixing, and acceleration [8]. Whilst AWJM demonstrates capability in cutting difficult-to-machine materials, they still experience some challenges. There have been reported issues in material response to AWJM concerning its behaviour, such as kerf tapering and low material removal, since the beginning of its applications. Kerf taper is the tapering angle generated during the AWJM process associated with the variation of kerf widths, which involves cut width of the material at the top and bottom [9,10]. Further, materials like AISI 304L have a relatively low material removal rate due to their relative machinability. The material removal rate in an AWJM for ductile materials like stainless steel is facilitated by a combination of cutting wear and deformation wear mechanism [9]. This involves determining the quantity of removed material from the workpiece per unit time, where the literature reveals that varied studies have been conducted on the effects of different parameters on the quality and efficiency of abrasive waterjet cutting performance. Therefore, an appropriate combination of AWJM input parameters, such as waterjet pressure, traverse speed, and mass rate of abrasive particles is important to achieve the required machining efficiency and material surface qualities [3]. For instance, Miao, et al. [11] studied quality defects such as kerf taper, cutting residue, and striation in AWJ cutting of AISI 304. Their study postulated that decreasing the jet energy is the cause of quality defects. Mohamad et al. [12] investigated the kerf taper angle generated in AWJ cutting of AISI 1090 mild steel with results indicating that the ratio of kerf taper increases at a higher level of standoff distance. They established that abrasive particles have higher kinetic energy at higher standoff distance leading to wider kerf taper angles; moreover, these particles gradually lose their kinetic energy as it moves towards from jet entry up to the exit. Kavya et al. [13] reported that the most influential parameters for MRR in AWJM of Al7075-TiB2 were traverse speed and abrasive mass flow rate. In their study, traverse speed is the most influential factor in achieving higher volumetric MRR. Ishfaq et al. [14] studied how traverse speed and abrasive mass flow rate are significant parameters for material removal rate, where traverse speed is considered the most influencing factor on AWJM of stainless-clad steel workpieces. Babu et al. [15] concluded that a slower feed rate allows more abrasives to strike the material and its jet does not drop much of its energy during the machining process, resulting in a lower kerf taper angle and surface roughness on abrasive waterjet cutting of AISI 1018 with 5 mm thickness. Thakkar et al. [16] investigated the effect of traverse speed, abrasive mass flow rate, and standoff distance on material removal rate in abrasive waterjet cutting of mild steel. Their experimental results showed that a higher traverse speed and abrasive mass flow rate increased the material removal rate. Moreover, a higher traverse speed has been shown to decrease kerf taper in AWJM straight line of AISI 304 [17]. Traverse speed regulates the quality of cut surfaces generated by AWJM applications, measured in mm/min [3]. Challenges of material reactions to AWJM have been investigated since the inception of this technique, where they continue to be studied, with regards to performance, including low material removal rate and distorted kerf geometries when employing varied traverse speed levels. A summary of experimental results obtained from several reviewed studies that investigated the impact of traverse speed on MRR and KTA in different metals in AWJM i.e., TRIP steel sheets, AISI 304, AISI 1018 and Inconel 600 is given in Figure 1 [8,15,18–22].



**Figure 1.** Statistics of impacts of traverse speed in (a) Material removal rate and (b) Kerf taper angle AWJ straight line cutting of various metals [8,15,18–22].

It is evident from Figure 1 that a lower kerf taper angle can be attained by utilising a lower traverse speed, whereas a higher rate of material removal can be obtained by increasing traverse speed. Accordingly, traverse speed is directly proportional to the material removal rate but inversely proportional to kerf taper [23]. Previous studies have applied specific material thicknesses in their AWJM experiments. However, in stainless steel fabrication industries, cutting involves different thicknesses for product formation, where it is necessary to investigate the influence of material thickness in precise AWJ cutting. Khan et al. [22] conducted machinability study in cutting low alloy steel of different thicknesses (5, 10, 15, 20 mm). Their experiments reported that material thickness impacts machine performance, including aspects of material removal rate, surface roughness, and kerf wall inclination. Further, their study showed that increasing the thickness of the material requires a higher traverse speed and water jet pressure in order to achieve better results. Additionally, Kechagias et al. [8] investigated the influence of sheet thickness, nozzle diameter, standoff distance, and traverse speed to kerf geometry and surface roughness in AWJM of transformation-induced plasticity (TRIP) sheet steel with varied thickness of 0.9 and 1.25 mm. They concluded that for higher thickness material, decreased kerf width and roughness can be achieved by applying a low standoff distance, a lower rate of traverse speed, and by using a smaller nozzle diameter. This could be due to the combination of high-level standoff distance and high rate traverse speed that effectively lower the contact time of abrasive particles within the cutting process.

The literature to date indicates that AWJM experiments and studies have been used specifically in relation to cutting straight line profiles, with only limited investigations regarding the machining of complicated shapes, such as curves with differing radii. Further, the cutting of complex geometries is more frequently applied in manufacturing industries than straight-slit or linear cutting [24]. Due to the taper and deceleration of a jet inside the kerf, challenges such as deformation of the material during the machining process can arise, particularly when cutting corners and curvature [25]. Therefore, this research gap requires further investigation.

AWJM is extensively used in the metal fabrication industry due to its capability to generate contours. This technology can produce contours due to their unidirectional cutting path system [26]. In addition, contour cutting is much more commonly applied rather than straight-slit cutting for metal product formation. Contour cutting involves various convex and concave arcs that make the process more challenging when compared to linear cutting.

To achieve precision in contour cutting, proper management of the process parameters are essential. In this research, austenitic stainless steel grade 304L material is utilised to examine the performance of abrasive waterjet contour-cutting. Key variables, such as material thickness and traverse speed, were considered in addressing issues relating to the differing radii of curvature, acute edges, and straight cutting path of AWJM.

## 2. Materials and Methods

In this work, AISI 304L was investigated. Austenitic stainless steel grades, such as 304L, are characterised as the most corrosion-resistant among other steel grades with high formability, ductility, and weldability because they contain a high percentage of chromium and nickel content [1]. This is the reason behind gaining higher volumes in a variety of manufacturing settings. This rising market demand has led to further studies aimed at achieving greater efficiency in the quality of cut during the machining process of abrasive waterjet.

The chemical composition and mechanical properties of AISI 304L are detailed in Table 1. The material thicknesses applied within this study were 4, 8, and 12 mm, with a uniform gap to observe the relative differences in AWJM behaviour towards this material. This experiment was conducted on an abrasive waterjet contour-cutting operation to investigate the impacts of traverse speed.

**Table 1.** Chemical and mechanical properties of AISI 304L in wt%.

Chemical	Carbon	Silicon	Manganese	Phosphorus	Sulphur	Nickel	Chromium	Nitrogen
Mechanical	0.03	0.75	2.00	0.045	0.03	8.00–0.50	18–20	0.10
	0.2% Proof Stress			205	Elongation%			40
	Tensile Strength <i>Mpa</i>			520–750	Hardness Brinell (HB) Max			202

An abrasive waterjet machine, model OMAX MAXIEM 1515, was used for contour cutting of the AISI 304L material. The machine has a built-in PC-based CAD/CAM with many distinct programming features including: adjustment of cutting model; six levels of quality; estimating the time needed for machining; generating data and reports; forming and tracking several sites, and rotating, ascending, reversing, and counterpoising. The specifications of the machine are further detailed in Table 2 and the corresponding set-up for experiments is illustrated in Figure 2 [23].

**Table 2.** Abrasive Waterjet Machine MAXIEM 1515 (OMAX Corp., Kent, WA, USA) specifications.

Parameters	Range
Max Pressure (MPa)	413.7 (4137 bar)
Max Traverse Speed (mm/min)	12,700 (500 in/min)
Table Size (L × W) (mm)	2235 × 1727
XY Cutting Envelope (mm)	1575 × 1575
Z-Axis travel (mm)	305
Max cut depth (mm)	152 (6 in) of mild steel

As presented in Figure 2a, the abrasive waterjet machine generates high-pressure water from the pump machine, which is then driven to the nozzle system. The nozzle system includes an abrasive hopper, an orifice, a mixing chamber, and a focusing tube. The water, travelling with a high level of velocity, is forced out of the orifice in a very thin stream structure [27]. The hopper consists of a plastic tube holding the abrasive particles and dispensing them to the cutting head, where the abrasive particles are drawn into a waterjet stream in the mixing chamber. The high-speed waterjet together with the abrasive particles are then mixed and accelerated to create an abrasive waterjet [27].

The workpiece is secured in a clamping tool to hold it in position during machining, as shown in Figure 2b. This is done to preclude the possibility of deflection during cutting





The input parameters selected in this study were traverse speed and material thickness, while waterjet pressure, abrasive mass flow rate, standoff distance, abrasive type, and mesh number were held constant. Three levels of material thickness and traverse speed were applied, as shown in Table 4. The selection of variable parameters, and the assignment of levels, was made following an intensive review of current research data. Input parameter settings were constantly redefined, due to limitations with the machine and/or constraints in effectiveness shown in previous AWJM experiments [8,15,18–22]. The input parameters that were kept constant during the tests are shown in Table 5.

**Table 4.** Variable input parameters values.

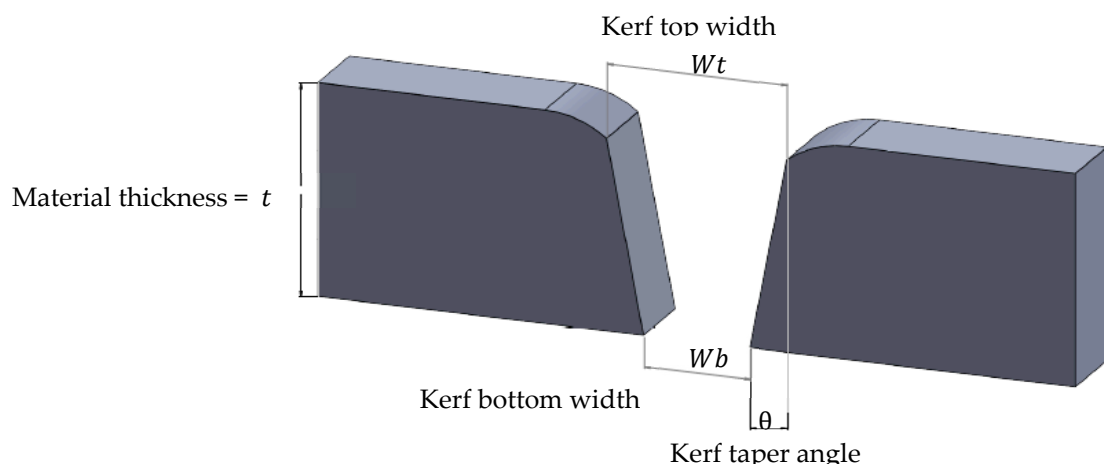
Parameters	Level 1	Level 2	Level 3
Material thickness, (mm)	4	8	12
Traverse speed, (mm/min)	90	120	150

**Table 5.** Constant input parameters values.

Parameters	Values
Orifice diameter (mm)	0.28
Nozzle/focusing diameter (mm)	0.56
Abrasive type	Garnet
Abrasive mesh number (#)	80
Waterjet pressure (MPa)	275
Abrasive mass flow rate (g/min)	300
Standoff distance (mm)	1.5

The performance of AWJM is determined by the amount of material removed from the target workpiece and by the accuracy of the geometry of the cut relying on the kerf width and taper angle [32]. Therefore, the kerf taper angle and material removal rate have been selected for consideration as output parameters in this study. Kerf taper angle resulting from abrasive waterjet contour cutting is measured according to the proportion of the sum of kerf top width and kerf bottom and thickness of the workpiece [10]. Kerf width refers to the ratio of entry and exit cut width. Kerf width dimensions are measured on the top as well as bottom by using an optical microscope, model LEICA M80, with a precision scale of 100  $\mu\text{m}$ . Equation (1) was utilised to calculate the kerf taper angle following abrasive waterjet cutting of AISI 304L [33]. A scheme of the applied kerf geometries is illustrated in Figure 3 [14].

$$\text{Kerf Taper Angle } \theta = \text{Arctan} \frac{W_t - W_b}{2t} \quad (1)$$



**Figure 3.** Scheme of AWJM kerf geometries.



The material removal rate, which is the volume of material removed from the material per unit of time, is measured by kerf width, traverse speed, and depth of cut. The material removal rate was calculated using Equation (2) [32]:

$$MRR = h_t \cdot W \cdot V_f \quad (2)$$

wherein:  $W = \frac{Wt+Wb}{2}$

Finally, analysis of variance (ANOVA) was applied to quantify the influence of the selected variable parameters. The ANOVA was employed to identify the significant effect of input parameters and their corresponding levels [34]. ANOVA was performed with a confidence interval of 95%, which has typically been applied in several related studies. The confidence interval determines how precise the estimated statistics are, whereby a 95% confidence interval denotes a 5% chance of having an incorrect estimation [35,36]. The percentage contribution assesses the effect of each input parameter on the output, where  $p$ -values estimated at more than 0.05 or 5%, are considered insignificant [37].

### 3. Results and Discussion

#### 3.1. Kerf Top Width and Bottom Results


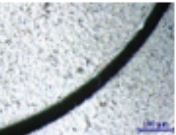
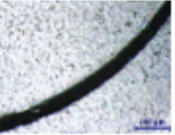

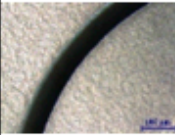
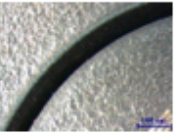
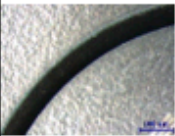
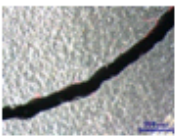
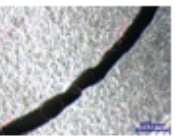
Figure 4 shows microscopic observations of AISI 304L with a thickness of 4, 8, and 12 mm at traverse speeds of 90, 120, and 150 mm/min, where kerf geometries such as kerf top width, and kerf bottom width. It can be seen from Figure 4 that aspects of the cut have irregular shapes, whereas material thickness increases cut quality deterioration at the bottom cut. The microscopic observation also revealed that increasing traverse speed generates a wider kerf top width than kerf bottom width. Kerf geometric inaccuracies imparted to machined samples are more prominent with higher material thickness. AWJM transpires through an erosion process where abrasives are suspended in a high velocity of water jet stream, leading in increasing acceleration of the abrasive particles [9]. The kinetic energy impingement and collisions of these abrasive particles gradually decrease during cutting resulting in incremental kerf taper angle as the material thickness increases. The initial collision of the abrasive particle towards the workpiece generates forces that are greater than the crushing load, causing particles to become fractured and reduced during the cutting process. Accordingly, denser abrasive particles move towards the target material and decrease forces, causing a narrowing of the kerf at the bottom part [3].

The results summarised in Table A1 of the Appendix A section represent the average values of kerf top and bottom widths obtained by conducting three contour cutting runs for each profile cut. Regardless of whether cut geometry occurred in arcs or a straight profile, lowering of the kerf at the exit cut dimension and irregularities of shape were observed. The experimental results reveal a reduction in the dimensions of both the top and bottom kerf widths. This differentiation between top and bottom kerf width was observed to increase as a higher traverse speed rate was employed. Figure 5 demonstrates the percentage rate of change in the narrowing top and bottom kerf widths for AWJM of AISI304L, with thicknesses of 4, 8, and 12 mm.

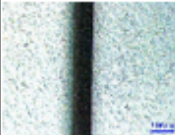
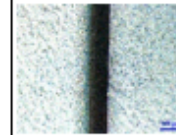


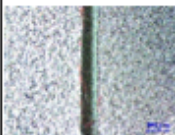
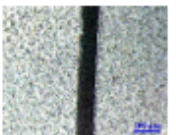
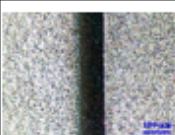


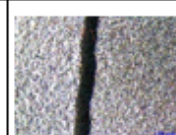
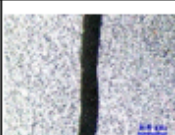





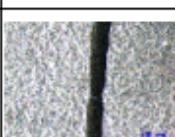
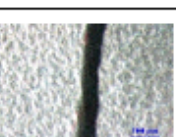
The experimental data obtained from cutting twelve different profiles at three varying levels of material thickness expressed similar results, indicating that a lower traverse speed is more favourable to use than a higher level. The difference between the top and bottom kerf width obtained is at the highest percentage ranging from 33–34% when employing a rate of 150 mm/min traverse speed. A slower traverse speed rate of 90 mm/min showed better results with a percentage rate ranging from 31–33%.

The kinetic energy of the abrasive particles is particularly high on first impact, though it gradually decreases during the machining process [14]. The narrowing of the top and bottom kerf widths is directly dependent on a decreasing amount of abrasive particles used during the machining process. In this work, a lower rate of traverse speed at 90 mm/min amounted to lower variation in kerf widths as compared to a higher rate of 120–150 mm/min. A lower gap in the kerf width geometry indicates better performance in AWJ cutting operations. The explanation for this is that a low traverse speed rate carries a

vast number of abrasive particles that can impinge on the target workpiece [9]; whereas a faster or higher traverse speed reduces the number of abrasive particles that execute cutting operations or machining motions [33].

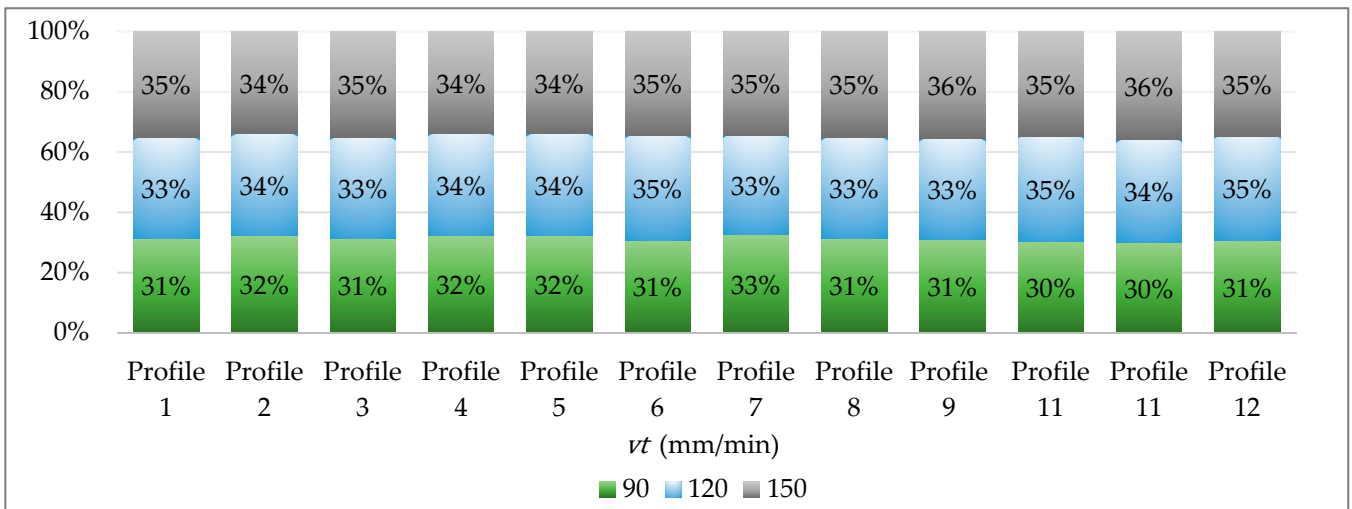
Output		Kerf Top Width			Kerf Bottom Width		
Traverse speed mm/min		90	120	150	90	120	150
Material thickness (mm)	4						
	8						
	12						

(a) Arcs profile

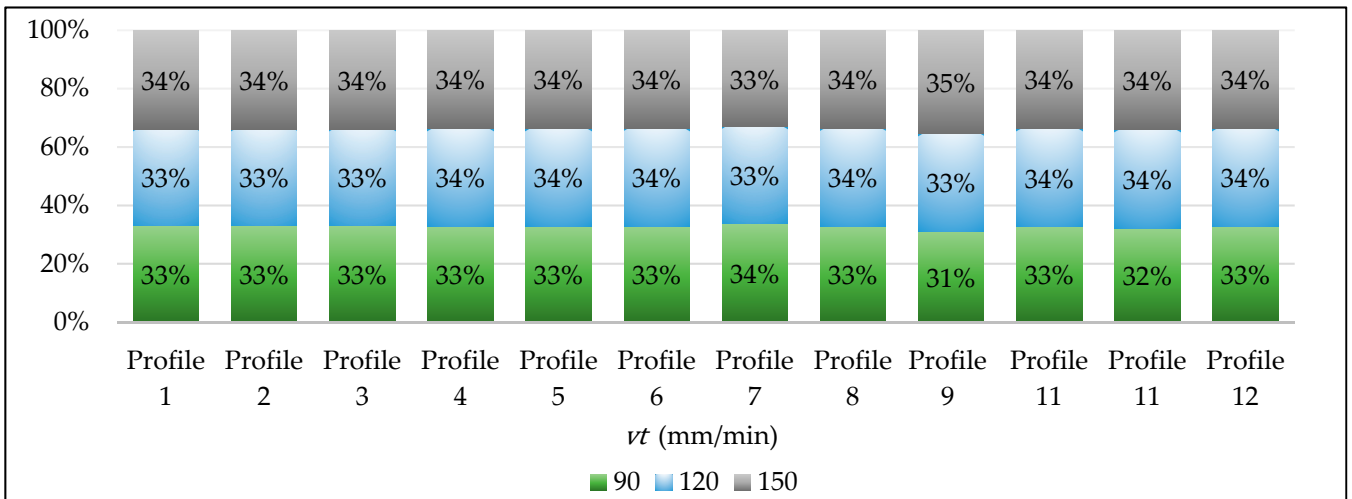
Output		Kerf Top Width			Kerf Bottom Width		
Traverse speed mm/min		90	120	150	90	120	150
Material thickness (mm)	4						
	8						
	12						

(b) Straight profile

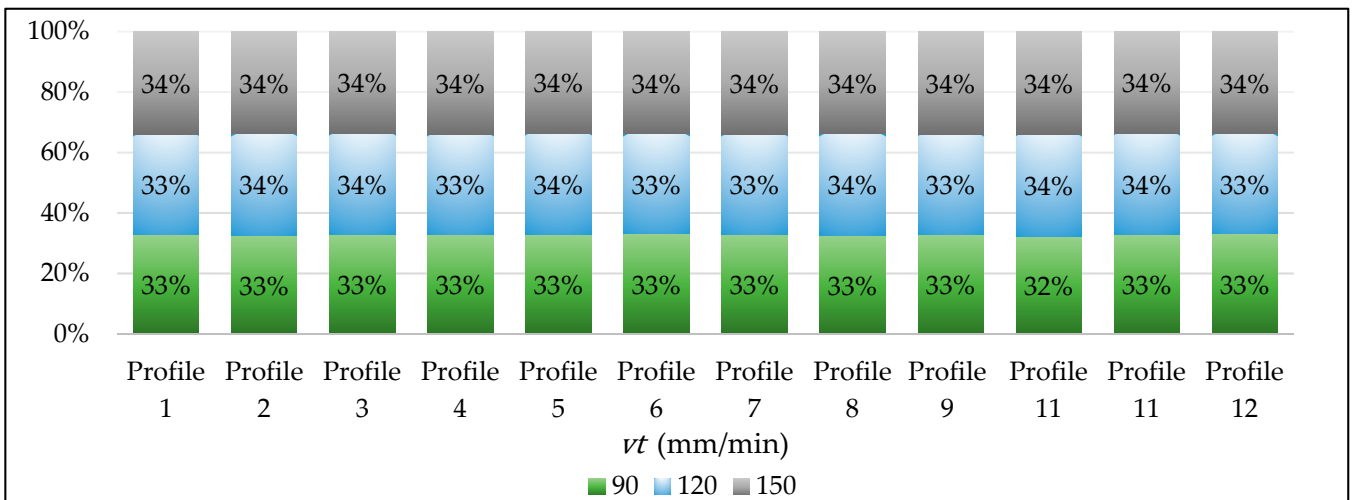
Figure 4. Sample of kerf width images of arcs and straight profiles cut in 100 μm.



(a)



(b)



(c)

**Figure 5.** Percentage of variation between top and bottom kerf widths for AISI 304L with material thickness of (a) 4 mm, (b) 8 mm, and (c) 12 mm.

### 3.2. Analysis of Kerf Taper Angle

Figure 6 shows the Kerf taper angles obtained in abrasive waterjet profile cutting of AISI 304L, where the experiment ranged from  $0.825^\circ$  to  $1.550^\circ$  for 4 mm,  $1.092^\circ$  to  $1.575^\circ$  for 8 mm, and  $1.235^\circ$  to  $1.660^\circ$  for 12 mm material thicknesses with traverse speed levels of 90, 120, and 150 mm/min. Gradual machining with a low level of traverse speed of 90 mm/min achieved the smallest kerf taper angle value of  $0.825^\circ$  for 4 mm,  $1.092^\circ$  for 8 mm, and  $1.235^\circ$  for 12 mm material thicknesses. For materials such as stainless steel, a disparity in taper cut is due to deformation-induced from ductile material during machining operations [25]. The formation of kerf taper inherent in AWJM is due to the changing conditions at the interface. Kerf tapering has been observed at the entrance and exit of the jet, initiated by low energy abrasive particles suspended at the exterior of the coherent jet [38]. It has been noted in findings by Wang et al. [39] that kerf taper correlates with traverse speed and material thickness.

In this research study, the values of KTA were visibly higher at 8 and 12 mm thickness than 4 mm AISI 304L. The results indicate that kerf geometry inaccuracies within machined AISI 304L can be recognised at a higher or increasing traverse speed. Initially, these abrasive particles have high kinetic energy and gradually decrease along with the cutting operation; thus, as material thickness increases, the kinetic energy continuously reduces, causing a higher tapering angle [14]. With the feature of abrasive particles, a lower traverse speed increased the influence of cohesion on metal material to create kerf taper angles.

### 3.3. Material Removal Rate Results and Analysis

In accordance with review of the obtained data, Figure 7 presents a graphical analysis of the behaviour of material removal rate towards different traverse speed and material thickness in abrasive waterjet profile cutting of AISI 304L.

In this study, the lowest value of KTA of  $0.825^\circ$  for arcs profile and  $0.916^\circ$  for straight profile were achieved at the lowest level of traverse speed at 90 mm/min rate. The maximum value of MRR of  $769.50 \text{ mm}^3/\text{min}$  was obtained from machining of curvature profile and  $751.50 \text{ mm}^3/\text{min}$  achieved when cutting straight line profiles at a higher value of traverse speed at 150 mm/min rate. A similar trend linking increased levels of input parameters with increasing values for output parameters has been observed for both curvature (i.e., arcs and straight line profiles) and different thicknesses of materials. The process of material removal for AWJM in ductile material, such as steel, takes place through erosion caused by impinging abrasive particles from the waterjet stream. Hence, higher kinetic energy generates higher erosion rates and leads to higher material removal rate. With a higher level of traverse speed, the machining rate increases, resulting in more material being removed from the workpiece. In turn, the material removal rate is noted to be mainly influenced by traverse speed, where these findings accord with previous studies [16]. In this work, the amount of material removed increased by approximately 60–80% as the value of material thickness increased from 4 mm to 12 mm. The study showed that a higher material thickness obtained a higher value of MRR  $346.50 \text{ mm}^3/\text{min}$  for 4 mm,  $612.00 \text{ mm}^3/\text{min}$  for 8 mm, and  $769.50 \text{ mm}^3/\text{min}$  for 12 mm material thickness of AISI 304L material. The results also show that traverse speed is an essential factor in obtaining a higher material removal rate, demonstrating a direct proportional trend to MRR.

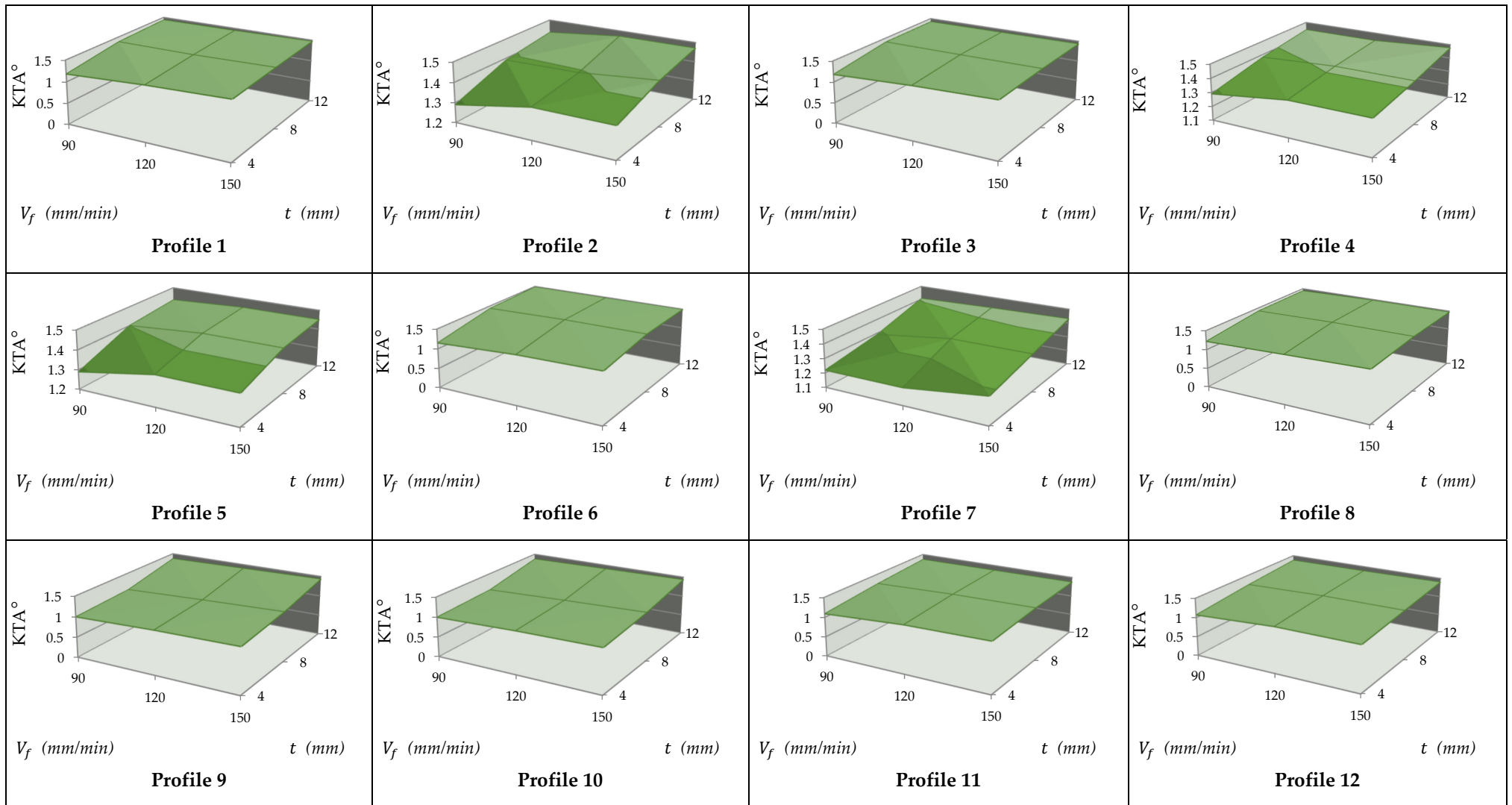
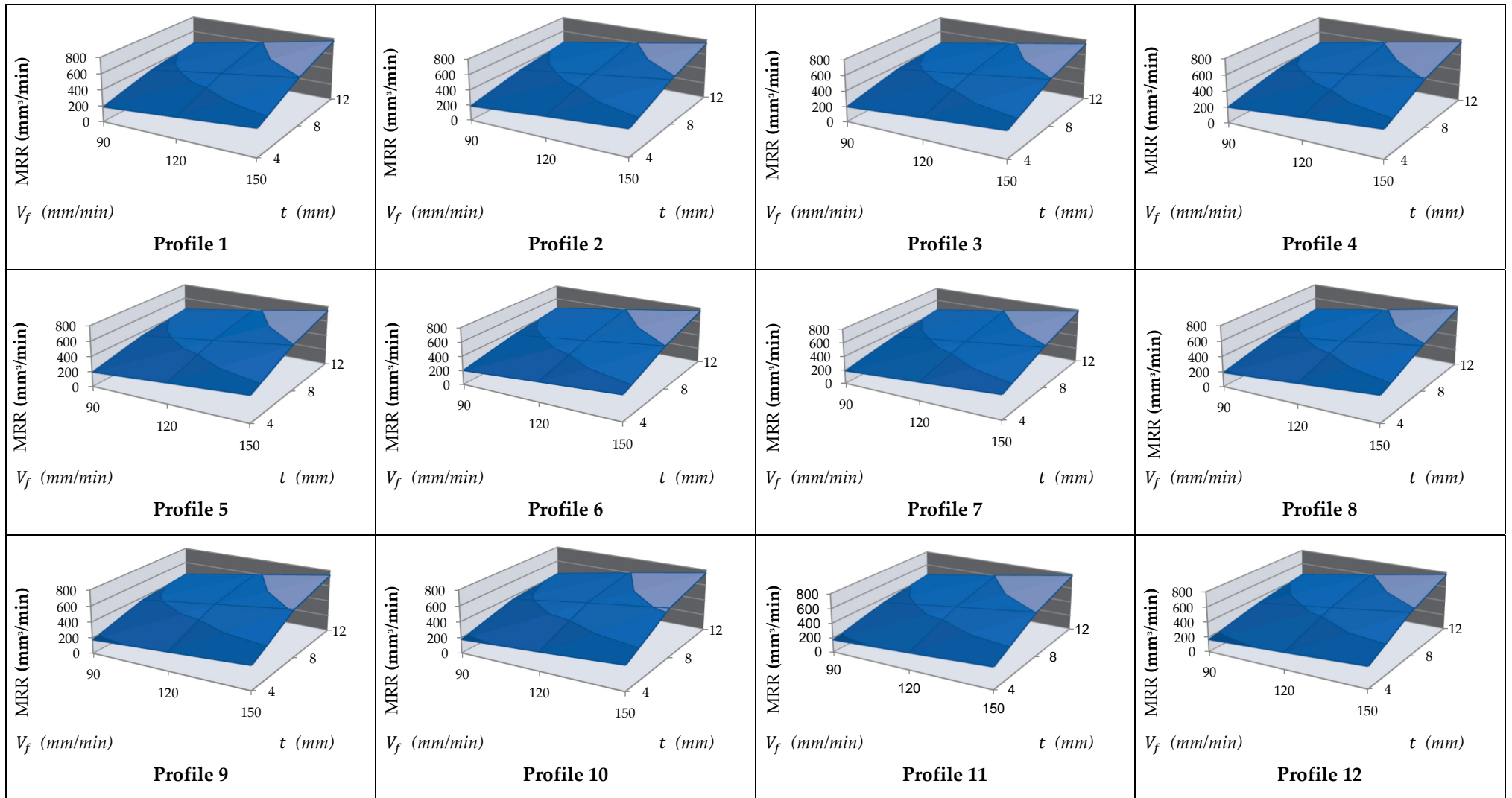


Figure 6. Impacts of material thickness and traverse speed on Kerf taper angle in AWJ profile cutting of AISI304L.





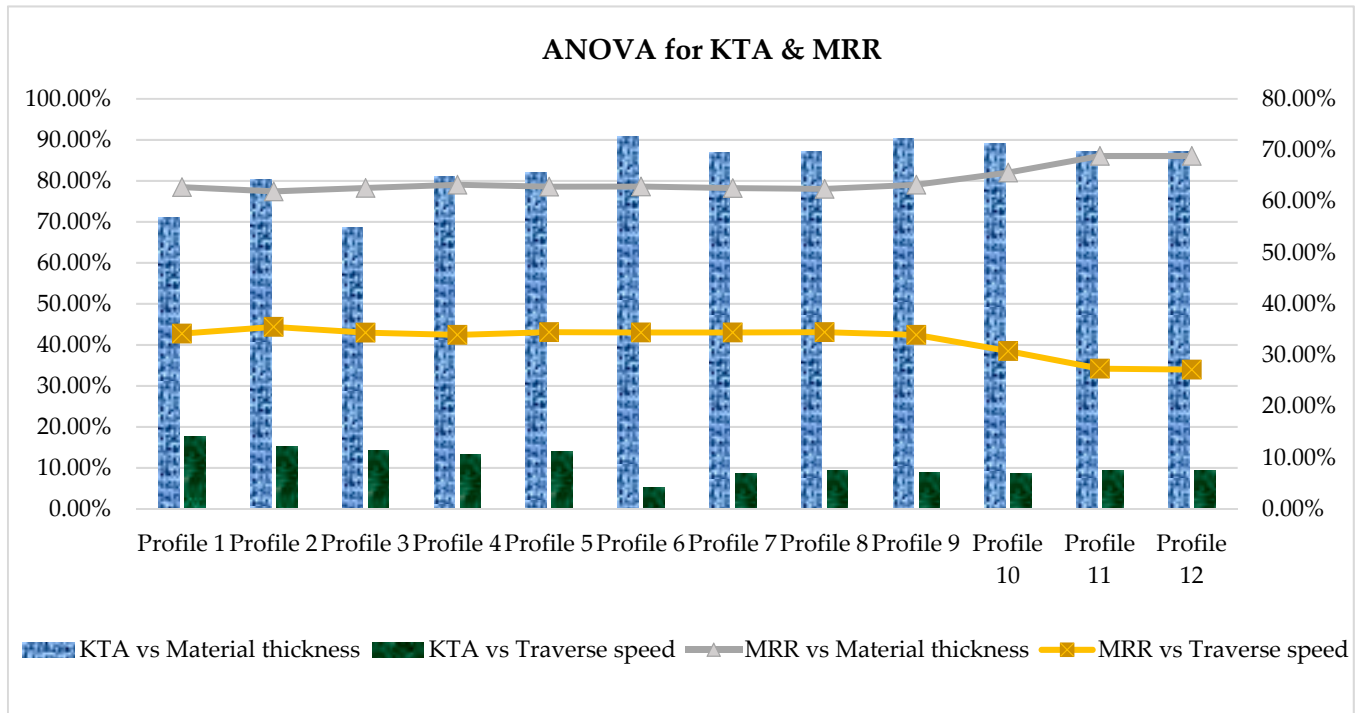
Material removal rate: MRR (mm<sup>3</sup>/min), Traverse speed:  $V_f$  (mm/min), Material thickness:  $t$  (mm)

Figure 7. Impacts of material thickness and traverse speed towards material removal rate in AWJ profile cutting of AISI304L.

### 3.4. Statistical Analysis

#### Analysis of Variance for Kerf Taper Angle and Material Removal Rate

Analysis of variance (ANOVA) was performed to validate kerf taper angle and material removal rate from the machining twelve profile, as given in Figure 8.



Kerf taper angle: KTA ( $^{\circ}$ ), Material removal rate: MRR ( $\text{mm}^3/\text{min}$ )

**Figure 8.** ANOVA results of KTA and MRR for AWJ contour cutting of AISI 304L with varied thickness.

The ANOVA results in Figure 8 denote that the percentage contribution of material thickness on kerf taper angle ranges from 69–91% with 5–18% for traverse speed. The kerf tapering results show the proportion of kerf top width to kerf bottom width. The variation between the top and bottom geometries denotes a higher kerf tapering. Kerf top or entry width is relatively higher than the exit width because the kinetic energy of abrasive particles is primarily at a high level and consistently decreases during the machining process [15]. An increase in material thickness denotes prolonged cutting operations, which continuously decrease the kinetic energy of abrasive particles, producing a higher taper angle.

Figure 8 also shows the material removal rate obtained under variable conditions. The percentage contribution of material thickness on material removal rate ranges from 62–69%, with 27–36% for traverse speed. According to this statistical analysis, material thickness directly influences the measured output parameter in this case. Referring to ANOVA Tables A2 and A3 in the appendices, the obtained  $p$ -values are less than 0.05. Therefore, the impacts of material thickness and traverse speed are statistically significant.

In AWJ cutting, machining is fundamentally executed by the cohering action produced through impact by a number of abrasive particles travelling at high velocity, towards a workpiece [14]. As a result, material removal rate and thickness are directly proportional, where it becomes possible to achieve higher MRR even when machining samples with increasing thickness.

## 4. Conclusions

In this experimental study, an abrasive waterjet machining application was investigated for contour cutting of AISI 304L. The impact of traverse speed and material thickness

on kerf geometries and material removal rate was examined, enabling the application to achieve precise and higher efficiency in cutting. AWJM exhibits similar behaviour in cutting curvature and straight line profiles of AISI 304L workpieces, in terms of kerf geometries and rate of material removal responses; thus, a minimum kerf taper angle value of  $0.825^\circ$  and maximum MRR of  $769.50 \text{ mm}^3/\text{min}$  were obtained from machining of curvature profile, whereas a minimum of  $0.916^\circ$  KTA and maximum of  $751.5 \text{ mm}^3/\text{min}$  occurred when cutting straight line profiles. The cutting performance of AWJM was found to achieve better kerf geometries at a lower rate of traverse speed. However, a higher traverse speed was shown to be more effective in achieving a higher MRR. It was also observed that a traverse speed of  $90 \text{ mm}/\text{min}$  provided the lowest KTA values of  $0.825^\circ$  or  $4 \text{ mm}$ ,  $1.092^\circ$  for  $8 \text{ mm}$ , and  $1.235^\circ$  for  $12 \text{ mm}$  material thickness. A higher traverse speed rate of  $150 \text{ mm}/\text{min}$  obtained the maximum values of MRR  $346.5 \text{ mm}^3/\text{min}$  for  $4 \text{ mm}$ ,  $609.0 \text{ mm}^3/\text{min}$  for  $8 \text{ mm}$ , and  $769.5 \text{ mm}^3/\text{min}$  for  $12 \text{ mm}$  thickness of AISI 304L material. Both traverse speed and material thickness were shown to impact the quality of cut regardless of the cutting profile; however, the material thickness was more influential than traverse speed. Using analysis of variance, the material thickness generated a contribution ranging from 69–91% in kerf taper angle and 62–69% for material removal rate, whereas traverse speed was revealed to obtain a percentage contribution ranging from 5–18% in kerf taper angle and 27–36% for MRR.

**Author Contributions:** Conceptualization, M.T.-R., A.V., and J.M.L.; methodology, investigation and writing original draft, J.M.L.; review and supervision, M.T.-R., A.V., and M.A.; editing, and project administration, M.A. and J.M.L. All authors have read and agreed to the published version of the manuscript.

**Funding:** This research received no external funding.

**Institutional Review Board Statement:** Not applicable.

**Informed Consent Statement:** Not applicable for studies not involving humans.

**Acknowledgments:** The authors would like to thank the School of Engineering, Edith Cowan University, Australia, for providing and administering the needed requirements in accomplishing this research and open access funding support.

**Conflicts of Interest:** The authors declare no conflict of interest.

## Abbreviations

The following abbreviations and nomenclatures are used in this paper:

$h_t$	Depth of penetration
$V_f$	Traverse speed
$W$	Kerf width
$W_t$	Kerf top width
$W_b$	Kerf bottom width.
$t$	Thickness of the material
AISI	Austenitic stainless steel
ANOVA	Analysis of variance
AWJ	Abrasive waterjet
AWJM	Abrasive waterjet machining
KTA	Kerf taper angle
MRR	Material removal rate



## Appendix A

Table A1. Kerf top width and kerf bottom width results.

Material Thickness (mm)	Traverse Speed (mm/min)	Profile 1		Profile 2		Profile 3		Profile 4	
		Wt (mm)	W <sub>b</sub> (mm)	Wt (mm)	W <sub>b</sub> (mm)	Wt (mm)	W <sub>b</sub> (mm)	Wt (mm)	W <sub>b</sub> (mm)
4	90	0.61	0.44	0.62	0.44	0.63	0.46	0.64	0.46
4	120	0.64	0.46	0.67	0.48	0.66	0.48	0.67	0.48
4	150	0.67	0.48	0.68	0.49	0.67	0.48	0.68	0.49
8	90	0.68	0.29	0.67	0.28	0.69	0.3	0.69	0.3
8	120	0.69	0.3	0.68	0.29	0.69	0.3	0.7	0.3
8	150	0.7	0.3	0.69	0.29	0.7	0.3	0.71	0.31
12	90	0.7	0.1	0.7	0.1	0.69	0.1	0.71	0.11
12	120	0.72	0.11	0.72	0.1	0.71	0.11	0.73	0.12
12	150	0.74	0.12	0.73	0.11	0.72	0.12	0.74	0.12
Material Thickness (mm)	Traverse Speed (mm/min)	Profile 5		Profile 6		Profile 7		Profile 8	
		Wt (mm)	W <sub>b</sub> (mm)	Wt (mm)	W <sub>b</sub> (mm)	Wt (mm)	W <sub>b</sub> (mm)	Wt (mm)	W <sub>b</sub> (mm)
4	90	0.63	0.45	0.64	0.48	0.61	0.44	0.61	0.44
4	120	0.66	0.47	0.67	0.49	0.64	0.47	0.64	0.46
4	150	0.67	0.48	0.68	0.5	0.67	0.49	0.67	0.48
8	90	0.68	0.29	0.69	0.29	0.68	0.26	0.68	0.28
8	120	0.69	0.29	0.7	0.29	0.69	0.28	0.69	0.28
8	150	0.7	0.3	0.71	0.3	0.7	0.29	0.7	0.29
12	90	0.7	0.1	0.72	0.1	0.7	0.11	0.7	0.1
12	120	0.71	0.1	0.73	0.11	0.72	0.12	0.72	0.1
12	150	0.72	0.11	0.74	0.11	0.74	0.13	0.74	0.12
Material Thickness (mm)	Traverse Speed (mm/min)	Profile 9		Profile 10		Profile 11		Profile 12	
		Wt (mm)	W <sub>b</sub> (mm)	Wt (mm)	W <sub>b</sub> (mm)	Wt (mm)	W <sub>b</sub> (mm)	Wt (mm)	W <sub>b</sub> (mm)
4	90	0.56	0.42	0.56	0.42	0.55	0.4	0.54	0.39
4	120	0.57	0.42	0.58	0.42	0.56	0.39	0.55	0.38
4	150	0.58	0.42	0.6	0.44	0.58	0.4	0.56	0.39
8	90	0.66	0.36	0.67	0.34	0.65	0.3	0.63	0.28
8	120	0.67	0.35	0.69	0.35	0.68	0.31	0.65	0.29
8	150	0.68	0.34	0.69	0.35	0.69	0.32	0.67	0.31
12	90	0.69	0.12	0.67	0.11	0.69	0.13	0.69	0.12
12	120	0.7	0.12	0.71	0.12	0.71	0.14	0.7	0.13
12	150	0.71	0.12	0.72	0.13	0.72	0.15	0.72	0.14



## References

1. Kaladhar, M.; Subbaiah, K.V.; Rao, C.S. Machining of austenitic stainless steels—A review. *Int. J. Mach. Mach. Mater.* **2012**, *12*, 178–192. [[CrossRef](#)]
2. Supriya, S.B.; Srinivas, S. Machinability Studies on Stainless steel by abrasive water jet-Review. *Mater. Today Proc.* **2018**, *5*, 2871–2876. [[CrossRef](#)]
3. Liu, X.C.; Liang, Z.W.; Wen, G.L.; Yuan, X.F. Waterjet machining and research developments: A review. *Int. J. Adv. Manuf. Tech.* **2019**, *102*, 1337–1338. [[CrossRef](#)]
4. Sureban, R.; Kulkarni, V.N.; Gaitonde, V. Modern Optimization Techniques for Advanced Machining Processes—A Review. *Mater. Today Proc.* **2019**, *18*, 3034–3042. [[CrossRef](#)]
5. Babu, M.K.; Chetty, O.K. A study on recycling of abrasives in abrasive water jet machining. *Wear* **2003**, *254*, 763–773. [[CrossRef](#)]
6. Schramm, A.; Morczinek, F.; Götze, U.; Putz, M. Technical-economic evaluation of abrasive recycling in the suspension fine jet process chain. *Int. J. Adv. Manuf. Technol.* **2020**, *106*, 981–992. [[CrossRef](#)]
7. Aydin, G.; Kaya, S.; Karakurt, I. Effect of abrasive type on marble cutting performance of abrasive waterjet. *Arab. J. Geosci.* **2019**, *12*, 1–8. [[CrossRef](#)]
8. Kechagias, J.; Petropoulos, G.; Vaxevanidis, N. Application of Taguchi design for quality characterization of abrasive water jet machining of TRIP sheet steels. *Int. J. Adv. Manuf. Technol.* **2012**, *62*, 635–643. [[CrossRef](#)]
9. Natarajan, Y.; Murugesan, P.K.; Mohan, M.; Khan, S.A.L.A. Abrasive Water Jet Machining process: A state of art of review. *J. Manuf. Process.* **2020**, *49*, 271–322. [[CrossRef](#)]
10. Saravanan, S.; Vijayan, V.; Suthahar, S.J.; Balan, A.; Sankar, S.; Ravichandran, M. A review on recent progresses in machining methods based on abrasive water jet machining. *Mater. Today Proc.* **2020**, *21*, 116–122. [[CrossRef](#)]
11. Miao, X.; Qiang, Z.; Wu, M.; Song, L.; Ye, F. Research on quality improvement of the cross section cut by abrasive water jet based on secondary cutting. *Int. J. Adv. Manuf. Technol.* **2018**, *97*, 71–80. [[CrossRef](#)]
12. Mohamad, W.; Kasim, M.; Norazlina, M.; Hafiz, M.; Izamshah, R.; Mohamed, S. Effect of standoff distance on the kerf characteristic during abrasive water jet machining. *Results Eng.* **2020**, *6*, 100101. [[CrossRef](#)]
13. Kavya, J.; Keshavamurthy, R.; Kumar, G.P. Studies on parametric optimization for abrasive water jet machining of Al7075-TiB2 in-situ composite. In Proceedings of the IOP Conference Series: Materials Science and Engineering, Bangalore, India, 14–16 July 2016; p. 012024.
14. Ishfaq, K.; Ahmad Mufti, N.; Ahmed, N.; Pervaiz, S. Abrasive waterjet cutting of clad material: Kerf taper and MRR analysis. *Mater. Manuf. Process.* **2019**, *34*, 544–553. [[CrossRef](#)]
15. Babu, M.N.; Muthukrishnan, N. Exploration on Kerf-angle and surface roughness in abrasive waterjet machining using response surface method. *J. Inst. Eng. Ser. C* **2018**, *99*, 645–656. [[CrossRef](#)]
16. Thakkar, P.; Prajapati, P.; Thakkar, S.A. A machinability study of mild steel using abrasive water jet machining technology. *Int. J. Eng. Res. Appl.* **2013**, *3*, 1063–1066.
17. Sanghani, C.; Korat, M. Performance analysis of abrasive water jet machining process for AISI 304 stainless steel. *J. Exp. Appl. Mech.* **2018**, *8*, 53–55.
18. Uthayakumar, M.; Khan, M.A.; Kumaran, S.T.; Slota, A.; Zajac, J. Machinability of nickel-based superalloy by abrasive water jet machining. *Mater. Manuf. Process.* **2016**, *31*, 1733–1739. [[CrossRef](#)]
19. Rao, R.V.; Rai, D.P.; Balic, J. Multi-objective optimization of abrasive waterjet machining process using Jaya algorithm and PROMETHEE Method. *J. Intell. Manuf.* **2019**, *30*, 2101–2127. [[CrossRef](#)]
20. Kumar, K.R.; Sreebalaji, V.S.; Pridhar, T. Characterization and optimization of Abrasive Water Jet Machining parameters of aluminium/tungsten carbide composites. *Measurement* **2018**, *117*, 57–66. [[CrossRef](#)]
21. Kumbhar, M.A.D.; Chatterjee, M.; Student, M. Optimization of Abrasive Water Jet Machining Process Parameters Using Response Surface Method on Inconel-188. *Int. J. Recent Trends Eng. Res.* **2018**, *11*, 2455–2457.
22. Khan, M.A.; Gupta, K. Machinability Studies on Abrasive Water Jet Machining of Low Alloy Steel for Different Thickness. In Proceedings of the IOP Conference Series: Materials Science and Engineering, Sevastopol, WI, USA, 9–13 September 2019; p. 044099.
23. Llanto, J.M.; Tolouei-Rad, M.; Vafadar, A.; Aamir, M. Recent Progress Trend on Abrasive Waterjet Cutting of Metallic Materials: A Review. *Appl. Sci.* **2021**, *11*, 3344. [[CrossRef](#)]
24. Wang, J.; Liu, H. Profile cutting on alumina ceramics by abrasive waterjet. Part 1: Experimental investigation. *Proc. Inst. Mech. Eng. Part C J. Mech. Eng. Sci.* **2006**, *220*, 703–714. [[CrossRef](#)]
25. Hlavac, L.M.; Hlavacova, I.M.; Geryk, V.; Plancar, S. Investigation of the taper of kerfs cut in steels by AWJ. *Int. J. Adv. Manuf. Tech.* **2015**, *77*, 1811–1818. [[CrossRef](#)]
26. El-Domiatiy, A.; Shabara, M.; Abdel-Rahman, A.; Al-Sabeeh, A. On the modelling of abrasive waterjet cutting. *Int. J. Adv. Manuf. Technol.* **1996**, *12*, 255–265. [[CrossRef](#)]
27. Radovanović, M. Multi-objective Optimization of Process Performances when Cutting Carbon Steel with Abrasive Water Jet. *Tribol. Ind.* **2016**, *38*, 454–462.
28. Wang, S.; Zhang, S.; Wu, Y.; Yang, F. A key parameter to characterize the kerf profile error generated by abrasive water-jet. *Int. J. Adv. Manuf. Technol.* **2017**, *90*, 1265–1275. [[CrossRef](#)]

29. Pawar, P.J.; Vidhate, U.S.; Khalkar, M.Y. Improving the quality characteristics of abrasive water jet machining of marble material using multi-objective artificial bee colony algorithm. *J. Comput. Des. Eng.* **2018**, *5*, 319–328. [[CrossRef](#)]
30. Hlavac, L.M.; Hlavacova, I.M.; Arleo, F.; Vigano, F.; Annoni, M.P.G.; Geryk, V. Shape distortion reduction method for abrasive water jet (AWJ) cutting. *Precis. Eng.* **2018**, *53*, 194–202. [[CrossRef](#)]
31. Kumar, R.; Chattopadhyaya, S.; Dixit, A.R.; Bora, B.; Zelenak, M.; Foldyna, J.; Hloch, S.; Hlavacek, P.; Scucka, J.; Klich, J. Surface integrity analysis of abrasive water jet-cut surfaces of friction stir welded joints. *Int. J. Adv. Manuf. Technol.* **2017**, *88*, 1687–1701. [[CrossRef](#)]
32. Gnanavelbabu, A.; Saravanan, P.; Rajkumar, K.; Karthikeyan, S. Experimental Investigations on Multiple Responses in Abrasive Waterjet Machining of Ti-6Al-4V Alloy. *Mater. Today Proc.* **2018**, *5*, 13413–13421. [[CrossRef](#)]
33. Li, M.; Huang, M.; Chen, Y.; Gong, P.; Yang, X. Effects of processing parameters on kerf characteristics and surface integrity following abrasive waterjet slotting of Ti6Al4V/CFRP stacks. *J. Manuf. Process.* **2019**, *42*, 82–95. [[CrossRef](#)]
34. Aamir, M.; Tolouei-Rad, M.; Giasin, K.; Vafadar, A. Machinability of Al2024, Al6061, and Al5083 alloys using multi-hole simultaneous drilling approach. *J. Mater. Res. Technol.* **2020**, *9*, 10991–11002. [[CrossRef](#)]
35. Aamir, M.; Tolouei-Rad, M.; Giasin, K.; Vafadar, A. Feasibility of tool configuration and the effect of tool material, and tool geometry in multi-hole simultaneous drilling of Al2024. *Int. J. Adv. Manuf. Technol.* **2020**, *111*, 861–879. [[CrossRef](#)]
36. Aamir, M.; Tu, S.; Giasin, K.; Tolouei-Rad, M. Multi-hole simultaneous drilling of aluminium alloy: A preliminary study and evaluation against one-shot drilling process. *J. Mater. Res. Technol.* **2020**, *9*, 3994–4006. [[CrossRef](#)]
37. Aamir, M.; Tu, S.; Tolouei-Rad, M.; Giasin, K.; Vafadar, A. Optimization and modeling of process parameters in multi-hole simultaneous drilling using taguchi method and fuzzy logic approach. *Materials* **2020**, *13*, 680. [[CrossRef](#)]
38. Pahuja, R.; Ramulu, M. Abrasive water jet machining of Titanium (Ti6Al4V)-CFRP stacks-A semi-analytical modeling approach in the prediction of kerf geometry. *J. Manuf. Process.* **2019**, *39*, 327–337. [[CrossRef](#)]
39. Wang, S.; Zhang, S.; Wu, Y.; Yang, F. Exploring kerf cut by abrasive waterjet. *Int. J. Adv. Manuf. Technol.* **2017**, *93*, 2013–2020. [[CrossRef](#)]

## **Chapter 4 Analysis and optimisation of process parameters AWJ contour cutting of AISI 304L**

This chapter has been published as a research article in the *“Metals, in a special issue: Optimisation and analysis of metal cutting processes”*, an official journal of MDPI. In order to maintain uniformity in the presentation of the thesis, the publication format was changed but the contents are the same. After determining the impacts of traverse speed and material thickness, as detailed in Chapter 3, other critical input parameters affecting the performance of abrasive waterjet contour cutting, such as waterjet pressure and abrasive mass flow rate were considered. In order to achieve the goal of a better surface integrity and higher efficiency, this chapter presents an experimental study in abrasive waterjet machining of austenitic stainless steel 304L with three level of thicknesses. It demonstrates the utilisation of Taguchi method in executing the experiments and performing a single-objective optimisation, in order to determine the optimum value of the process parameters with the objectives of either maximisation rate of material removal or minimisation of surface roughness. Moreover, this chapter reveals the percentage contribution of the selected influencing input parameters.

Sections 4.1 to 5 of Thesis have been published as the following article.

## Article

# Analysis and Optimization of Process Parameters in Abrasive Waterjet Contour Cutting of AISI 304L

Jennifer Milaor Llanto , Ana Vafadar , Muhammad Aamir  and Majid Tolouei-Rad

School of Engineering, Edith Cowan University, Joondalup, WA 6027, Australia;  
a.vafadarshamasbi@ecu.edu.au (A.V.); m.aamir@ecu.edu.au (M.A.); m.rad@ecu.edu.au (M.T.-R.)

\* Correspondence: j.llanto@ecu.edu.au; Tel.: +61-404-138-991

**Abstract:** Abrasive waterjet machining is applied in various industries for contour cutting of heat-sensitive and difficult-to-cut materials like austenitic stainless steel 304L, with the goal of ensuring high surface integrity and efficiency. In alignment with this manufacturing aspiration, experimental analysis and optimization were carried out on abrasive waterjet machining of austenitic stainless steel 304L with the objectives of minimizing surface roughness and maximizing material removal rate. In this machining process, process parameters are critical factors influencing contour cutting performance. Accordingly, Taguchi's S/N ratio method has been used in this study for the optimization of process parameters. Further in this work, the impacts of input parameters are investigated, including waterjet pressure, abrasive mass flow rate, traverse speed and material thickness on material removal rate and surface roughness. The study reveals that an increasing level of waterjet pressure and abrasive mass flow rate achieved better surface integrity and higher material removal values. The average S/N ratio results indicate an optimum value of waterjet pressure at 300 MPa and abrasive mass flow rate of 500 g/min achieved minimum surface roughness and maximum material removal rate. It was also found that an optimized value of a traverse speed at 90 mm/min generates the lowest surface roughness and 150 mm/min produces the highest rate of material removed. Moreover, analysis of variance in the study showed that material thickness was the most influencing parameter on surface roughness and material removal rate, with a percentage contribution ranging 90.72–97.74% and 65.55–78.17%, respectively.

**Keywords:** abrasive waterjet machining; metal contour cutting; surface roughness; material removal rate; Taguchi method; ANOVA



**Citation:** Llanto, J.M.; Vafadar, A.; Aamir, M.; Tolouei-Rad, M. Analysis and Optimization of Process Parameters in Abrasive Waterjet Contour Cutting of AISI 304L. *Metals* **2021**, *11*, 1362. <https://doi.org/10.3390/met11091362>

Academic Editors:  
Tadeusz Mikolajczyk, Danil Yurievich Pimenov and Munish Kumar Gupta

Received: 30 July 2021  
Accepted: 27 August 2021  
Published: 30 August 2021

**Publisher's Note:** MDPI stays neutral with regard to jurisdictional claims in published maps and institutional affiliations.

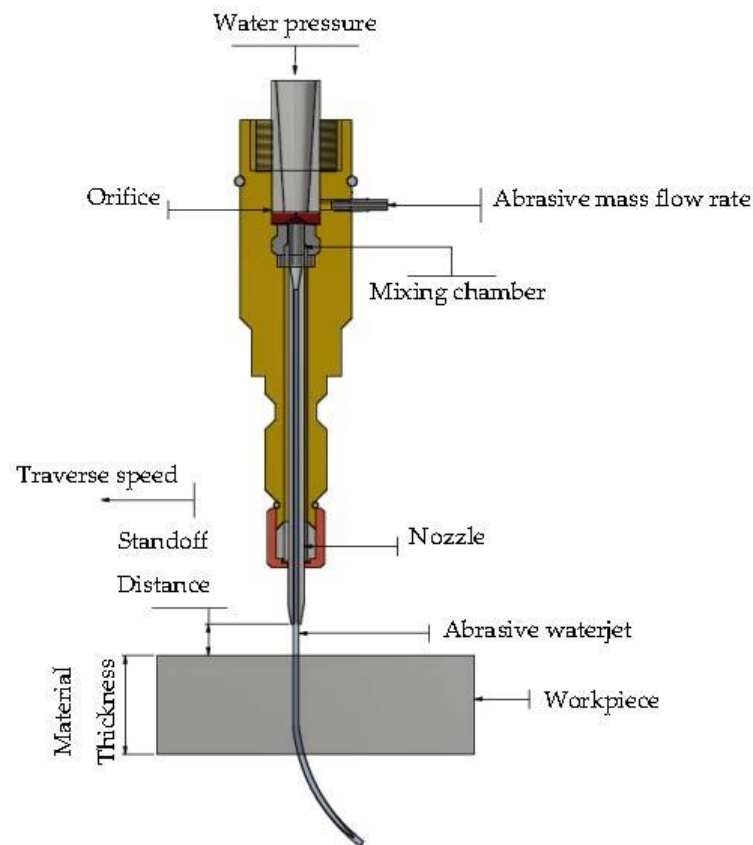


**Copyright:** © 2021 by the authors. Licensee MDPI, Basel, Switzerland. This article is an open access article distributed under the terms and conditions of the Creative Commons Attribution (CC BY) license (<https://creativecommons.org/licenses/by/4.0/>).

## 1. Introduction

Abrasive waterjet machining (AWJM) is a non-traditional cold processing technology used for material processing, with considerable advantages including the absence of heat affected zones, low tool wear, low reaction force, high flexibility, as well as broad application range [1]. In general, the AWJM system consists of four major elements: (1) a high pressure pump producing a flow of pressurized water; (2) an abrasive flow control systems and a cutting head that generates the abrasive water jet machining; (3) a computer-based controller that controls the activity of the cutting head motion; and (4) a water-filled tank that disseminates energy of the abrasive water jet upon completion of machining the workpiece [2]. The fundamental mechanism of abrasive waterjet cutting is material erosion through waterjet eroding, with force and disparity in the momentum of the abrasives colliding on the target material.

An AWJM nozzle system consists of an abrasive hopper and feeder, a water nozzle/orifice, a mixing/vacuum chamber, and a focusing tube or inserts. The abrasive particles are carried out from the plastic tube into the hopper, where they are released to the cutting head and extracted by a waterjet stream in the vacuum chamber. The high-pressure waterjet is then combined with abrasive particles and accelerated to produce the abrasive waterjet [3]. Figure 1 represents the scheme of abrasive waterjet nozzle and parameters.



**Figure 1.** Schematic representation of AWJM cutting.

Abrasive waterjet is extensively used in machining of difficult-to-cut materials including titanium, steel and Inconel, with the capability to produce contour profiles in thickness of a workpiece possessing a value of up to 100 mm for stainless steel and up to 120 mm for aluminum [4]. For metallic materials, the material removal in an abrasive waterjet machine occurs through shear deformation, which is comprised of micro-chip formation, ploughing and rubbing [5]. Whilst AWJM exhibited feasibility in cutting difficult-to-machine materials, they still experience cutting issues such as high occurrences of surface roughness and low material removal rate. For instance, Veerappan et al. [6] studied abrasive waterjet performance in machining of nickel-based superalloy. The effects of cutting factors, such as traverse speed, waterjet pressure, standoff distance and abrasive mass flow rate against surface roughness and material removal rate were investigated. They obtained maximum surface roughness and material removal at a high level of waterjet pressure and abrasive mass flow rate. Therefore, both material removal rate and surface roughness increase with an increase in both the abrasive mass flow rate and waterjet pressure. Begic-Hajdarevic et al. [7] carried out experiments on the effect of traverse speed, abrasive mass flow rate, and material thickness on the surface roughness of AWJM of aluminum. Their experimental results indicated that increasing material thickness produces a higher value of surface roughness, particularly on the bottom area of the cut. They established that the traverse speed has no great effect on the surface roughness due to a minimal change occurred at the lower traverse speeds. Hence, increasing traverse speed increases the surface roughness value. Moreover, Bhandarkar et al. [8] presented an experimental investigation in machining Inconel 718 by AWJM. They considered input parameters i.e., traverse speed and pressure in achieving the required geometric accuracy and surface integrity. They concluded that a higher rate of traverse speed and lower pressure are the favorable conditions for achieving an improved roughness of the cut surface.



An abrasive waterjet is predominantly applied for cutting hard-to-machine materials like austenitic stainless steels [9]. Due to its excellent corrosion resistance, austenitic stainless steel has been applied to a variety of industrial applications, such as architectural paneling, molding, trimming, construction materials for buildings, kitchen equipment, railings, chemical containers, aerospace, automotive etc. [10,11]. This capability of AISI 304L is owing to its low carbon content and molybdenum, which restrains chloride corrosion and has low sensitivity to intergranular corrosion and good wear and friction properties [11]. AWJM is highly suitable for machining heat-sensitive materials such as austenitic stainless steel 304L due to its absence of the heat-affected zone [9]. Despite noteworthy advancements in the AWJM of austenitic stainless steel, there are still constraints and hindrances in utilizing this modern mechanical technology. Challenges associated with AWJM of austenitic stainless steel have been reported, particularly its low rate of the eroded material and high roughness of the cut surface. In an abrasive waterjet, cutting is generated by material removal caused by abrasive particles that hit the workpiece at high velocity and are influenced by the thickness and hardness of the target material [12]. Fundamentally, the productivity performance of AWJM is indicated by the removed material per unit of time [13]. In addition, surface roughness is the primary indicator of surface quality level which defines the scale of smoothness of the machined parts [14]. In general, the surface finishing profile cut by an abrasive waterjet is characterized by the degree of roughness it acquires during the machining process [15,16]. Comprehensive knowledge of the impacts of AWJM settings on the quality of the acquired cuts is an essential requisite in achieving precise cutting [17]. Hence, there is a necessity for optimization method as AWJM is faced with uncertainties in the selection of the most suitable parameter combination to improve quality and productivity relating to surface roughness and material removal rate. AWJM incorporates several independent input parameters that directly affect machine performance in terms of efficiency and quality. Generally, there are four sets of AWJM input parameters that include: (1) hydraulic parameters, (2) cutting parameters, (3) abrasive parameters and (4) mixing and acceleration parameters. The issues of material responses and behaviors, such as surface roughness, material removal rate and kerf taper angle to AWJM, have been studied since the emergence of abrasive waterjet applications in 1980s. Yet, it continues to be investigated as a means of effectively controlling AWJM input process parameters to achieve better cutting performance [18]. Accordingly, this determines the influence of AWJM process parameters on surface quality characteristics and material removal rate of difficult-to-cut materials such as AISI 304L.

The impacts of input parameters such as transverse speed, standoff distance, abrasive flow rate, and water pressure on material removal rate and surface roughness of austenitic stainless steel 304 by AWJM have been evaluated by Singh et al. [19]. Within the above study, an abrasive flow rate of 300 g/min, a waterjet pressure of 340 MPa, a stand-off distance of 2.5 mm, and a traverse speed of 90 mm/min were derived as the optimum process parameter values. Further, the above study divulged that traverse speed is the most significant factor, whilst standoff distance is the least significant factor affecting the selected responses. Löschnera et al. [20] have demonstrated an investigation of AWJM process parameters responses in reducing roughness in the straight cut surface of AWJM of AISI 316L with 10 mm thickness. Their results revealed that employing a higher rate of cutting speed with decreasing kinetic energy of abrasive particles showed visible roughness in the lower cut part. Therefore, a lower rate of cutting speed prevents loss of kinetic energy of the abrasive water jet, resulting in a better quality of surface cut. Moreover, Karthik et al. [21] have studied the influences of water jet pressure, feed rate and abrasive flow rate on material removal rate and kerf top width in AWJM of stainless steel grade 304. Their experimental results indicate that higher values of material removal rate occur at higher values of water pressure and feed rate. Further, minimum kerf top width was achieved in the study by increasing the rate of waterjet pressure and decreasing value feed rate. Hence, their work has revealed that abrasive mass flow rate is an insignificant factor in material removal rate. Furthermore, Kmec et al. [22] have performed machining of AISI 304 with

straight line directions, considering input parameters such as waterjet pressure, abrasive nozzle diameter, standoff distance, cutting feed rate, abrasive mass flow rate, and material thickness in order to minimize surface roughness. Their study has shown that a higher value of abrasive mass flow rate produces a large number of abrasives during cutting processes, resulting in lower surface roughness. However, increasing waterjet pressure with a wider diameter of abrasive nozzle generates inconsistent impacts between particles inside the stream and a loss in kinetic energy, leading to higher roughness value. Further, material thickness was shown to be an insignificant factor for surface roughness in the above study. Therefore, an increasing abrasive mass flow rate and decreasing values of waterjet pressure, cutting feed rate and standoff distance were shown as preferable for minimizing surface roughness.

A number of research studies have been conducted on the straight-slit cutting of austenitic stainless steel with an abrasive waterjet; however, very few studies have been conducted in contour cutting of difficult-to-cut and heat-sensitive materials like AISI 304L. The retardation of the jet inside the kerf of cut generates the deformation of the target material, specifically when machining corner and curvatures profiles [23]. Hence, this machining challenge requires further investigation.

In order to establish the optimum parameters in machining applications, Taguchi-based optimization has been employed using Minitab software in this study. The Taguchi method is useful for discovering the most suitable combination of factors under specifically required experimental conditions, lessening the requisite number of experiments in conventional experiments as the number of process parameters increase [24]. In the Taguchi method, selection of suitable orthogonal array relies on aspects such as the number of input and response parameters along with correlations that are of key significance, figures of levels of data for input parameters; required objectives of the experiment; and constraints cited in the value and its performance [24,25]. This technique enables researchers to simultaneously establish independent and interrelating effects of several parameters affecting an outcome in any configuration. Therefore, in this study, the Taguchi method indicates S/N ratio calculation equations according to the maximization and minimization objectives in the abrasive waterjet contour cutting of AISI 304L.

Several studies relating to AWJM using the Taguchi method have demonstrated the effectiveness of this technique in establishing the optimal combination of process parameters in minimizing surface roughness. For instance, Kechagias et al. [5] have performed an experiment on AWJM using the Taguchi methodology, with results showing that by employing a lower level of traverse speed and standoff distance, a lower value of kerf width and surface roughness during AWJM of steel sheets (TRIP 800 HR-FH and TRIP 700 CR-FH) was produced. In addition, an increasing thickness of material generated a decreasing value of surface roughness. Accordingly, the optimization of process parameters using the Taguchi method can be applied to various machining processes to provide sufficient approximation of performance and process control. Maneiah et al. [26] have presented the influence of various AWJM parameters such as standoff distance, feed rate, and abrasive flow rate in machining metal matrix composites (MMCs). The Taguchi  $L_9$  orthogonal array was shown to achieve the appropriate combination of designated process parameters to attain better surface quality characteristics. The authors determined that a feed rate of 135 mm/min, distance stand of 0.5 mm, and abrasive flow rate of 450 gm/min were the most favorable process parameters to achieve lower surface roughness on MMCs. Thus, the response of the S/N ratio indicates that feed rate provides greater impact on surface roughness, whilst stand of distance has minor impacts as compared to abrasive flow rate. Moreover, Sharma et al. [27] have presented an application of the Taguchi method to obtain desired surface roughness of aluminum AL-6061 via AWJM. The researchers of this study established that traverse speed has a greater influence on surface roughness, where pressure was the utmost impacting parameter for material removal rate. Hence, the application of an  $L_{16}$  orthogonal array can effectively optimize process variables for the achievement of desired surface roughness and material removal rates in AWJM processes.

Furthermore, it should be noted that traditional experimental studies have been used to analyze the impacts of process parameters. Therefore, an optimization method is required in order to establish the best contributing factors. Amongst differing optimization techniques, the Taguchi method has become increasingly popular for developing engineered products [28]. The method addresses challenges with traditional experimental procedure of having a further increment in experimental works as the number of process parameters increases. With this specific advantage, this method minimizes time and cost spent in conducting experiments and in discovering significant factors.

From the above literature review, it is concluded that further investigation is required to comprehensively understand the impacts of process parameters in abrasive waterjet contour cutting to achieve better quality and higher productivity. In general, contour cutting is more challenging than linear cutting process. In addition, high-quality surface finish of the contour cut is an intensified requirement in various manufacturing industries, in particular, for difficult-to-cut metals such as such as stainless steel AISI 304L, where it is a significant performance indicator for machining. Therefore, this foregoing challenge requires continuous further investigation to be addressed.

In this research project, responses including material removal rate and surface roughness have been considered, as these are important quality characteristics of profile cut and aspects of productivity. To achieve these objectives, experimental and numerical studies have been conducted in this work to investigate interactions between AWJM input parameters, including water jet pressure, traverse speed, and abrasive mass flow rate, on surface roughness and rate of material removal in abrasive waterjet contour cutting of AISI 304L with differing level thicknesses. An optimization is implemented using Taguchi method in determining input parameter values resulting in minimum surface roughness and maximum material removal rate.

## 2. Materials and Methods

### 2.1. Workpiece and Contour Cutting Profiles

In this work, austenitic stainless steel (AISI) 340L was used at varied thicknesses of 4 mm, 8 mm and 12 mm. The selected material thicknesses with uniform incremental gap were assigned to capture variations of AWJM behavior and to study its impacts on the machining characteristics of steel. The chemical composition and properties of AISI 304L are given in Tables 1 and 2.

The widely used difficult-to-cut AISI 304L is distinguished from other alloy steels for its high strength, high corrosion and heat resistance because of its high contents of Cr and Ni [29]. Surface integrity and low material removal rate have been reported when machining AISI 304L, requiring improved industrial applications and further scientific research [30].

**Table 1.** Chemical composition in wt% of AISI 304L [11].

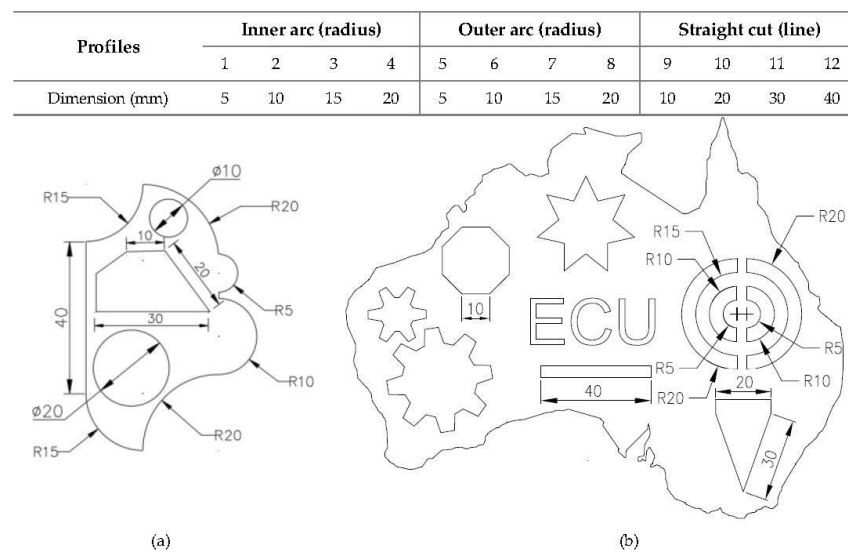
Chemical Composition (wt %).									
Fe	C	Mn	Si	Mo	Co	Cr	Cu	Ni	Others
70.780	0.025	1.140	0.410	0.360	0.210	18.40	0.180	8.190	0.305

**Table 2.** Mechanical Properties of AISI 304L [11,31].

Properties of AISI 304L	
Hardness, Rockwell B	82
Tensile Strength, Ultimate, MPa	564
Tensile Strength, Yield, MPa	210
Elongation at Break %	58%
Modulus of Elasticity, GPa	193–200

In general, contour cutting is employed in steel fabrication industries because of its ability to deal with complicated and complex geometries, enabling the production of various products. The contour cutting process is mostly applied in metalworking industries as compared with the straight-slit cutting process, involving various convex and concave arcs and straight-lines to form a particular geometry. In this research, four levels of inner and outer arcs and straight-lines have been used to study the impacts of contour profiles on abrasive waterjet machining responses.

Figure 2 presents the cutting path containing the identified profiles for the execution of the Taguchi design of experiments and confirmatory tests. Figure 2a summarizes the execution of 27 experimental runs, while Figure 2b illustrates a confirmatory test using the obtained optimum combination of input parameters.



**Figure 2.** AWJM contour cutting path for (a) Taguchi  $L_{27}$  tests [32]. (b) Confirmation test.

The abovementioned profiles were selected to accommodate a broad array of complicated machining profiling applications. A straight-line cut ranging from 10 to 40 mm is adequate to acquire a constant phase of feed rate, covering the acceleration and retardation phase [33]. The levels of arcs profile, i.e., 10–40 mm, showed manifestation of surface roughness, low machining rate and imprecision of cut geometries from previous works [34–36], indicating the necessity for further studies, particularly for hard-to-cut materials such as AISI 304L.

## 2.2. AWJ Machining Setup and Parameters

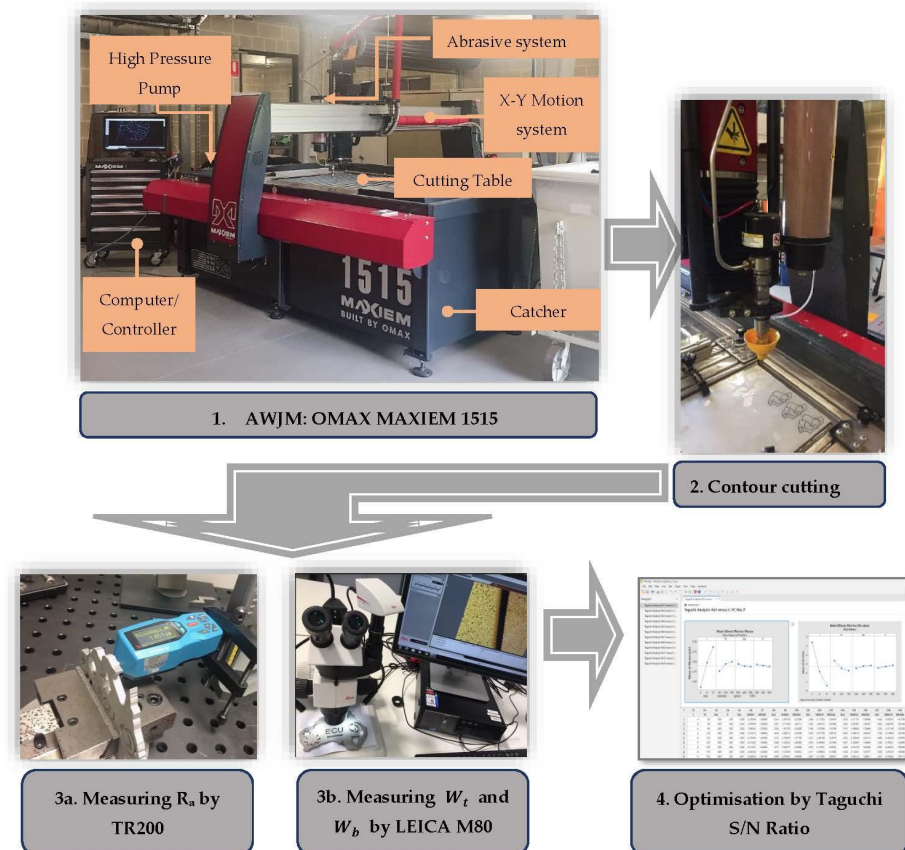
The experiments were conducted on an OMAX–MAXIEM 1515 abrasive waterjet machine. Clamping was required to hold the workpiece in the catcher tank. The water temperature was maintained at 50–32 °C during cutting operations, using a chiller tank. These machine components included a pneumatically-controlled valve, an abrasive hopper with gravity feed type, an abrasive feeder system and a cutting table of 1575 mm × 1575 mm. To attain accuracy in contour cutting, an appropriate assignment of the process parameters is critical. In this research, waterjet pressure, abrasive mass flow rate, traverse speed and material thickness have been considered as variable input parameters at three different levels.

The machining setup and input parameters employed in the cutting test of AISI 304L are given in Table 3. The designated levels of variable and constant input parameters were based on consensus from recommended control ranges for abrasive waterjet machining in previous investigations [37–39]. Abrasive type efficiency is indicated by level of hardness; thus, a more rigid material requires a harder abrasive particle [15,40]. A Garnet of 80 mesh size with a hardness of MOHS 7–8 was used in this study due to its better surface integrity results, in accordance with previous related studies [15].

**Table 3.** Machine specifications and cutting input parameters.

Abrasive Waterjet Conditions	Details	Range/Values
OMAX MAXIEM 1515	Max Pressure, MPA	413.7
	Max Traverse Speed, mm/min	12,700
	Table Size (L × W), mm	2235 × 1727
	XY Cutting Envelope, mm	1575 × 1575
	z-Axis travel, mm	305
Variable cutting input parameters	Abrasive mass flow rate, g/min	300, 400, 500
	Waterjet pressure, MPa	200, 250, 300
	Traverse speed, mm/min	90, 120, 150
	Material thickness, mm	4, 8, 12
Constant cutting input parameters	Orifice diameter, mm	2.8
	Abrasive type	Garnet
	Abrasive mesh number, #	80
	Standoff distance, mm	1.5

In this work, three major steps were executed, comprising of abrasive waterjet contour cutting experiments, measuring of results and optimization. The overall experimental and optimization procedures are shown in Figure 3. The defined machining conditions of OMAX MAXIEM 1515 are employed to execute contour cutting of AISI 304L experiments. The roughness resulted from the machined surfaces are measured using the TR200 model surface roughness tester. Subsequently, the surface images of the cut profiles were captured and topographically analyzed using LEICA M80. The kerf widths of the cut workpiece, which were the function of material removal rate, were measured using a LEICA M80 optical microscope model. Further, the Taguchi S/N ratio was employed to optimize the process parameters using MINITAB 19 software (version 19.1, Minitab Pty Ltd. Sydney, Australia).

**Figure 3.** AWJM contour cutting experiment and analysis setup.



The rate of material removal and surface roughness are selected as output parameters to be optimized. The rate of material removal, which is the volume of metal eroded from the target workpiece per unit of time, is quantified by traverse speed, width of kerf and penetration of cut. Thus, material removal rate was calculated using Equation (1) [41].

$$MRR = ht .W.vf \quad (1)$$

where kerf width is calculated by the following formula:  $W = \frac{W_t + W_b}{2}$ .

### 2.3. Design of Experiment

To accommodate several variable parameters in the abrasive waterjet contour cutting of AISI 304L, a standardized Taguchi Orthogonal array  $L_{27}$  was employed in this study to execute the experiment using four factors with three levels, as shown in Table 4.

**Table 4.** The  $L_{27}$  orthogonal array of Taguchi.

Exp. Input Parameters				
No.	Material Thickness, $t$ (mm)	Traverse Speed, $V_f$ (mm/min)	Abrasive Mass Flow Rate, $m_a$ (g/min)	Waterjet Pressure, $P$ (MPa)
1	4	90	300	200
2	4	90	400	250
3	4	90	500	300
4	4	120	300	250
5	4	120	400	300
6	4	120	500	200
7	4	150	300	300
8	4	150	400	200
9	4	150	500	250
10	8	90	300	200
11	8	90	400	250
12	8	90	500	300
13	8	120	300	250
14	8	120	400	300
15	8	120	500	200
16	8	150	300	300
17	8	150	400	200
18	8	150	500	250
19	12	90	300	200
20	12	90	400	250
21	12	90	500	300
22	12	120	300	250
23	12	120	400	300
24	12	120	500	200
25	12	150	300	300
26	12	150	400	200
27	12	150	500	250

Relying on this design, 27 experimental runs were executed with combination levels for each variable parameter. The Taguchi method has a diverse signal-to-noise (S/N) ratio, including “the larger the better”, “the nominal the better” and “the smaller the better” [42]. This work’s objectives sought to obtain results with minimum surface roughness and maximum material removal rate. Therefore, signal-to-noise ratios have been calculated according to the “lower-is-the better” category for surface roughness and “higher-is-the better” for material removal rate. In computing SNR (signal-to noise ratios), the lower-

the-better and the higher-the-better categories are expressed in Equations (2) and (3), respectively [43].

$$S/N_{SR} = \eta_{ij} = -10 \log \left( \frac{1}{n_i} \sum_{j=1}^n (y_{ij})^2 \right) \quad (2)$$

$$S/N_{MRR} = \eta_{ij} = -10 \log \left( \frac{1}{n_i} \sum_{j=1}^n \frac{1}{(y_{ij})^2} \right), \quad (3)$$

where  $y_i$  is the result obtained in present;  $\eta$  shows the number of tests.

Furthermore, Analysis of variance (ANOVA) was utilized to establish the percentage contribution of each input parameter regarding surface roughness and material removal rate.  $p$ -Values estimated at more than 0.05 or 5% were considered insignificant because ANOVA in this research was run with a confidence interval of 95%, in alignment with previous studies [24,44–46].

### 3. Results and Discussions

#### 3.1. Effects of Input Parameters on Surface Roughness and Material Removal Rate

The cut surfaces produced during AWJM of AISI 304L are topographically presented in Figures 4–12. The cut samples from a straight profile demonstrated different material responses towards the application of three levels of traverse speed, waterjet pressure and abrasive mass flow rate for 4 mm, 8 mm and 12 mm thickness of AISI 304L.

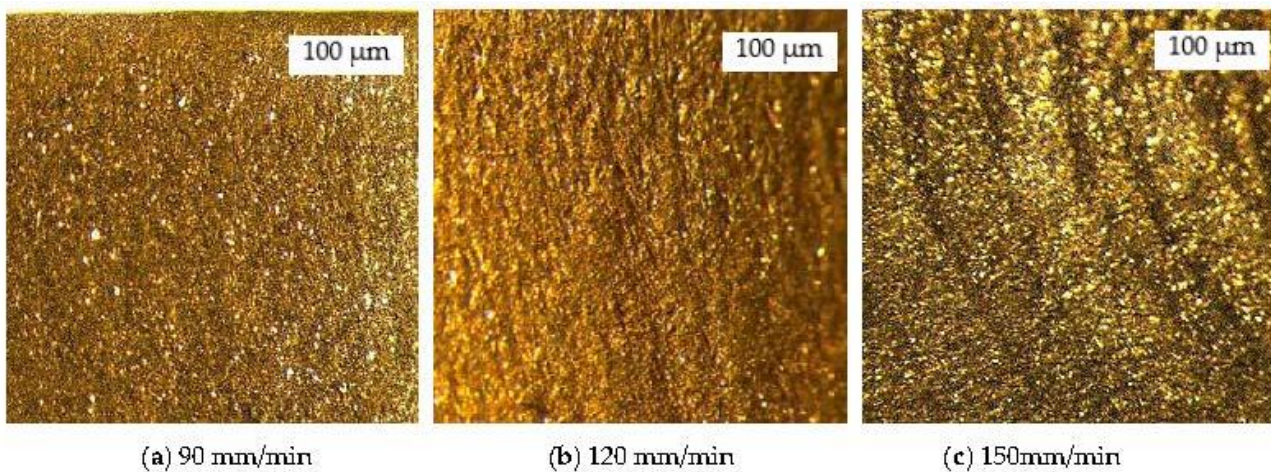


Figure 4. Topography of AISI 304L cut surface with 4 mm thickness using varied traverse speed.

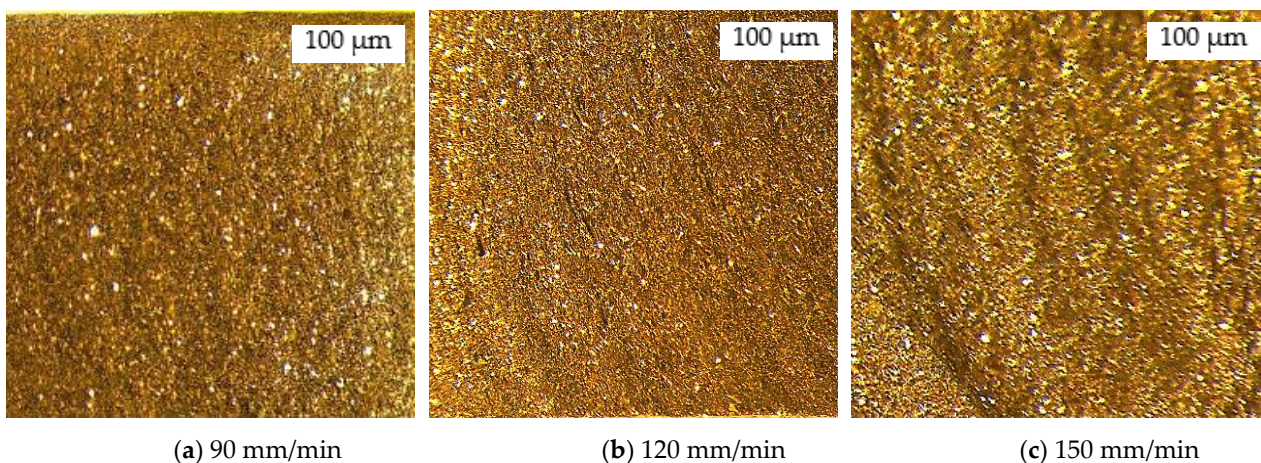
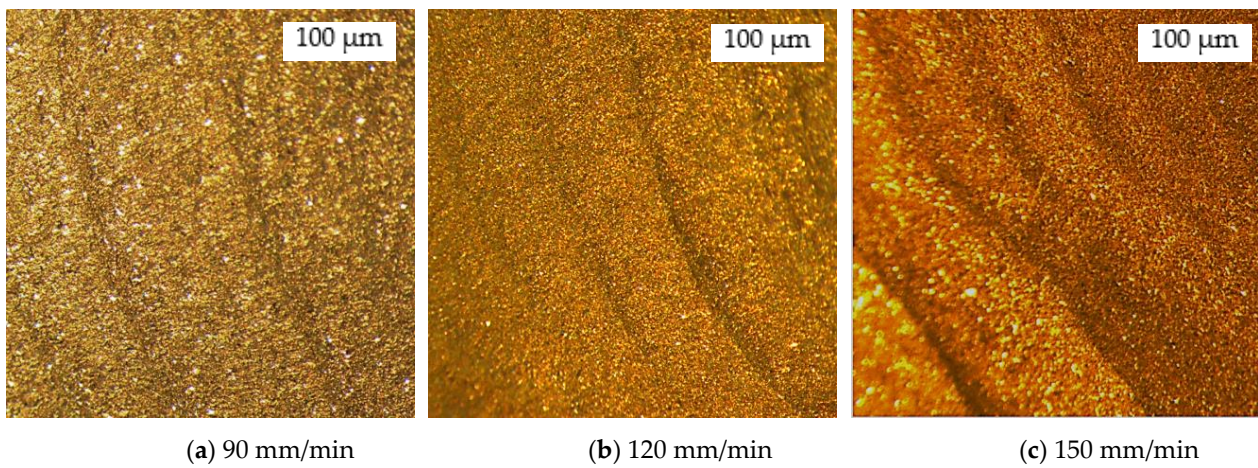
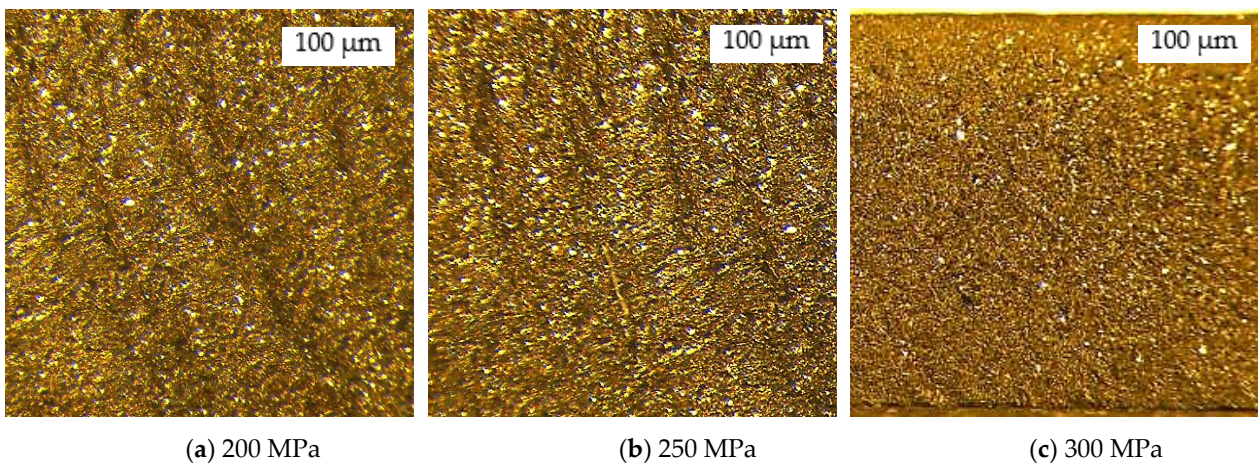


Figure 5. Topography of AISI 304L cut surface with 8 mm thickness using varied traverse speed.

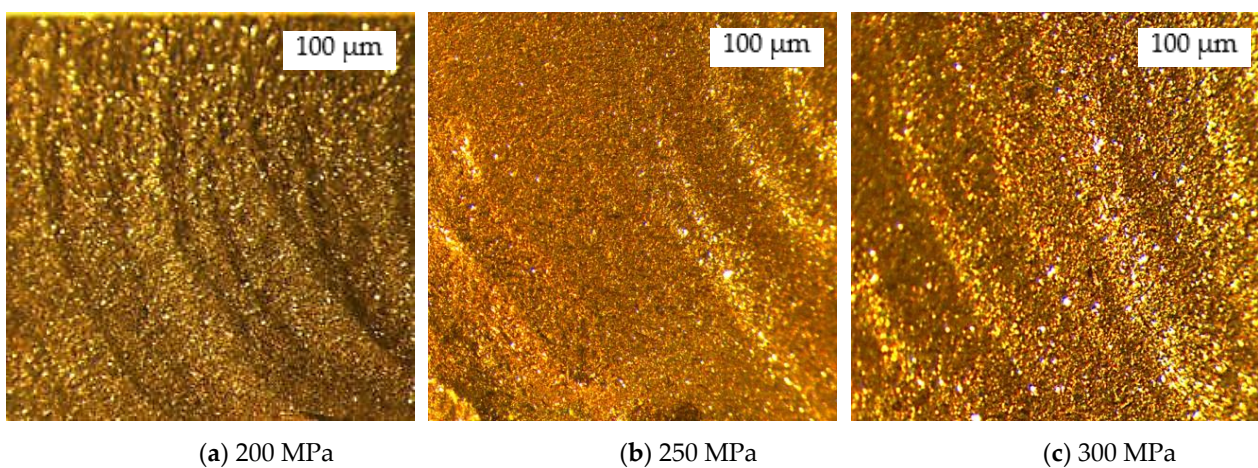




**Figure 6.** Topography of AISI 304L cut surface with 12 mm thickness using varied traverse speed.

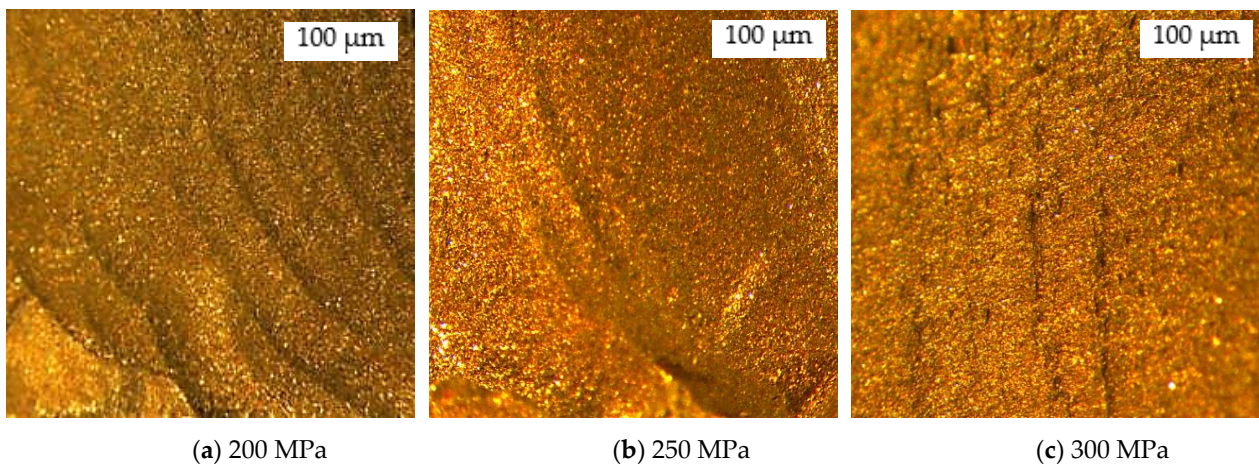


**Figure 7.** Topography of AISI 304L cut surface with 4 mm thickness using varied waterjet pressure.

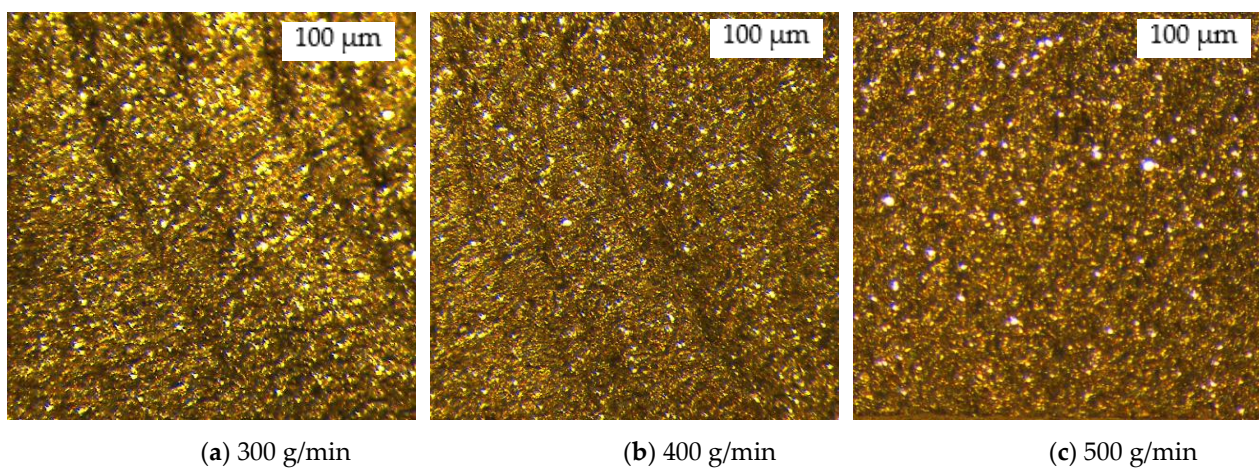


**Figure 8.** Topography of AISI 304L cut surface with 8 mm thickness using varied waterjet pressure.

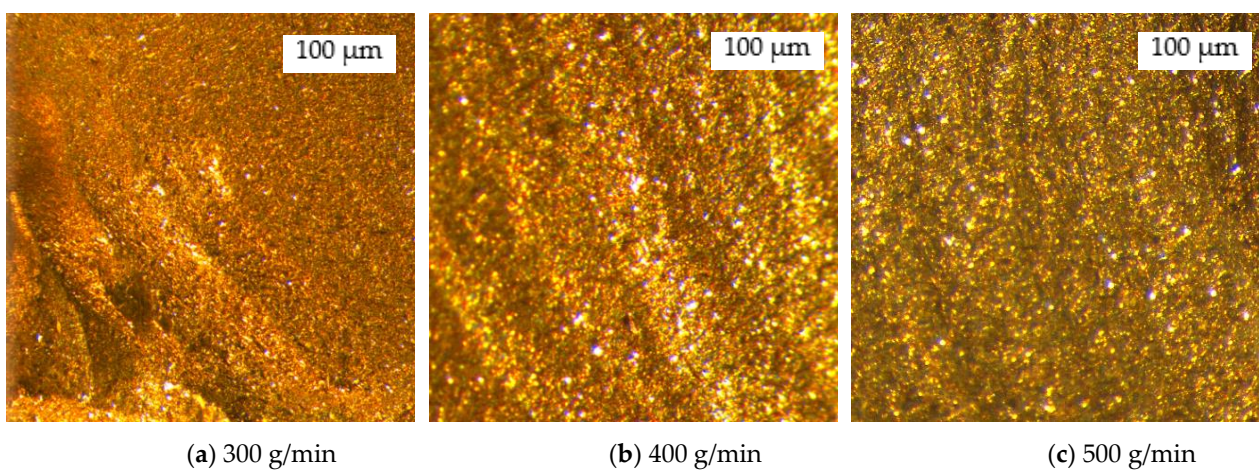




**Figure 9.** Topography of AISI 304L cut surface with 12 mm thickness using varied waterjet pressure.

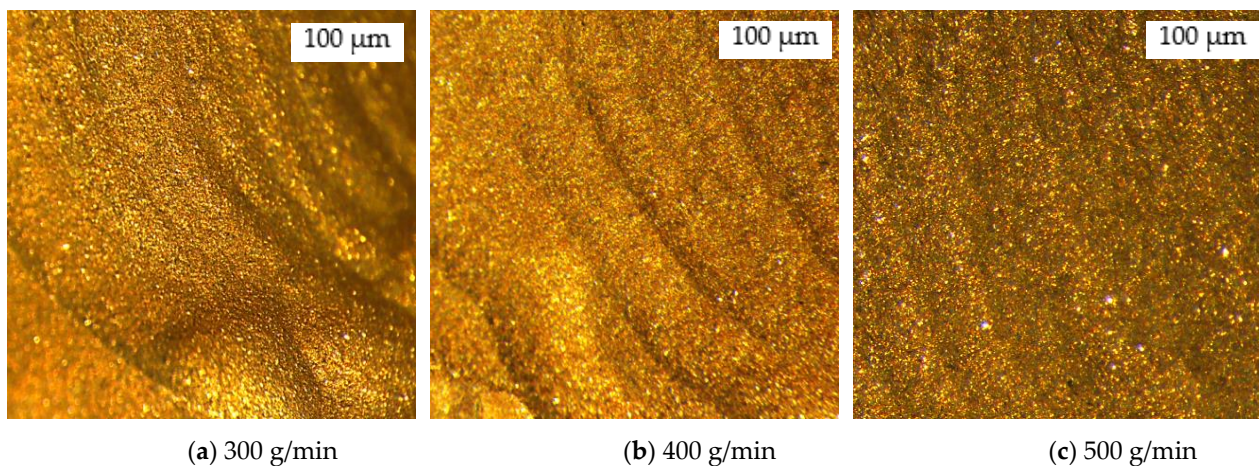


**Figure 10.** Topography of AISI 304L cut surface with 4 mm thickness using varied Abrasive mass flow rate.



**Figure 11.** Topography of AISI 304L cut surface with 8 mm thickness using varied Abrasive mass flow rate.





**Figure 12.** Topography of AISI 304L cut surface with 12 mm thickness using varied Abrasive mass flow rate.

Figures 4–6 showed that surface roughness and striation are visibly higher as the traverse speed value increases from 90 mm/min to 150 mm/min with constant values for waterjet pressure and abrasive mass flow rate of 300 MPa and 500 g/min, respectively. The cut samples displayed similar material behavior of incrementing occurrences of surface roughness as the traverse speed value increases. This is due to the fact that the increasing rate of traverse speed is losing the number of abrasive particles leading to the roughness of the cut surface [47]. The material responses of AISI 304L against waterjet pressure were presented in Figures 7–9. The cut specimens revealed comparable evidence of decreasing surface roughness as the waterjet pressure value increases from 200 MPa to 300 MPa with constant values for traverse speed and abrasive mass flow rate of 90 mm/min and 500 g/min, respectively. The increasing value of waterjet pressure denotes a higher energy reinforcing a larger amount of abrasive particles which results in lesser striation on the cut surface [5]. Figures 10–12 exhibited a similar trend of decreasing waviness pattern on the cut surface, as the abrasive mass flow rate is increasing from 300 g/min to 500 g/min with constant rates for traverse speed and waterjet pressure of 90 mm/min and 300 MPa, respectively. A higher abrasive mass flow results in a breakdown of abrasive particles into smaller scales, producing more sharp edges which are responsible for decreasing the roughness of the cut surface [40].

Images presented in Figures 4–12, denote higher visibility of surface striations and waviness as the material thickness increases. It is observed that striations are turned in the opposite direction of the cutting path. The curvature of striations depends on the AWJM cutting velocity and material type [48]. The topmost cut surface demonstrated smoothness and the bottom part is rough with wavy lines patterns. The striation is formed due to the movements of the jets during the machining process, which is linked to the changing of the cutting path or profiles [49]. In addition, the wavy distribution of the kinetic energy of the intergranular abrasive inside the abrasive waterjet leads to the formation of striation on the surface cut. Hence, as the depth of cut or material thickness increases, the kinetic energy decreases generating a higher occurrence of wavy lines. The abrasive waterjet holds high kinetic energy with a large number of abrasive particles from the beginning of the erosion process that gradually subsiding during machining, resulting in manifestations of higher surface roughness [47]. Topographically, material thickness is the topmost impacting parameter followed by the waterjet pressure, abrasive mass flow rate and traverse speed.

The experimental results presented in Table 5 display the response of surface roughness ( $R_a$ ) for various levels of material thickness ( $t$ ), abrasive flow rate ( $m_a$ ), waterjet pressure ( $P$ ) and traverse speed ( $V_f$ ). The lowest values of  $R_a$  achieved in abrasive waterjet contour cutting of AISI 304L were 1.142  $\mu\text{m}$  for 4 mm, 1.529  $\mu\text{m}$  for 8 mm, and 1.993  $\mu\text{m}$  for 12 mm material thicknesses.

Table 5. The  $L_{27}$  orthogonal array of Taguchi for surface roughness results.

Exp.	Input Parameters				Output Parameter ( $R_a = \mu\text{m}$ )											
	No.	$t$ (mm)	$V_f$ (mm/min)	$m_a$ (g/min)	$P$ (MPa)	Profiles										
					1	2	3	4	5	6	7	8	9	10	11	12
1	4	90	300	200	1.298	1.324	1.284	1.305	1.428	1.396	1.356	1.248	1.285	1.250	1.248	1.235
2	4	90	400	250	1.256	1.281	1.243	1.263	1.382	1.351	1.313	1.208	1.243	1.210	1.208	1.195
3	4	90	500	300	1.200	1.204	1.168	1.187	1.320	1.291	1.254	1.154	1.188	1.156	1.154	1.142
4	4	120	300	250	1.398	1.426	1.383	1.405	1.538	1.504	1.461	1.344	1.384	1.346	1.344	1.331
5	4	120	400	300	1.345	1.372	1.331	1.352	1.480	1.447	1.406	1.293	1.332	1.295	1.293	1.280
6	4	120	500	200	1.399	1.468	1.424	1.447	1.539	1.505	1.462	1.345	1.385	1.347	1.345	1.332
7	4	150	300	300	1.448	1.477	1.433	1.456	1.593	1.558	1.513	1.392	1.434	1.394	1.392	1.378
8	4	150	400	200	1.426	1.455	1.411	1.434	1.569	1.534	1.490	1.371	1.412	1.373	1.371	1.357
9	4	150	500	250	1.401	1.409	1.367	1.389	1.541	1.507	1.464	1.347	1.387	1.349	1.347	1.333
10	8	90	300	200	1.886	1.924	1.866	1.896	2.075	2.029	1.971	1.813	1.867	1.816	1.813	1.795
11	8	90	400	250	1.825	1.861	1.806	1.835	2.007	1.963	1.907	1.755	1.807	1.757	1.755	1.737
12	8	90	500	300	1.744	1.576	1.529	1.553	1.918	1.876	1.822	1.676	1.726	1.679	1.676	1.660
13	8	120	300	250	2.031	2.072	2.010	2.042	2.234	2.185	2.123	1.953	2.011	1.956	1.953	1.933
14	8	120	400	300	1.954	1.893	1.836	1.866	2.150	2.102	2.042	1.879	1.935	1.882	1.879	1.860
15	8	120	500	200	2.033	2.073	2.011	2.044	2.236	2.187	2.124	1.954	2.012	1.958	1.954	1.935
16	8	150	300	300	2.104	2.146	2.082	2.115	2.314	2.263	2.199	2.023	2.083	2.026	2.023	2.003
17	8	150	400	200	2.072	2.113	2.050	2.083	2.279	2.229	2.165	1.992	2.051	1.995	1.992	1.972
18	8	150	500	250	2.036	1.998	1.938	1.969	2.239	2.19	2.127	1.957	2.015	1.960	1.957	1.938
19	12	90	300	200	2.265	2.310	2.241	2.277	2.492	2.437	2.367	2.178	2.242	2.181	2.178	2.156
20	12	90	400	250	2.192	2.236	2.169	2.203	2.411	2.358	2.290	2.107	2.170	2.111	2.107	2.086
21	12	90	500	300	2.094	2.136	2.072	2.105	2.303	2.253	2.188	2.013	2.073	2.017	2.013	1.993
22	12	120	300	250	2.440	2.408	2.336	2.373	2.684	2.625	2.549	2.345	2.415	2.349	2.345	2.322
23	12	120	400	300	2.347	2.308	2.239	2.275	2.582	2.525	2.453	2.256	2.324	2.260	2.256	2.234
24	12	120	500	200	2.441	2.490	2.415	2.454	2.685	2.626	2.551	2.347	2.417	2.351	2.347	2.324
25	12	150	300	300	2.527	2.658	2.578	2.620	2.780	2.718	2.641	2.429	2.502	2.433	2.429	2.405
26	12	150	400	200	2.488	2.538	2.462	2.502	2.737	2.677	2.600	2.392	2.464	2.396	2.392	2.368
27	12	150	500	250	2.445	2.393	2.321	2.359	2.689	2.630	2.555	2.350	2.420	2.354	2.350	2.327

Surface roughness corresponding to S/N ratio values for this study is listed in Table A1 of the Appendix A. The results indicate the feasibility of obtaining lowest surface roughness with higher values of waterjet pressure and abrasive mass flow rate at a rate of 300 MPa and 500 g/min, respectively. In AWJM, higher waterjet pressure leads to a greater amount of abrasives, providing a uniform cutting energy that results in a better surface finish during the erosion process [50].

In this work, the obtained results of  $R_a$  are greater at thicknesses of 8 and 12 mm, as compared to 4 mm AISI 304L. Additionally, the lowest  $R_a$  value was achieved by decreasing traverse speed to a rate of 90 mm/min. At the initial strike, the abrasive waterjet possesses high kinetic energy with vast number of abrasive particles which gradually decrease as the material thickness and traverse speed increases [51], resulting in an incremental value of surface roughness.

Table 6 displays the AISI 304L reaction for material removal rate (MRR) within the three levels of each selected input parameter in this study. The highest values of MRR were achieved in abrasive waterjet contour cutting of AISI 304L, with 421.2 mm<sup>3</sup>/min for 4 mm, 767.10 mm<sup>3</sup>/min for 8 mm, and 811.4 mm<sup>3</sup>/min for 12 mm material thicknesses. Regardless of whether contour cutting covered an arc or a straight profile, higher material removal rates were attained via a high-level of abrasive mass flow rate and waterjet pressure. Increasing the waterjet pressure in conjunction with abrasive mass flow rate has been shown to improve material erosion, invoking a large amount of abrasives that result in lower surface roughness [22]. These results reveal an increasing MRR can be attained by incrementally increasing the level of traverse speed. An increasing traverse speed enhances the contact time of the waterjet with the abrasive on the target material, creating more volume of material to erode [22].

**Table 6.** The L<sub>27</sub> orthogonal array of Taguchi for material removal rate results.

Exp. No.	Input Parameters				Output Parameter (MRR = mm <sup>3</sup> /min)											
	<i>t</i> (mm)	<i>V<sub>f</sub></i> (mm/min)	<i>m<sub>a</sub></i> (g/min)	<i>P</i> (MPa)	Profiles											
					1	2	3	4	5	6	7	8	9	10	11	12
1	4	90	300	200	224.50	214.20	210.30	220.70	212.10	227.10	224.80	236.10	221.90	208.20	215.80	211.30
2	4	90	400	250	225.60	225.30	211.30	234.30	223.10	248.60	246.10	258.40	242.90	209.20	236.20	231.30
3	4	90	500	300	227.40	257.00	213.00	219.40	250.60	254.40	244.30	256.00	240.60	210.90	234.50	229.60
4	4	120	300	250	351.10	335.10	328.90	348.50	331.70	355.20	351.60	369.20	347.00	325.60	337.50	330.50
5	4	120	400	300	358.20	351.90	335.50	345.60	343.10	348.30	334.40	350.50	329.40	332.20	321.00	314.30
6	4	120	500	200	353.60	377.50	331.20	388.80	373.70	400.10	396.10	415.90	391.00	327.90	380.30	372.30
7	4	150	300	300	413.00	395.00	386.90	406.50	387.00	418.70	401.90	421.20	395.90	383.00	385.80	377.80
8	4	150	400	200	403.40	390.00	377.80	401.70	386.10	404.00	400.00	420.00	394.80	374.10	384.00	376.00
9	4	150	500	250	411.70	390.90	385.60	398.50	385.10	401.80	397.80	417.70	392.60	381.80	381.90	373.90
10	8	90	300	200	383.40	365.90	359.20	376.90	362.30	387.90	384.00	403.20	379.00	355.60	368.70	361.00
11	8	90	400	250	384.70	377.20	360.40	392.20	373.40	399.80	395.80	415.60	390.60	356.80	380.00	372.00
12	8	90	500	300	381.10	403.80	357.00	367.70	393.70	399.70	383.70	402.20	378.00	353.50	368.40	360.70
13	8	120	300	250	458.20	437.30	429.20	454.80	432.90	461.50	456.90	479.80	451.00	424.90	438.60	429.50
14	8	120	400	300	467.40	456.10	437.80	450.90	444.70	451.50	433.40	454.20	427.00	433.40	416.10	407.40
15	8	120	500	200	472.00	437.50	442.20	450.60	433.10	463.80	459.10	482.10	453.20	437.70	440.80	431.60
16	8	150	300	300	656.00	626.10	614.50	632.90	610.40	619.80	595.00	623.60	586.20	608.30	571.20	559.30
17	8	150	400	200	682.20	661.10	639.00	680.90	654.50	700.80	693.80	728.40	684.70	632.70	666.00	652.10
18	8	150	500	250	687.50	696.20	644.00	724.00	689.20	737.90	730.60	767.10	721.10	637.60	701.30	686.70
19	12	90	300	200	426.50	407.10	399.50	419.30	403.00	431.50	427.20	448.50	421.60	395.50	410.10	401.60
20	12	90	400	250	428.60	419.10	401.50	435.90	414.90	444.20	439.80	461.80	434.10	397.50	422.20	413.40
21	12	90	500	300	432.00	452.30	404.70	416.80	441.00	447.80	429.90	450.50	423.50	400.60	412.70	404.10
22	12	120	300	250	667.00	636.60	624.80	662.10	630.20	674.80	668.10	701.50	659.40	618.60	641.30	628.00
23	12	120	400	300	680.60	659.50	637.50	656.60	643.10	652.90	626.80	656.90	617.50	631.10	601.80	589.20
24	12	120	500	200	671.80	631.20	629.30	650.10	624.90	669.00	662.30	695.50	653.70	623.00	635.90	622.60
25	12	150	300	300	784.70	748.90	735.10	763.70	734.00	785.90	754.50	811.40	761.80	725.40	724.30	709.20
26	12	150	400	200	766.40	741.40	717.90	757.10	730.20	740.50	733.10	769.70	723.50	710.70	703.70	689.10
27	12	150	500	250	782.20	726.50	732.70	755.60	719.20	779.60	754.50	810.40	762.70	727.70	731.00	725.50

Material removal rate S/N ratios are presented in Table A2 of the Appendix A, where it is evident that with a material thickness of 4 mm the best combination of input parameters to achieve the highest MRR were 300 g/min of abrasive flow rate (*m<sub>a</sub>*), 300 MPa of waterjet pressure (*P*) and 150 mm/min of traverse speed (*V<sub>f</sub>*) for all types of profiles. This combination also achieved the highest MRR for 12 mm thickness, but only for cutting arc profiles. In AWJM of straight-line profiles for 12 mm AISI 304L, the best combination was 500 g/min of *m<sub>a</sub>*, 250 MPa of *P* and 150 mm/min of *V<sub>f</sub>*. This combination was also found to generate the highest MRR for 8 mm thickness of the target workpiece.

According to the results obtained via ANOVA for surface roughness detailed in Table 7, material thickness emerges as the most influencing input parameter, followed by waterjet pressure and abrasive mass flow rate with a percent contribution ranging 90.72–97.74%, 0.76–2.74% and 0.11–11%, respectively for all profiles. This is in agreement with the topographical features shown in Figures 1–9. Waterjet pressure impacts the distribution of water and jet abrasive particles during erosion processes. Similarly, waterjet pressure alongside abrasive flow rate indicates comparable performance within AWJM. According to this statistical analysis, traverse speed provided the least contribution, where it was dominated by material thickness with a percentage contribution from 0.08% to 1.165%. The effects of the parameters for all profiles demonstrate a similar trend, denoting that material thickness, waterjet pressure and abrasive mass flow rate are significant factors for acquiring *p*-values lower than 0.05, as detailed in Table 7. Accordingly, this study has revealed traverse speed to be insignificant for achieving *p*-values > 0.05, ranging from 0.090 to 0.575.

In reference to results obtained from ANOVA for material removal rate that are presented in Table 8, waterjet pressure and abrasive mass flow rate provided the minimal effect on MRR, with a percentage ranging 7.88–12.65% and 0.2–1.45% accordingly. Material thickness featured in the ANOVA as the utmost impacting factor, followed by traverse speed with a percent contribution ranging 65.55–78.17% and 13.15–18.62%, respectively for all profiles. The obtained *p*-values for material thickness, traverse speed and waterjet pressure were all less than 0.05, as illustrated in Table 8. Therefore, the influences of material thickness, waterjet pressure and traverse speed are all shown to be statistically significant. Contrastingly, abrasive mass flow rate achieved *p*-values ranging from 0.070 to 0.445, indicating an insignificant factor affecting material removal rate.



### 3.2. Optimisation with Taguchi S/N Ratio

The average S/N ratios shown in Table A3 in the Appendix A were attained from contour cutting of twelve different profiles with differing levels of selected input parameters. The lowest value of S/N ratio obtained for each factor represents the best experimental result. These express similar results to Table A1, indicating the optimal combination of input parameters as Level 1 for traverse speed and Level 3 for abrasive mass flow rate and waterjet pressure, set at 90 mm/min, 500 g/min and 300 MPa respectively. Table 9 summarizes the minimum value of surface roughness attained in abrasive waterjet contour cutting of AISI 304L, for three level material thicknesses for all profiles, according to the L<sub>27</sub> orthogonal array experiment setup.

**Table 9.** Optimum parameters for surface roughness.

Input Process Parameters	Optimum Values	Condition	Surface Roughness ( $\mu\text{m}$ )		
Abrasive flow rate (g/min)	500	↑	Condition: minimised		
Waterjet pressure (MPa)	300	↑	$t = 4 \text{ mm}$	$t = 8 \text{ mm}$	$t = 12 \text{ mm}$
Traverse speed (mm/min)	90	↓	1.142	1.529	1.993

The interaction of independent variables, i.e., material thickness ( $t$ ), abrasive flow rate ( $m_a$ ), waterjet pressure ( $P$ ), traverse speed ( $V_f$ ) on surface roughness ( $R_a$ ) were indicated in the main effect plots shown in Figure 13. The main effect plots display the means for each profile within a particular variable. The surface roughness was shown to decrease by approximately 10–20% as the value of the waterjet pressure increases and the abrasive mass flow rate from 200 MPa to 300 MPa and 300 g/min to 500 g/min, respectively. In AWJM, a higher level of waterjet pressure indicates an equivalent performance with abrasive mass flow rate [52]. An increasing water pressure along with the flow of abrasives, generates high velocity, resulting in a stronger impact of abrasive particles, which in turn decreases the roughness of the cut surface [53]. Hence, it is evident from the results of this study that increases in abrasive flow rate and waterjet pressure up until a particular level enhances the smoothening of cut surfaces.

Moreover, increasing the rate of traverse speed and thickness of a material increases the value of surface roughness. Surface roughness in this study was established to increase by approximately 50–60% as the level of material thickness and traverse speed increases from 4 mm to 12 mm and from 90 mm/min to 150 mm/min, respectively. The abrasive particles containing high kinetic energy occur at the initial strike and gradually decrease during the machining process [51]. Accordingly, reduced amounts of collision and cutting edges can be obtainable per unit of area over time, resulting in higher incidences of rough surfaces. Hence, it can be predicted that a lower level of traverse speed can yield a better-machined surface. Further, an increasing speed and thickness of a material denotes prolongment of the machining process, which continuously reduces the kinetic energy and generates higher roughness of a cut surface.

In the Taguchi method, the obtained S/N ratios are averaged to configure the optimum combination of parameters applicable for all conditions or profiles. Table A4 in the Appendix A presents the average S/N ratios calculated for each profile with different levels of input parameters, denoting that a traverse speed at level 3, an abrasive mass flow rate at level 3 and pressure at level 3 are the optimal combination of input parameters. Table 10 summarizes the optimum values input parameters and material removal rate obtained in abrasive waterjet contour cutting of AISI 304L, according to average S/N Ratios and the L<sub>27</sub> orthogonal array experiment setup.

The nomination of the optimal level of each input parameter is further evidenced by the main effect plots. Figure 14 shows the main effect plots for means in abrasive waterjet contour cutting of AISI 304L in terms of maximizing MRR. The figure shows that an increasing level of material thickness and traverse speed denotes an improvement of the rate of material removal for all profiles.



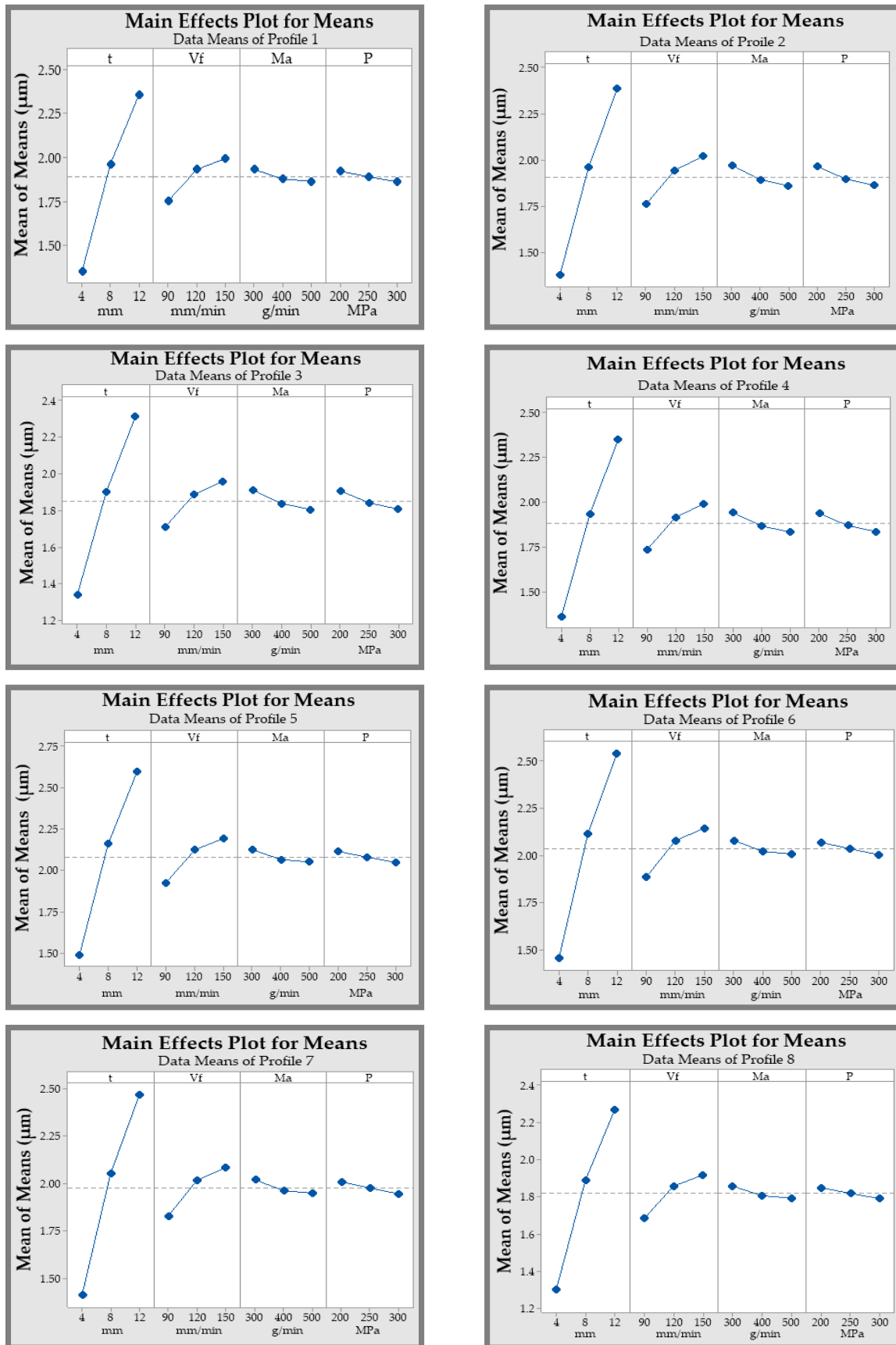


Figure 13. Cont.

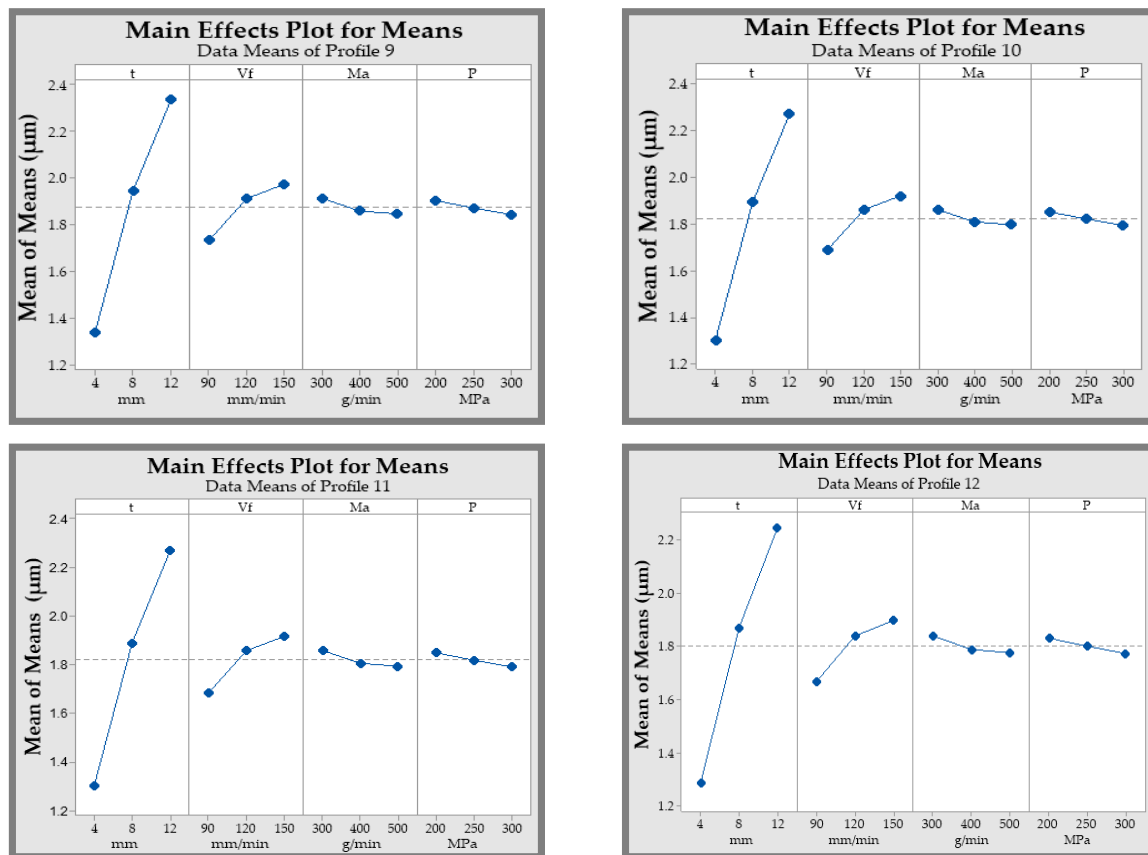


Figure 13. Main effect plot of means of surface roughness against input parameters.

Table 10. Optimum parameters for material removal rate.

Input Process Parameters	Optimum Values	Condition	Material Removal Rate (mm <sup>3</sup> /min)		
			t = 4 mm	t = 8 mm	t = 12 mm
Abrasive flow rate (g/min)	500	↑	Condition: maximised		
Waterjet pressure (MPa)	300	↑	421.2	767.1	811.4
Traverse speed (mm/min)	150	↑			

The material removal rate was shown to increase by approximately 70% when higher values of material thickness and traverse speed are used. AWJM is primarily processed by cohering action generated from the impacts of a large amount of abrasive particles in the direction of the target material [51]. In addition, material removal rate is directly proportional to abrasive mass flow rate and waterjet pressure. An increase of approximately 70% of material removal rate was obtained as the rate of abrasive mass flow rate and waterjet pressure were increased from 200 MPa to 300 MPa and 300 g/min to 500 g/min, respectively. AWJM of ductile material, such as AISI 304L, occurs via erosion generated by impinging abrasive particles from the waterjet stream. Generation of a high level of kinetic energy relating to a higher level of waterjet pressure generates higher erosion or cutting rate leading to a larger amount of material eroded from the workpiece [22]. Therefore, the rate of material removal is highly dictated by waterjet pressure and abrasive mass flow rate.



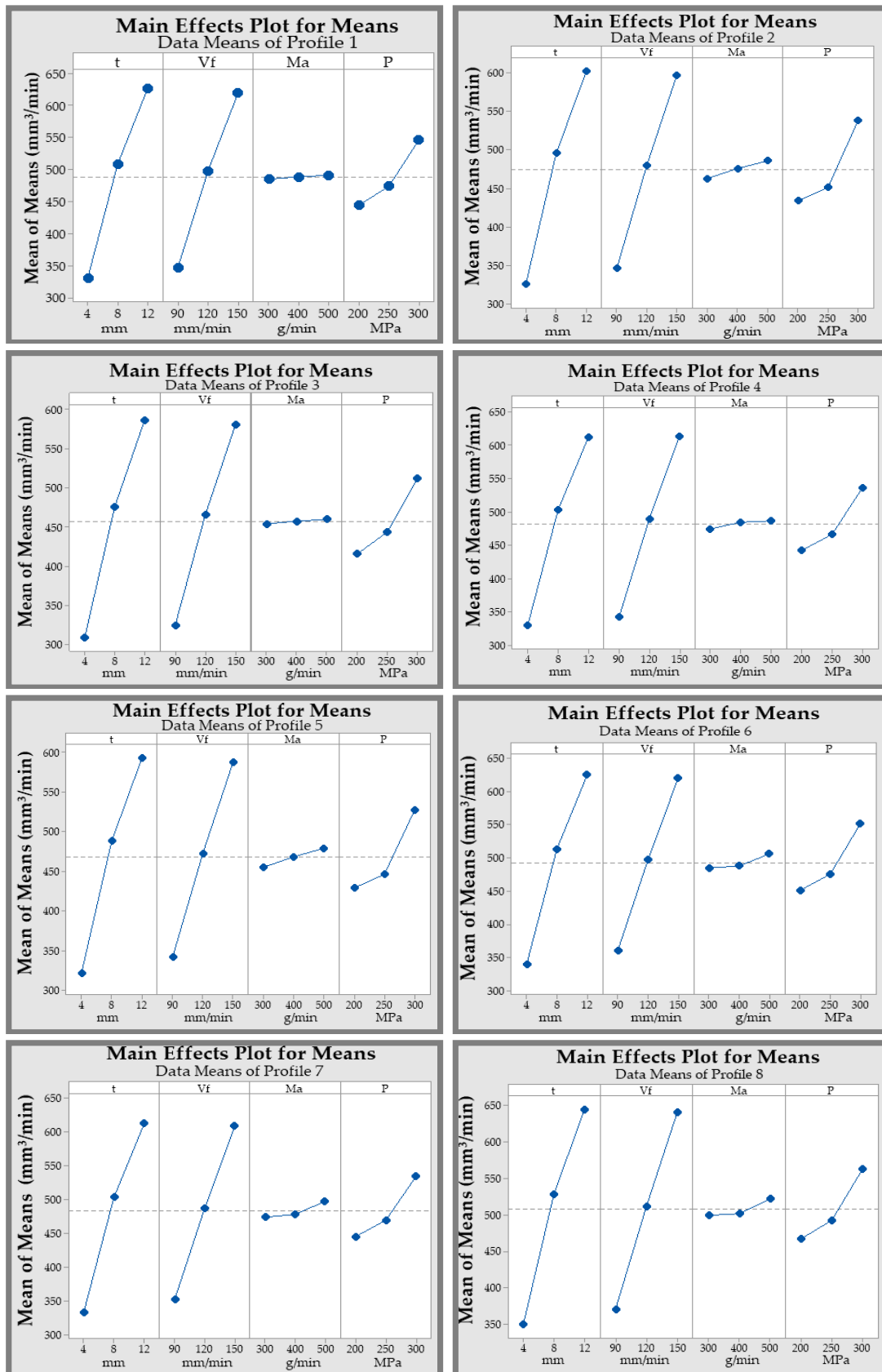


Figure 14. Cont.

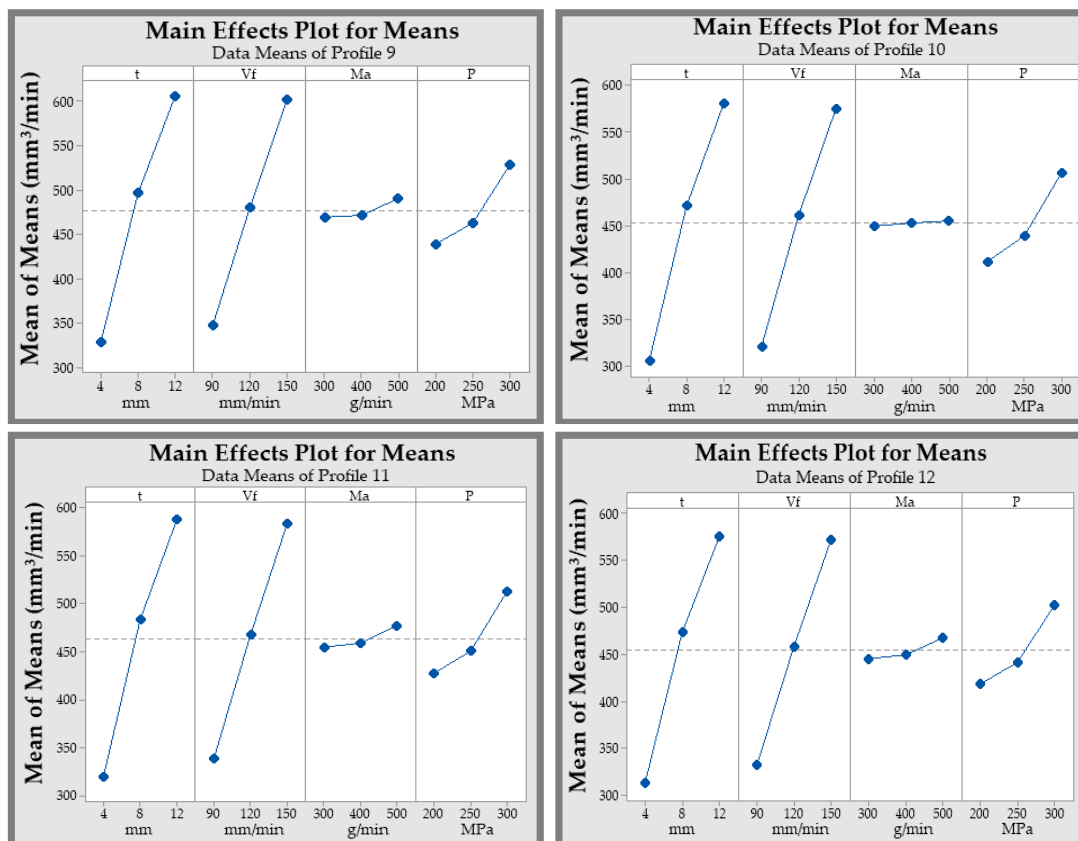


Figure 14. Main effect plot of means for material removal rate against input parameters.

#### 4. Confirmation Test

Validation of the optimal process parameters via a combination derived from the Taguchi methodology was established by confirmation experiments. Three sets of confirmatory test run for abrasive waterjet contour cutting of AISI 304L were conducted utilizing the derived optimal levels of traverse speed, abrasive mass flow rate and waterjet pressure based on the average S/N ratio.

The parametric combination of  $V_f$  at level 1 (90 mm/min),  $m_a$  at level 3 (500 g/min) and  $P$  at level 3 (300 MPa) achieved  $R_a$  values of 1.133  $\mu\text{m}$  for 4 mm, 1.372  $\mu\text{m}$  for 8 mm, and 1.901  $\mu\text{m}$  for 12 mm material thicknesses, demonstrating relative values to results achieved from the  $L_{27}$  orthogonal array experiment setup.

The derived optimal process parameter mix obtained to achieve maximum material removal rate was  $V_f$  at Level 3 (150 mm/min),  $m_a$  at Level 3 (500 g/min) and  $P$  at Level 3 (300 MPa) attaining MRR values of 425.4 mm<sup>3</sup>/min for 4 mm, 751.6 mm<sup>3</sup>/min for 8 mm, and 809.7 mm<sup>3</sup>/min for 12 mm material thicknesses.

#### 5. Conclusions

This article presents an optimization of abrasive waterjet contour cutting process parameters to minimize surface roughness and maximize material removal rate. In addition, the impacts of material thickness, traverse speed, waterjet pressure and abrasive mass flow rate were investigated, facilitating the process to achieve better surface integrity and machining rates. On the basis of Taguchi-based optimization and analysis of variance, the following conclusions were acquired:

- A minimum value of surface roughness achieved, where 1.142  $\mu\text{m}$  for 4 mm, 1.529  $\mu\text{m}$  for 8 mm, and 1.993  $\mu\text{m}$  for 12 mm material thicknesses according to  $L_{27}$  orthogonal array experiment setup. The average S/N ratios expressed similar results to all profiles, indicating the optimal combination of input parameters of Level 1 for traverse speed, Level 3 for abrasive mass flow rate and waterjet pressure at 90 mm/min, 500 g/min and 300 MPa respectively.
- The optimal settings observed for increasing material removal rate are traverse speed at Level 3 (150 mm/min), abrasive mass flow rate at Level 3 (500 g/min) and pressure at Level 3 (300 MPa). Increasing the value of these selected parameters was found to increase material thickness by approximately 70%.
- By employing analysis of variance, material thickness features as the most influencing and significant factor in governing responses on surface roughness and material removal rate, generating a contribution ranging 90.72–97.74% and 65.55–78.17% for all profiles, respectively.
- An increasing level of waterjet pressure and abrasive mass flow rate denotes an improvement in contour cutting performance by decreasing the surface roughness. In contrast, an increasing speed of traverse and material thickness drives a negative impact, whereby it increases the roughness of the cut surface.

**Author Contributions:** Conceptualization and methodology: M.T.-R., A.V., J.M.L. and M.A.; investigation and writing original draft: J.M.L.; review and supervision: M.T.-R., A.V., J.M.L. and M.A.; editing, project administration and software application: J.M.L. and M.A. All authors have read and agreed to the published version of the manuscript.

**Funding:** This research received an open access funding from School of Engineering, Edith Cowan University, Australia.

**Institutional Review Board Statement:** Not applicable.

**Informed Consent Statement:** Not applicable.

**Data Availability Statement:** Not applicable.

**Acknowledgments:** The authors would like to thank the School of Engineering, Edith Cowan University, Australia, for providing and administering the needed requirements in accomplishing this research. The authors would like to thank the technical staff, Adrian Davis for his assistance in experiments and Michael Stein for his assistance in writing structure and proficiency.

**Conflicts of Interest:** The authors declare no conflict of interest.

## Abbreviations and Nomenclature

$ht$	Depth of cut
$m_a$	Abrasive mass flow rate
$P$	Water pressure
$R_a$	Surface roughness
$V_f$	Traverse speed
$W$	Kerf width
$W_t$	Kerf top width
$W_b$	Kerf bottom width
$t$	Thickness of the material
AISI	Austenitic stainless steel
ANOVA	Analysis of variance
AWJM	Abrasive waterjet machining
MRR	Material removal rate

## Appendix A

Table A1. Signal-to-noise ratios for surface roughness (smaller is better).

Exp.	Input Parameters				Signal to Noise Ratios (S/NR = dB)												
	No.	<i>t</i> (mm)	<i>V<sub>f</sub></i> (mm/min)	<i>m<sub>a</sub></i> (g/min)	<i>P</i> (MPa)	Profiles											
						1	2	3	4	5	6	7	8	9	10	11	12
1	4	90	300	200		-2.265	-2.437	-2.173	-2.312	-3.093	-2.900	-2.648	-1.924	-2.178	-1.938	-1.924	-1.836
2	4	90	400	250		-1.980	-2.152	-1.887	-2.026	-2.808	-2.614	-2.362	-1.638	-1.892	-1.652	-1.638	-1.551
3	4	90	500	300		-1.584	-1.613	-1.348	-1.487	-2.411	-2.218	-1.966	-1.242	-1.496	-1.256	-1.242	-1.154
4	4	120	300	250		-2.910	-3.082	-2.818	-2.956	-3.738	-3.545	-3.292	-2.568	-2.823	-2.583	-2.568	-2.481
5	4	120	400	300		-2.574	-2.746	-2.482	-2.62	-3.402	-3.209	-2.957	-2.233	-2.487	-2.247	-2.233	-2.145
6	4	120	500	200		-2.916	-3.335	-3.070	-3.209	-3.744	-3.551	-3.299	-2.574	-2.829	-2.589	-2.574	-2.487
7	4	150	300	300		-3.215	-3.387	-3.123	-3.261	-4.043	-3.850	-3.598	-2.873	-3.128	-2.888	-2.873	-2.786
8	4	150	400	200		-3.082	-3.254	-2.990	-3.128	-3.910	-3.717	-3.465	-2.740	-2.995	-2.755	-2.740	-2.653
9	4	150	500	250		-2.929	-2.978	-2.714	-2.852	-3.757	-3.563	-3.311	-2.587	-2.841	-2.601	-2.587	-2.500
10	8	90	300	200		-5.511	-5.683	-5.418	-5.557	-6.339	-6.145	-5.893	-5.169	-5.424	-5.183	-5.169	-5.082
11	8	90	400	250		-5.225	-5.397	-5.133	-5.271	-6.053	-5.860	-5.607	-4.883	-5.138	-4.898	-4.883	-4.796
12	8	90	500	300		-4.829	-3.951	-3.687	-3.825	-5.657	-5.464	-5.211	-4.487	-4.742	-4.502	-4.487	-4.400
13	8	120	300	250		-6.155	-6.327	-6.063	-6.201	-6.983	-6.790	-6.538	-5.814	-6.068	-5.828	-5.814	-5.726
14	8	120	400	300		-5.820	-5.543	-5.278	-5.417	-6.648	-6.454	-6.202	-5.478	-5.732	-5.492	-5.478	-5.391
15	8	120	500	200		-6.162	-6.334	-6.069	-6.208	-6.99	-6.796	-6.544	-5.820	-6.074	-5.834	-5.820	-5.732
16	8	150	300	300		-6.461	-6.633	-6.368	-6.507	-7.289	-7.095	-6.843	-6.119	-6.373	-6.133	-6.119	-6.031
17	8	150	400	200		-6.328	-6.500	-6.235	-6.374	-7.156	-6.962	-6.710	-5.986	-6.240	-6.000	-5.986	-5.898
18	8	150	500	250		-6.174	-6.012	-5.747	-5.886	-7.002	-6.809	-6.556	-5.832	-6.087	-5.847	-5.832	-5.745
19	12	90	300	200		-7.102	-7.274	-7.009	-7.148	-7.930	-7.736	-7.484	-6.760	-7.014	-6.774	-6.760	-6.672
20	12	90	400	250		-6.816	-6.988	-6.723	-6.862	-7.644	-7.451	-7.198	-6.474	-6.729	-6.489	-6.474	-6.387
21	12	90	500	300		-6.420	-6.592	-6.327	-6.466	-7.248	-7.054	-6.802	-6.078	-6.333	-6.092	-6.078	-5.991
22	12	120	300	250		-7.746	-7.633	-7.369	-7.507	-8.574	-8.381	-8.129	-7.404	-7.659	-7.419	-7.404	-7.317
23	12	120	400	300		-7.411	-7.265	-7.000	-7.139	-8.238	-8.045	-7.793	-7.069	-7.323	-7.083	-7.069	-6.981
24	12	120	500	200		-7.753	-7.925	-7.660	-7.799	-8.58	-8.387	-8.135	-7.411	-7.665	-7.425	-7.411	-7.323
25	12	150	300	300		-8.052	-8.491	-8.227	-8.365	-8.879	-8.686	-8.434	-7.710	-7.964	-7.724	-7.710	-7.622
26	12	150	400	200		-7.919	-8.091	-7.826	-7.965	-8.746	-8.553	-8.301	-7.577	-7.831	-7.591	-7.577	-7.489
27	12	150	500	250		-7.765	-7.579	-7.314	-7.453	-8.593	-8.400	-8.147	-7.423	-7.678	-7.438	-7.423	-7.336

Table A2. Signal-to-noise ratios for material removal rate (larger is better).

Exp.	Input Parameters				Signal to Noise Ratios (S/NR = dB)												
	No.	<i>t</i> (mm)	<i>V<sub>f</sub></i> (mm/min)	<i>m<sub>a</sub></i> (g/min)	<i>P</i> (MPa)	Profiles											
						1	2	3	4	5	6	7	8	9	10	11	12
1	4	90	300	200		47.00	46.60	46.50	46.90	46.50	47.10	47.00	47.50	46.90	46.40	46.70	46.50
2	4	90	400	250		47.10	47.10	46.50	47.40	47.00	47.90	47.80	48.20	47.70	46.40	47.50	47.30
3	4	90	500	300		47.10	48.20	46.60	46.80	48.00	48.10	47.80	48.20	47.60	46.50	47.40	47.20
4	4	120	300	250		50.90	50.50	50.30	50.80	50.40	51.00	50.90	51.30	50.80	50.30	50.60	50.40
5	4	120	400	300		51.10	50.90	50.50	50.80	50.70	50.80	50.50	50.90	50.40	50.40	50.10	49.90
6	4	120	500	200		51.00	51.50	50.40	51.80	51.50	52.00	52.00	52.40	51.80	50.30	51.60	51.40
7	4	150	300	300		52.30	51.90	51.80	52.20	51.80	52.40	52.10	52.50	52.00	51.70	51.70	51.50
8	4	150	400	200		52.10	51.80	51.50	52.10	51.70	52.10	52.00	52.50	51.90	51.50	51.70	51.50
9	4	150	500	250		52.30	51.80	51.70	52.00	51.70	52.10	52.00	52.40	51.90	51.60	51.60	51.50
10	8	90	300	200		51.70	51.30	51.10	51.50	51.20	51.80	51.70	52.10	51.60	51.00	51.30	51.10
11	8	90	400	250		51.70	51.50	51.10	51.90	51.40	52.00	51.90	52.40	51.80	51.00	51.60	51.40
12	8	90	500	300		51.60	52.10	51.10	51.30	51.90	52.00	51.70	52.10	51.60	51.00	51.30	51.10
13	8	120	300	250		53.20	52.80	52.70	53.20	52.70	53.30	53.20	53.60	53.10	52.60	52.80	52.70
14	8	120	400	300		53.40	53.20	52.80	53.10	53.00	53.10	52.70	53.10	52.60	52.70	52.40	52.20
15	8	120	500	200		53.50	52.80	52.90	53.10	52.70	53.30	53.20	53.70	53.10	52.80	52.90	52.70
16	8	150	300	300		56.30	55.90	55.80	56.00	55.70	55.80	55.50	55.90	55.40	55.70	55.10	55.00
17	8	150	400	200		56.70	56.40	56.10	56.70	56.30	56.90	56.80	57.20	56.70	56.00	56.50	56.30
18	8	150	500	250		56.70	56.90	56.20	57.20	56.80	57.40	57.30	57.70	57.20	56.10	56.90	56.70
19	12	90	300	200		52.60	52.20	52.00	52.50	52.10	52.70	52.60	53.00	52.50	51.90	52.30	52.10
20	12	90	400	250		52.60	52.40	52.10	52.80	52.40	53.00	52.90	53.30	52.80	52.00	52.50	52.30
21	12	90	500	300		52.70	53.10	52.10	52.40	52.90	53.00	52.70	53.10	52.50	52.10	52.30	52.10
22	12	120	300	250		56.50	56.10	55.90	56.40	56.00	56.60	56.50	56.90	56.40	55.80	56.10	56.00
23	12	120	400	300		56.70	56.40	56.10	56.30	56.20	56.30	55.90	56.40	55.80	56.00	55.60	55.40
24	12	120	500	200		56.50	56.00	56.00	56.30	55.90	56.50	56.40	56.80	56.30	55.90	56.10	55.90
25	12	150	300	300		57.90	57.50	57.30	57.70	57.30	57.90	57.60	58.20	57.60	57.20	57.20	57.00
26	12	150	400	200		57.70	57.40	57.10	57.60	57.30	57.40	57.30	57.70	57.20	57.00	56.90	56.80
27	12	150	500	250		57.90	57.20	57.30	57.60	57.10	57.80	57.60	58.20	57.60	57.20	57.40	57.20

**Table A3.** Average response table for signal-to-noise ratios for surface roughness (smaller is better).

Profile 1				Profile 2				Profile 3				Profile 4				
Level	<i>t</i>	<i>V<sub>f</sub></i>	<i>m<sub>a</sub></i>	<i>P</i>	<i>t</i>	<i>V<sub>f</sub></i>	<i>m<sub>a</sub></i>	<i>P</i>	<i>t</i>	<i>V<sub>f</sub></i>	<i>m<sub>a</sub></i>	<i>P</i>	<i>t</i>	<i>V<sub>f</sub></i>	<i>m<sub>a</sub></i>	<i>P</i>
1	−2.606	−4.637	−5.491	−5.449	−2.776	−4.676	−5.661	−5.648	−2.512	−4.412	−5.396	−5.383	−2.650	−4.550	−5.535	−5.522
2	−5.852	−5.494	−5.239	−5.300	−5.820	−5.577	−5.326	−5.350	−5.555	−5.312	−5.062	−5.085	−5.694	−5.451	−5.200	−5.224
3	−7.442	−5.769	−5.170	−5.152	−7.537	−5.881	−5.146	−5.136	−7.273	−5.616	−4.882	−4.871	−7.411	−5.755	−5.020	−5.010
Delta	4.836	1.133	0.321	0.297	4.761	1.204	0.515	0.512	4.761	1.204	0.515	0.512	4.761	1.204	0.515	0.512
Rank	1	2	3	4	1	2	3	4	1	2	3	4	1	2	3	4
Profile 5				Profile 6				Profile 7				Profile 8				
Level	<i>t</i>	<i>V<sub>f</sub></i>	<i>m<sub>a</sub></i>	<i>P</i>	<i>t</i>	<i>V<sub>f</sub></i>	<i>m<sub>a</sub></i>	<i>P</i>	<i>t</i>	<i>V<sub>f</sub></i>	<i>m<sub>a</sub></i>	<i>P</i>	<i>t</i>	<i>V<sub>f</sub></i>	<i>m<sub>a</sub></i>	<i>P</i>
1	−3.434	−5.465	−6.319	−6.276	−3.241	−5.271	−6.125	−6.083	−2.989	−5.019	−5.873	−5.831	−2.264	−4.295	−5.149	−5.107
2	−6.679	−6.322	−6.067	−6.128	−6.486	−6.129	−5.874	−5.935	−6.234	−5.876	−5.622	−5.682	−5.510	−5.152	−4.897	−4.958
3	−8.270	−6.597	−5.998	−5.979	−8.077	−6.404	−5.805	−5.786	−7.825	−6.152	−5.552	−5.534	−7.101	−5.427	−4.828	−4.810
Delta	4.836	1.133	0.321	0.297	4.836	1.133	0.321	0.297	4.836	1.133	0.321	0.297	4.836	1.133	0.321	0.297
Rank	1	2	3	4	1	2	3	4	1	2	3	4	1	2	3	4
Profile 9				Profile 10				Profile 11				Profile 12				
Level	<i>t</i>	<i>V<sub>f</sub></i>	<i>m<sub>a</sub></i>	<i>P</i>	<i>t</i>	<i>V<sub>f</sub></i>	<i>m<sub>a</sub></i>	<i>P</i>	<i>t</i>	<i>V<sub>f</sub></i>	<i>m<sub>a</sub></i>	<i>P</i>	<i>t</i>	<i>V<sub>f</sub></i>	<i>m<sub>a</sub></i>	<i>P</i>
1	−2.519	−4.550	−5.404	−5.361	−2.264	−4.295	−5.149	−5.107	−2.177	−4.208	−5.062	−5.019	−2.279	−4.309	−5.164	−5.121
2	−5.764	−5.407	−5.152	−5.213	−5.510	−5.152	−4.897	−4.958	−5.422	−5.065	−4.810	−4.871	−5.524	−5.167	−4.912	−4.973
3	−7.355	−5.682	−5.083	−5.064	−7.101	−5.427	−4.828	−4.810	−7.013	−5.340	−4.741	−4.722	−7.115	−5.442	−4.843	−4.824
Delta	4.836	1.133	0.321	0.297	4.836	1.133	0.321	0.297	4.836	1.133	0.321	0.297	4.836	1.133	0.321	0.297
Rank	1	2	3	4	1	2	3	4	1	2	3	4	1	2	3	4

**Table A4.** Average response table for signal-to-noise ratios for material removal rate (larger is better).

Profile 1				Profile 2				Profile 3				Profile 4				
Level	<i>t</i>	<i>V<sub>f</sub></i>	<i>m<sub>a</sub></i>	<i>P</i>	<i>t</i>	<i>V<sub>f</sub></i>	<i>m<sub>a</sub></i>	<i>P</i>	<i>t</i>	<i>V<sub>f</sub></i>	<i>m<sub>a</sub></i>	<i>P</i>	<i>t</i>	<i>V<sub>f</sub></i>	<i>m<sub>a</sub></i>	<i>P</i>
1	50.10	50.46	53.16	52.44	50.05	50.50	52.76	52.28	49.53	49.90	52.59	51.87	50.09	50.38	52.99	52.42
2	53.87	53.64	53.22	53.04	53.66	53.36	53.02	52.66	53.30	53.07	52.66	52.47	53.77	53.53	53.18	52.95
3	55.68	55.55	53.26	54.17	55.37	55.21	53.30	54.14	55.11	54.98	52.69	53.61	55.50	55.44	53.18	53.98
Delta	5.58	5.08	0.10	1.74	5.32	4.71	0.54	1.86	5.58	5.08	0.10	1.74	5.41	5.06	0.20	1.55
Rank	1	2	4	3	1	2	4	3	1	2	4	3	1	2	4	3
Profile 5				Profile 6				Profile 7				Profile 8				
Level	<i>t</i>	<i>V<sub>f</sub></i>	<i>m<sub>a</sub></i>	<i>P</i>	<i>t</i>	<i>V<sub>f</sub></i>	<i>m<sub>a</sub></i>	<i>P</i>	<i>t</i>	<i>V<sub>f</sub></i>	<i>m<sub>a</sub></i>	<i>P</i>	<i>t</i>	<i>V<sub>f</sub></i>	<i>m<sub>a</sub></i>	<i>P</i>
1	49.92	50.37	52.63	52.18	50.41	50.85	53.18	52.64	50.23	50.68	53.01	52.52	50.65	51.09	53.45	52.94
2	53.53	53.23	52.89	52.56	53.96	53.67	53.28	53.12	53.79	53.49	53.11	53.00	54.20	53.91	53.53	53.42
3	55.24	55.08	53.17	53.95	55.69	55.54	53.59	54.30	55.51	55.37	53.42	54.01	55.96	55.81	53.83	54.44
Delta	5.32	4.71	0.54	1.77	5.28	4.69	0.41	1.67	5.28	4.69	0.41	1.49	5.30	4.72	0.38	1.50
Rank	1	2	4	3	1	2	4	3	1	2	4	3	1	2	4	3
Profile 9				Profile 10				Profile 11				Profile 12				
Level	<i>t</i>	<i>V<sub>f</sub></i>	<i>m<sub>a</sub></i>	<i>P</i>	<i>t</i>	<i>V<sub>f</sub></i>	<i>m<sub>a</sub></i>	<i>P</i>	<i>t</i>	<i>V<sub>f</sub></i>	<i>m<sub>a</sub></i>	<i>P</i>	<i>t</i>	<i>V<sub>f</sub></i>	<i>m<sub>a</sub></i>	<i>P</i>
1	50.11	50.56	52.91	52.41	49.45	49.81	52.51	51.78	49.88	50.32	52.65	52.17	49.70	50.14	52.47	51.98
2	53.67	53.37	52.99	52.89	53.22	52.98	52.57	52.38	53.43	53.13	52.75	52.65	53.25	52.95	52.57	52.46
3	55.42	55.27	53.30	53.91	55.02	54.89	52.61	53.52	55.16	55.01	53.06	53.65	54.97	54.83	52.88	53.47
Delta	5.30	4.72	0.38	1.50	5.58	5.08	0.10	1.74	5.28	4.69	0.41	1.49	5.28	4.69	0.41	1.49
Rank	1	2	4	3	1	2	4	3	1	2	4	3	1	2	4	3

## References

- Miao, X.; Wu, M.; Qiang, Z.; Wang, Q.; Miao, X. Study on optimization of a simulation method for abrasive water jet machining. *Int. J. Adv. Manuf. Technol.* **2017**, *93*, 587–593. [[CrossRef](#)]
- Alsoufi, M.S. State-of-the-art in abrasive water jet cutting technology and the promise for micro-and nano-machining. *Int. J. Mech. Eng. Appl.* **2017**, *5*, 1. [[CrossRef](#)]
- El-Domiaty, A.; Shabara, M.; Abdel-Rahman, A.; Al-Sabeeh, A. On the modelling of abrasive waterjet cutting. *Int. J. Adv. Manuf. Technol.* **1996**, *12*, 255–265. [[CrossRef](#)]
- Radovanovic, M. Multi-Objective Optimization of Abrasive Water Jet Cutting Using MOGA. *Procedia Manuf.* **2020**, *47*, 781–787. [[CrossRef](#)]
- Kechagias, J.; Petropoulos, G.; Vaxevanidis, N. Application of Taguchi design for quality characterization of abrasive water jet machining of TRIP sheet steels. *Int. J. Adv. Manuf. Technol.* **2012**, *62*, 635–643. [[CrossRef](#)]

6. Veerappan, G.; Ravichandran, M. Experimental investigations on abrasive water jet machining of nickel-based superalloy. *J. Braz. Soc. Mech. Sci. Eng.* **2019**, *41*, 1–12. [[CrossRef](#)]
7. Begic-Hajdarevic, D.; Cekic, A.; Mehmedovic, M.; Djelmic, A. Experimental study on surface roughness in abrasive water jet cutting. *Procedia Eng.* **2015**, *100*, 394–399. [[CrossRef](#)]
8. Bhandarkar, V.; Singh, V.; Gupta, T. Experimental analysis and characterization of abrasive water jet machining of Inconel 718. *Mater. Today Proc.* **2020**, *23*, 647–650. [[CrossRef](#)]
9. Lehocka, D.; Botko, F.; Klich, J.; Sitek, L.; Hvizdos, P.; Fides, M.; Cep, R. Effect of pulsating water jet disintegration on hardness and elasticity modulus of austenitic stainless steel AISI 304L. *Int. J. Adv. Manuf. Technol.* **2020**, *107*, 1–12. [[CrossRef](#)]
10. Supriya, S.; Srinivas, S. Machinability studies on stainless steel by abrasive water jet-Review. *Mater. Today Proc.* **2018**, *5*, 2871–2876. [[CrossRef](#)]
11. Desu, R.K.; Krishnamurthy, H.N.; Balu, A.; Gupta, A.K.; Singh, S.K. Mechanical properties of Austenitic Stainless Steel 304L and 316L at elevated temperatures. *J. Mater. Res. Technol.* **2016**, *5*, 13–20. [[CrossRef](#)]
12. Barabas, S.A.; Florescu, A. Optimization Method of Abrasive Water Jet Cutting of Welded Overlay Materials. *Metals* **2019**, *9*, 1046. [[CrossRef](#)]
13. Kuntoğlu, M.; Acar, O.; Gupta, M.K.; Sağlam, H.; Sarikaya, M.; Giasin, K.; Pimenov, D.Y. Parametric Optimization for Cutting Forces and Material Removal Rate in the Turning of AISI 5140. *Machines* **2021**, *9*, 90. [[CrossRef](#)]
14. Kuntoğlu, M.; Aslan, A.; Pimenov, D.Y.; Giasin, K.; Mikolajczyk, T.; Sharma, S. Modeling of cutting parameters and tool geometry for multi-criteria optimization of surface roughness and vibration via response surface methodology in turning of AISI 5140 steel. *Materials* **2020**, *13*, 4242. [[CrossRef](#)]
15. Natarajan, Y.; Murugesan, P.K.; Mohan, M.; Khan, S.A.L.A. Abrasive Water Jet Machining process: A state of art of review. *J. Manuf. Process.* **2020**, *49*, 271–322. [[CrossRef](#)]
16. Aamir, M.; Giasin, K.; Tolouei-Rad, M.; Vafadar, A. A review: Drilling performance and hole quality of aluminium alloys for aerospace applications. *J. Mater. Res. Technol.* **2020**, *9*, 12484–12500. [[CrossRef](#)]
17. Sutowska, M.; Kapłonek, W.; Pimenov, D.Y.; Gupta, M.K.; Mia, M.; Sharma, S. Influence of variable radius of cutting head trajectory on quality of cutting kerf in the abrasive water jet process for soda–lime glass. *Materials* **2020**, *13*, 4277. [[CrossRef](#)]
18. Liu, X.; Liang, Z.; Wen, G.; Yuan, X. Waterjet machining and research developments: A review. *Int. J. Adv. Manuf. Technol.* **2019**, *102*, 1257–1335. [[CrossRef](#)]
19. Singh, D.; Chaturvedi, V. Investigation of optimal processing condition for abrasive water jet machining for stainless steel AISI 304 using grey relational analysis coupled with S/N ratio. *Appl. Mech. Mater.* **2014**, *592–594*, 438–443. [[CrossRef](#)]
20. Löschner, P.; Jarosz, K.; Niesłony, P. Investigation of the effect of cutting speed on surface quality in abrasive water jet cutting of 316L stainless steel. *Procedia Eng.* **2016**, *149*, 276–282. [[CrossRef](#)]
21. Karthik, K.; Sundarsingh, D.S.; Harivignesh, M.; Karthick, R.G.; Praveen, M. Optimization of machining parameters in abrasive water jet cutting of stainless steel 304. *Mater. Today Proc.* **2021**, *46*, 1384–1389. [[CrossRef](#)]
22. Kmec, J.; Gombár, M.; Harničárová, M.; Valíček, J.; Kušnerová, M.; Kříž, J.; Kadnár, M.; Karková, M.; Vagaská, A. The Predictive Model of Surface Texture Generated by Abrasive Water Jet for Austenitic Steels. *Appl. Sci.* **2020**, *10*, 3159. [[CrossRef](#)]
23. Hlaváč, L.M.; Hlaváčová, I.M.; Geryk, V.; Plančar, Š. Investigation of the taper of kerfs cut in steels by AWJ. *Int. J. Adv. Manuf. Technol.* **2015**, *77*, 1811–1818. [[CrossRef](#)]
24. Aamir, M.; Tu, S.; Tolouei-Rad, M.; Giasin, K.; Vafadar, A. Optimization and modeling of process parameters in multi-hole simultaneous drilling using taguchi method and fuzzy logic approach. *Materials* **2020**, *13*, 680. [[CrossRef](#)] [[PubMed](#)]
25. Lin, C. Use of the Taguchi method and grey relational analysis to optimize turning operations with multiple performance characteristics. *Mater. Manuf. Process.* **2004**, *19*, 209–220. [[CrossRef](#)]
26. Maneiah, D.; Shunmugasundaram, M.; Reddy, A.R.; Begum, Z. Optimization of machining parameters for surface roughness during abrasive water jet machining of aluminium/magnesium hybrid metal matrix composites. *Mater. Today Proc.* **2020**, *27*, 1293–1298. [[CrossRef](#)]
27. Sharma, M.K.; Chaudhary, H.; Kumar, A. Optimization of abrasive waterjet machining process parameters on aluminium AL-6061. *Int. J. Sci. Res.* **2017**, *6*, 869–874.
28. Otto, K.N.; Antonsson, E.K. Extensions to the Taguchi method of product design. *J. Mech. Des.* **1993**, *115*, 5–13. [[CrossRef](#)]
29. Jiang, W.; Cao, Y.; Jiang, Y.; Liu, Y.; Mao, Q.; Zhou, H.; Liao, X.; Zhao, Y. Effects of nanostructural hierarchy on the hardness and thermal stability of an austenitic stainless steel. *J. Mater. Res. Technol.* **2021**, *12*, 376–384. [[CrossRef](#)]
30. Kaladhar, M.; Subbaiah, K.V.; Rao, C.S. Machining of austenitic stainless steels—A review. *Int. J. Mach. Mach. Mater.* **2012**, *12*, 178–192. [[CrossRef](#)]
31. Ramana, M.V.; Kumar, B.R.; Krishna, M.; Rao, M.V.; Kumar, V. Optimization and influence of process parameters of dissimilar SS304L–SS430 joints produced by Robotic TIG welding. *Mater. Today Proc.* **2020**, *23*, 479–482. [[CrossRef](#)]
32. Llanto, J.M.; Tolouei-Rad, M.; Vafadar, A.; Aamir, M. Impacts of Traverse Speed and Material Thickness on Abrasive Waterjet Contour Cutting of Austenitic Stainless Steel AISI 304L. *Appl. Sci.* **2021**, *11*, 4925. [[CrossRef](#)]
33. Wang, S.; Zhang, S.; Wu, Y.; Yang, F. A key parameter to characterize the kerf profile error generated by abrasive water-jet. *Int. J. Adv. Manuf. Technol.* **2017**, *90*, 1265–1275. [[CrossRef](#)]
34. Pawar, P.J.; Vidhate, U.S.; Khalkar, M.Y. Improving the quality characteristics of abrasive water jet machining of marble material using multi-objective artificial bee colony algorithm. *J. Comput. Des. Eng.* **2018**, *5*, 319–328. [[CrossRef](#)]

35. Hlavac, L.M.; Hlavacova, I.M.; Arleo, F.; Vigano, F.; Annoni, M.P.G.; Geryk, V. Shape distortion reduction method for abrasive water jet (AWJ) cutting. *Precis. Eng.* **2018**, *53*, 194–202. [[CrossRef](#)]
36. Kumar, R.; Chattopadhyaya, S.; Dixit, A.R.; Bora, B.; Zelenak, M.; Foldyna, J.; Hloch, S.; Hlavacek, P.; Scucka, J.; Klich, J. Surface integrity analysis of abrasive water jet-cut surfaces of friction stir welded joints. *Int. J. Adv. Manuf. Technol.* **2017**, *88*, 1687–1701. [[CrossRef](#)]
37. Uthayakumar, M.; Khan, M.A.; Kumaran, S.T.; Slota, A.; Zajac, J. Machinability of nickel-based superalloy by abrasive water jet machining. *Mater. Manuf. Process.* **2016**, *31*, 1733–1739. [[CrossRef](#)]
38. Rao, R.V.; Rai, D.P.; Balic, J. Multi-objective optimization of abrasive waterjet machining process using Jaya algorithm and PROMETHEE Method. *J. Intell. Manuf.* **2019**, *30*, 2101–2127. [[CrossRef](#)]
39. Khan, M.A.; Gupta, K. Machinability Studies on Abrasive Water Jet Machining of Low Alloy Steel for Different Thickness. *IOP Conf. Ser. Mater. Sci. Eng.* **2020**, *709*, 044099. [[CrossRef](#)]
40. Llanto, J.M.; Tolouei-Rad, M.; Vafadar, A.; Aamir, M. Recent Progress Trend on Abrasive Waterjet Cutting of Metallic Materials: A Review. *Appl. Sci.* **2021**, *11*, 3344. [[CrossRef](#)]
41. Gnanavelbabu, A.; Saravanan, P.; Rajkumar, K.; Karthikeyan, S. Experimental investigations on multiple responses in abrasive waterjet machining of Ti-6Al-4V alloy. *Mater. Today Proc.* **2018**, *5*, 13413–13421. [[CrossRef](#)]
42. Barad, M. Taguchi Experimental-Design Techniques—Revisited. In *Transformation of Science and Technology into Productive Power, Supplement*; Taylor & Francis Ltd.: Oxfordshire, UK, 1991; pp. 1101–1104.
43. Patel Gowdru Chandrashekarappa, M.; Kumar, S.; Pimenov, D.Y.; Giasin, K. Experimental Analysis and Optimization of EDM Parameters on HcHcr Steel in Context with Different Electrodes and Dielectric Fluids Using Hybrid Taguchi-Based PCA-Utility and CRITIC-Utility Approaches. *Metals* **2021**, *11*, 419. [[CrossRef](#)]
44. Aamir, M.; Tolouei-Rad, M.; Giasin, K.; Vafadar, A. Machinability of Al2024, Al6061, and Al5083 alloys using multi-hole simultaneous drilling approach. *J. Mater. Res. Technol.* **2020**, *9*, 10991–11002. [[CrossRef](#)]
45. Aamir, M.; Giasin, K.; Tolouei-Rad, M.; Ud Din, I.; Hanif, M.I.; Kuklu, U.; Pimenov, D.Y.; Ikhlaq, M. Effect of Cutting Parameters and Tool Geometry on the Performance Analysis of One-Shot Drilling Process of AA2024-T3. *Metals* **2021**, *11*, 854. [[CrossRef](#)]
46. Aamir, M.; Tolouei-Rad, M.; Giasin, K.; Vafadar, A. Feasibility of tool configuration and the effect of tool material, and tool geometry in multi-hole simultaneous drilling of Al2024. *Int. J. Adv. Manuf. Technol.* **2020**, *111*, 861–879. [[CrossRef](#)]
47. Sasikumar, K.; Arulshri, K.; Ponappa, K.; Uthayakumar, M. A study on kerf characteristics of hybrid aluminium 7075 metal matrix composites machined using abrasive water jet machining technology. *Proc. Inst. Mech. Eng. Part B J. Eng. Manuf.* **2018**, *232*, 690–704. [[CrossRef](#)]
48. Yu, Y.; Sun, T.; Yuan, Y.; Gao, H.; Wang, X. Experimental investigation into the effect of abrasive process parameters on the cutting performance for abrasive waterjet technology: A case study. *Int. J. Adv. Manuf. Technol.* **2020**, *107*, 2757–2765. [[CrossRef](#)]
49. Selvan, M.C.P.; Raju, N.M.S.; Sachidananda, H. Effects of process parameters on surface roughness in abrasive waterjet cutting of aluminium. *Front. Mech. Eng.* **2012**, *7*, 439–444. [[CrossRef](#)]
50. Thamizhvalavan, P.; Arivazhagan, S.; Yuvaraj, N.; Ramesh, B. Machinability study of abrasive aqua jet parameters on hybrid metal matrix composite. *Mater. Manuf. Process.* **2019**, *34*, 321–344. [[CrossRef](#)]
51. Ishfaq, K.; Ahmad Mufti, N.; Ahmed, N.; Pervaiz, S. Abrasive waterjet cutting of clad material: Kerf taper and MRR analysis. *Mater. Manuf. Process.* **2019**, *34*, 544–553. [[CrossRef](#)]
52. Hashish, M. Optimization Factors in Abrasive-Waterjet Machining. *J. Eng. Ind. ASME* **1991**, *113*, 29–37. [[CrossRef](#)]
53. Liu, S.; Zhou, F.; Li, H.; Chen, Y.; Wang, F.; Guo, C. Experimental Investigation of Hard Rock Breaking Using a Conical Pick Assisted by Abrasive Water Jet. *Rock Mech. Rock Eng.* **2020**, *59*, 1–10. [[CrossRef](#)]

Chapter 5 is not available in this version of the Thesis as it is intended for publication.



## Chapter 6 Conclusion and potential future work

This chapter provides overall conclusions based on end of chapter conclusions given for each chapter. It also provides directions for future work in this research.

### 6.1 Conclusions

Establishing solution/s to the challenges faced with abrasive waterjet contour cutting of hard-to-machine materials has been the main objective of this work, where the optimisation approach leads to addressing quality and productivity issues. In this research work, the impacts of the independent input parameters i.e., traverse speed, abrasive mass flow rate and waterjet pressure against the AWJM material responses was performed in a manner where material removal rate, surface roughness and kerf taper angle during contouring of austenitic stainless steel 304L were investigated. The research achievements and findings are summarised below:

1. AWJM demonstrated similar trends of higher occurrences of roughness on the cut surface and kerf taper angle at an increasing rate of traverse speed and material thickness during machining curvature and straight line profiles of AISI 304L workpieces. This AWJM behavior denotes an unfavourable impact during application of a higher rate of traverse speed, in terms of surface roughness and kerf geometries. In contrast, an increasing value of traverse speed was recognised to be more effective in obtaining a higher material removal rate. The contour cutting performance of AWJM was established to achieve a higher rate of material removal, lower roughness on the cut surface and lower tapering angle of the kerf at a higher level of abrasive mass flow rate and waterjet pressure. The incrementing value of waterjet pressure denotes a higher energy reinforcing a larger amount of abrasive particles and acceleration of abrasive flow, which results in higher machining rates and higher quality of cut surfaces. The experimental study reveals that AWJM material responses were mainly influenced by material thickness. Initially, the abrasive waterjet comprised of high kinetic energy containing a large amount of abrasive particles gradually decreases as the thickness of the material increased, resulting in challenges encountered with the machining process.
2. With the objective of achieving higher productivity and better integrity of the cut surface, a single response optimisation using the Taguchi method was employed. The surface roughness conferred a reduction of approximately 10–20%, while material removal rate increased by approximately 60–80%. The experimental investigation indicates that traverse speed is one of the most influencing factors followed by the waterjet pressure

and abrasive mass flow rate in AWJM contour cutting performance. The effects of the input parameters on straight line and curvature profiles using three levels of material thicknesses exhibited the same response, showing that traverse speed and waterjet pressure were significant factors in machining of AISI 304L using abrasive waterjet cutting.

3. The selected responses are simultaneously optimised with the objectives of maximising material removal rate and minimising kerf taper angle and surface roughness. In order to properly select the suitable process parameters, a multi-linear regression model has been generated. The model has proven its adequacy by achieving percentage errors with values ranging from -6.59% to 6.71%, indicating that the predicted values correlate well with the experimental data. The predictive models for surface roughness, material removal rate and kerf taper angle were employed for multi-objective optimisation using response surface methodology. The input parameters optimal settings ( $V_f$ ) for 4 mm, 8 mm and 12 mm material thicknesses were respective 95 mm/min, 90 mm/min and 91 mm/min. The optimal settings for  $m_a$  and  $P$  were distinguished to be at the same value across all material thicknesses, at 500 g/min and 200 MPa, respectively. These results and key findings can be a basis for process planning to efficiently and effectively utilise abrasive waterjet as a feasible solution in the machining of difficult-to-cut materials.
4. Overall, this research work has proved the feasibility of utilising abrasive waterjet in contour cutting of hard to machine workpieces of varied thicknesses, confirming its distinct advantages such as, the absence of heat affected zone and lower cutting forces that may prevent destruction of the properties of the target material.

## 6.2 Potential future work

This research work has yielded a greater understanding of the mechanisms involved in machining process and has assisted in the optimisation of this process. The characteristics and behaviour of the various major machining performance measures, with respect to the variable process parameters, have been comprehensively analysed. However, the industrial utilisation of AWJM requires further progressions and improvements. After taking into consideration the discoveries found in this study, several potential future research areas are summarised below:

1. A number of noteworthy works have been fulfilled in evaluating AWJM performance in terms of quality and productivity. Further research could progress for optimisation governing mathematical modelling with an objective of minimising manufacturing cost.

The authors are currently working in this research area that is beyond the scope of this thesis.

2. There are limited studies considering other factors such as various type and size of abrasives, nozzle sizes and jet impact angle. Further study investigating the impacts of these critical parameters can provide prospective future works
3. There are numerous research studies and experiments conducted investigating through cut of AWJMs. Nonetheless, limited reports have manifested about AWJM performance in non-through or blind cutting for high machinability index materials, which is a potential area of further development. Providing an analytical study of the impacts of the process parameters in AWJ blind cutting would be essential to manufacturing processes in various industries.

# APPENDIX A Data for impacts of traverse speed and material thickness in AWJ contour cutting tests

Table A1. Kerf top width and kerf bottom width results.

Material Thickness (mm)	Traverse Speed (mm/min)	Profile 1		Profile 2		Profile 3		Profile 4	
		Wt (mm)	W <sub>b</sub> (mm)	Wt (mm)	W <sub>b</sub> (mm)	Wt (mm)	W <sub>b</sub> (mm)	Wt (mm)	W <sub>b</sub> (mm)
4	90	0.61	0.44	0.62	0.44	0.63	0.46	0.64	0.46
4	120	0.64	0.46	0.67	0.48	0.66	0.48	0.67	0.48
4	150	0.67	0.48	0.68	0.49	0.67	0.48	0.68	0.49
8	90	0.68	0.29	0.67	0.28	0.69	0.3	0.69	0.3
8	120	0.69	0.3	0.68	0.29	0.69	0.3	0.7	0.3
8	150	0.7	0.3	0.69	0.29	0.7	0.3	0.71	0.31
12	90	0.7	0.1	0.7	0.1	0.69	0.1	0.71	0.11
12	120	0.72	0.11	0.72	0.1	0.71	0.11	0.73	0.12
12	150	0.74	0.12	0.73	0.11	0.72	0.12	0.74	0.12
Material Thickness (mm)	Traverse Speed (mm/min)	Profile 5		Profile 6		Profile 7		Profile 8	
		Wt (mm)	W <sub>b</sub> (mm)	Wt (mm)	W <sub>b</sub> (mm)	Wt (mm)	W <sub>b</sub> (mm)	Wt (mm)	W <sub>b</sub> (mm)
4	90	0.63	0.45	0.64	0.48	0.61	0.44	0.61	0.44
4	120	0.66	0.47	0.67	0.49	0.64	0.47	0.64	0.46
4	150	0.67	0.48	0.68	0.5	0.67	0.49	0.67	0.48
8	90	0.68	0.29	0.69	0.29	0.68	0.26	0.68	0.28
8	120	0.69	0.29	0.7	0.29	0.69	0.28	0.69	0.28
8	150	0.7	0.3	0.71	0.3	0.7	0.29	0.7	0.29
12	90	0.7	0.1	0.72	0.1	0.7	0.11	0.7	0.1
12	120	0.71	0.1	0.73	0.11	0.72	0.12	0.72	0.1
12	150	0.72	0.11	0.74	0.11	0.74	0.13	0.74	0.12
Material Thickness (mm)	Traverse Speed (mm/min)	Profile 9		Profile 10		Profile 11		Profile 12	
		Wt (mm)	W <sub>b</sub> (mm)	Wt (mm)	W <sub>b</sub> (mm)	Wt (mm)	W <sub>b</sub> (mm)	Wt (mm)	W <sub>b</sub> (mm)
4	90	0.56	0.42	0.56	0.42	0.55	0.4	0.54	0.39
4	120	0.57	0.42	0.58	0.42	0.56	0.39	0.55	0.38
4	150	0.58	0.42	0.6	0.44	0.58	0.4	0.56	0.39
8	90	0.66	0.36	0.67	0.34	0.65	0.3	0.63	0.28
8	120	0.67	0.35	0.69	0.35	0.68	0.31	0.65	0.29
8	150	0.68	0.34	0.69	0.35	0.69	0.32	0.67	0.31
12	90	0.69	0.12	0.67	0.11	0.69	0.13	0.69	0.12
12	120	0.7	0.12	0.71	0.12	0.71	0.14	0.7	0.13
12	150	0.71	0.12	0.72	0.13	0.72	0.15	0.72	0.14

Table A2. Analysis of variance of kerf taper angle.

ANOVA:	Profile 1		Profile 2		Profile 3		Profile 4		Profile 5		Profile 6	
Source	Contribution	p-Value	Contribution	p-Value	Contribution	p-Value	Contribution	p-Value	Contribution	p-Value	Contribution	p-Value
Model	88.85%	0.035	95.64%	0.006	82.89%	0.078	94.26%	0.01	95.94%	0.005	95.90%	0.005
Linear	88.85%	0.035	95.64%	0.006	82.89%	0.078	94.26%	0.01	95.94%	0.005	95.90%	0.005
Materials thickness	71.14%	0.018	80.45%	0.003	68.62%	0.04	80.95%	0.004	82.03%	0.002	90.71%	0.002
Transverse speed	17.71%	0.149	15.19%	0.05	14.27%	0.297	13.31%	0.091	13.91%	0.051	5.20%	0.194
Error	11.15%		4.36%		17.11%		5.74%		4.06%		4.10%	
Total	100.00%		100.00%		100.00%		100.00%		100.00%		100.00%	
ANOVA:	Profile 7		Profile 8		Profile 9		Profile 10		Profile 11		Profile 12	
Source	Contribution	p-Value	Contribution	p-Value	Contribution	p-Value	Contribution	p-Value	Contribution	p-Value	Contribution	p-Value
Model	95.63%	0.006	94.30%	0.009	99.15%	0	97.67%	0.002	90.37%	0.026	96.50%	0.004
Linear	95.63%	0.006	94.30%	0.009	99.15%	0	97.67%	0.002	90.37%	0.026	96.50%	0.004
Materials thickness	87.04%	0.002	80.63%	0.004	90.39%	0	89.09%	0.001	67.56%	0.016	87.23%	0.001
Transverse speed	8.59%	0.114	13.67%	0.087	8.76%	0.008	8.58%	0.046	22.81%	0.088	9.27%	0.075
Error	4.37%		5.70%		0.85%		2.33%		9.63%		3.50%	
Total	100.00%		100.00%		100.00%		100.00%		100.00%		100.00%	

Table A3. Analysis of variance of material removal rate.

ANOVA:	Profile 1		Profile 2		Profile 3		Profile 4		Profile 5		Profile 6	
Source	Contribution	p-Value	Contribution	p-Value	Contribution	p-Value	Contribution	p-Value	Contribution	p-Value	Contribution	p-Value
Model	96.97%	0.003	97.46%	0.002	97.03%	0.003	97.19%	0.002	97.36%	0.002	97.33%	0.002
Linear	96.97%	0.003	97.46%	0.002	97.03%	0.003	97.19%	0.002	97.36%	0.002	97.33%	0.002
Materials thickness	62.77%	0.002	61.94%	0.002	62.63%	0.002	63.24%	0.002	62.87%	0.002	62.91%	0.002
Transverse speed	34.20%	0.007	35.51%	0.004	34.40%	0.006	33.95%	0.006	34.49%	0.005	34.41%	0.005
Error	3.03%		2.54%		2.97%		2.81%		2.64%		2.67%	
Total	100.00%		100.00%		100.00%		100.00%		100.00%		100.00%	
ANOVA:	Profile 7		Profile 8		Profile 9		Profile 10		Profile 11		Profile 12	
Source	Contribution	p-Value	Contribution	p-Value	Contribution	p-Value	Contribution	p-Value	Contribution	p-Value	Contribution	p-Value
Model	97.02%	0.003	96.92%	0.003	96.92%	0.003	96.41%	0.004	96.23%	0.004	96.03%	0.005
Linear	97.02%	0.003	96.92%	0.003	96.92%	0.003	96.41%	0.004	96.23%	0.004	96.03%	0.005
Materials thickness	62.59%	0.002	62.44%	0.002	69.72%	0.002	65.61%	0.003	68.85%	0.003	68.85%	0.003
Transverse speed	34.43%	0.006	34.47%	0.007	27.20%	0.01	30.80%	0.011	27.38%	0.015	27.18%	0.016
Error	2.98%		3.08%		3.08%		3.59%		3.77%		3.97%	
Total	100.00%		100.00%		100.00%		100.00%		100.00%		100.00%	

## APPENDIX B Data for single-objective optimisation of AWJ contour cutting process parameters

Table B1. Signal to noise ratios for surface roughness (smaller is better).

Exp.	Input Parameters				Signal to Noise Ratios (S/NR = dB)											
No.	$t$ (mm)	$V_f$ (mm/min)	$m_a$ (g/min)	$P$ (MPa)	Profiles											
					1	2	3	4	5	6	7	8	9	10	11	12
1	4	90	300	200	-2.265	-2.437	-2.173	-2.312	-3.093	-2.900	-2.648	-1.924	-2.178	-1.938	-1.924	-1.836
2	4	90	400	250	-1.980	-2.152	-1.887	-2.026	-2.808	-2.614	-2.362	-1.638	-1.892	-1.652	-1.638	-1.551
3	4	90	500	300	-1.584	-1.613	-1.348	-1.487	-2.411	-2.218	-1.966	-1.242	-1.496	-1.256	-1.242	-1.154
4	4	120	300	250	-2.910	-3.082	-2.818	-2.956	-3.738	-3.545	-3.292	-2.568	-2.823	-2.583	-2.568	-2.481
5	4	120	400	300	-2.574	-2.746	-2.482	-2.62	-3.402	-3.209	-2.957	-2.233	-2.487	-2.247	-2.233	-2.145
6	4	120	500	200	-2.916	-3.335	-3.070	-3.209	-3.744	-3.551	-3.299	-2.574	-2.829	-2.589	-2.574	-2.487
7	4	150	300	300	-3.215	-3.387	-3.123	-3.261	-4.043	-3.850	-3.598	-2.873	-3.128	-2.888	-2.873	-2.786
8	4	150	400	200	-3.082	-3.254	-2.990	-3.128	-3.910	-3.717	-3.465	-2.740	-2.995	-2.755	-2.740	-2.653
9	4	150	500	250	-2.929	-2.978	-2.714	-2.852	-3.757	-3.563	-3.311	-2.587	-2.841	-2.601	-2.587	-2.500
10	8	90	300	200	-5.511	-5.683	-5.418	-5.557	-6.339	-6.145	-5.893	-5.169	-5.424	-5.183	-5.169	-5.082
11	8	90	400	250	-5.225	-5.397	-5.133	-5.271	-6.053	-5.860	-5.607	-4.883	-5.138	-4.898	-4.883	-4.796
12	8	90	500	300	-4.829	-3.951	-3.687	-3.825	-5.657	-5.464	-5.211	-4.487	-4.742	-4.502	-4.487	-4.400
13	8	120	300	250	-6.155	-6.327	-6.063	-6.201	-6.983	-6.790	-6.538	-5.814	-6.068	-5.828	-5.814	-5.726
14	8	120	400	300	-5.820	-5.543	-5.278	-5.417	-6.648	-6.454	-6.202	-5.478	-5.732	-5.492	-5.478	-5.391
15	8	120	500	200	-6.162	-6.334	-6.069	-6.208	-6.99	-6.796	-6.544	-5.820	-6.074	-5.834	-5.820	-5.732
16	8	150	300	300	-6.461	-6.633	-6.368	-6.507	-7.289	-7.095	-6.843	-6.119	-6.373	-6.133	-6.119	-6.031
17	8	150	400	200	-6.328	-6.500	-6.235	-6.374	-7.156	-6.962	-6.710	-5.986	-6.240	-6.000	-5.986	-5.898
18	8	150	500	250	-6.174	-6.012	-5.747	-5.886	-7.002	-6.809	-6.556	-5.832	-6.087	-5.847	-5.832	-5.745
19	12	90	300	200	-7.102	-7.274	-7.009	-7.148	-7.930	-7.736	-7.484	-6.760	-7.014	-6.774	-6.760	-6.672
20	12	90	400	250	-6.816	-6.988	-6.723	-6.862	-7.644	-7.451	-7.198	-6.474	-6.729	-6.489	-6.474	-6.387
21	12	90	500	300	-6.420	-6.592	-6.327	-6.466	-7.248	-7.054	-6.802	-6.078	-6.333	-6.092	-6.078	-5.991
22	12	120	300	250	-7.746	-7.633	-7.369	-7.507	-8.574	-8.381	-8.129	-7.404	-7.659	-7.419	-7.404	-7.317
23	12	120	400	300	-7.411	-7.265	-7.000	-7.139	-8.238	-8.045	-7.793	-7.069	-7.323	-7.083	-7.069	-6.981
24	12	120	500	200	-7.753	-7.925	-7.660	-7.799	-8.58	-8.387	-8.135	-7.411	-7.665	-7.425	-7.411	-7.323
25	12	150	300	300	-8.052	-8.491	-8.227	-8.365	-8.879	-8.686	-8.434	-7.710	-7.964	-7.724	-7.710	-7.622
26	12	150	400	200	-7.919	-8.091	-7.826	-7.965	-8.746	-8.553	-8.301	-7.577	-7.831	-7.591	-7.577	-7.489
27	12	150	500	250	-7.765	-7.579	-7.314	-7.453	-8.593	-8.400	-8.147	-7.423	-7.678	-7.438	-7.423	-7.336

Table B2. Signal to noise ratios for material removal rate (larger is better).

Exp.	Input Parameters				Signal to Noise Ratios (S/NR = dB)											
	No.	$t$ (mm)	$V_f$ (mm/min)	$m_a$ (g/min)	$P$ (MPa)	Profiles										
					1	2	3	4	5	6	7	8	9	10	11	12
1	4	90	300	200	47.00	46.60	46.50	46.90	46.50	47.10	47.00	47.50	46.90	46.40	46.70	46.50
2	4	90	400	250	47.10	47.10	46.50	47.40	47.00	47.90	47.80	48.20	47.70	46.40	47.50	47.30
3	4	90	500	300	47.10	48.20	46.60	46.80	48.00	48.10	47.80	48.20	47.60	46.50	47.40	47.20
4	4	120	300	250	50.90	50.50	50.30	50.80	50.40	51.00	50.90	51.30	50.80	50.30	50.60	50.40
5	4	120	400	300	51.10	50.90	50.50	50.80	50.70	50.80	50.50	50.90	50.40	50.40	50.10	49.90
6	4	120	500	200	51.00	51.50	50.40	51.80	51.50	52.00	52.00	52.40	51.80	50.30	51.60	51.40
7	4	150	300	300	52.30	51.90	51.80	52.20	51.80	52.40	52.10	52.50	52.00	51.70	51.70	51.50
8	4	150	400	200	52.10	51.80	51.50	52.10	51.70	52.10	52.00	52.50	51.90	51.50	51.70	51.50
9	4	150	500	250	52.30	51.80	51.70	52.00	51.70	52.10	52.00	52.40	51.90	51.60	51.60	51.50
10	8	90	300	200	51.70	51.30	51.10	51.50	51.20	51.80	51.70	52.10	51.60	51.00	51.30	51.10
11	8	90	400	250	51.70	51.50	51.10	51.90	51.40	52.00	51.90	52.40	51.80	51.00	51.60	51.40
12	8	90	500	300	51.60	52.10	51.10	51.30	51.90	52.00	51.70	52.10	51.60	51.00	51.30	51.10
13	8	120	300	250	53.20	52.80	52.70	53.20	52.70	53.30	53.20	53.60	53.10	52.60	52.80	52.70
14	8	120	400	300	53.40	53.20	52.80	53.10	53.00	53.10	52.70	53.10	52.60	52.70	52.40	52.20
15	8	120	500	200	53.50	52.80	52.90	53.10	52.70	53.30	53.20	53.70	53.10	52.80	52.90	52.70
16	8	150	300	300	56.30	55.90	55.80	56.00	55.70	55.80	55.50	55.90	55.40	55.70	55.10	55.00
17	8	150	400	200	56.70	56.40	56.10	56.70	56.30	56.90	56.80	57.20	56.70	56.00	56.50	56.30
18	8	150	500	250	56.70	56.90	56.20	57.20	56.80	57.40	57.30	57.70	57.20	56.10	56.90	56.70
19	12	90	300	200	52.60	52.20	52.00	52.50	52.10	52.70	52.60	53.00	52.50	51.90	52.30	52.10
20	12	90	400	250	52.60	52.40	52.10	52.80	52.40	53.00	52.90	53.30	52.80	52.00	52.50	52.30
21	12	90	500	300	52.70	53.10	52.10	52.40	52.90	53.00	52.70	53.10	52.50	52.10	52.30	52.10
22	12	120	300	250	56.50	56.10	55.90	56.40	56.00	56.60	56.50	56.90	56.40	55.80	56.10	56.00
23	12	120	400	300	56.70	56.40	56.10	56.30	56.20	56.30	55.90	56.40	55.80	56.00	55.60	55.40
24	12	120	500	200	56.50	56.00	56.00	56.30	55.90	56.50	56.40	56.80	56.30	55.90	56.10	55.90
25	12	150	300	300	57.90	57.50	57.30	57.70	57.30	57.90	57.60	58.20	57.60	57.20	57.20	57.00
26	12	150	400	200	57.70	57.40	57.10	57.60	57.30	57.40	57.30	57.70	57.20	57.00	56.90	56.80
27	12	150	500	250	57.90	57.20	57.30	57.60	57.10	57.80	57.60	58.20	57.60	57.20	57.40	57.20

Table B3. Average response table for signal to noise ratios for surface roughness (smaller is better).

Profile 1		Profile 2			Profile 3			Profile 4								
Level	$t$	$V_f$	$m_a$	$P$	$t$	$V_f$	$m_a$	$P$	$t$	$V_f$	$m_a$	$P$	$t$	$V_f$	$m_a$	$P$
1	-2.606	-4.637	-5.491	-5.449	-2.776	-4.676	-5.661	-5.648	-2.512	-4.412	-5.396	-5.383	-2.650	-4.550	-5.535	-5.522
2	-5.852	-5.494	-5.239	-5.300	-5.820	-5.577	-5.326	-5.350	-5.555	-5.312	-5.062	-5.085	-5.694	-5.451	-5.200	-5.224
3	-7.442	-5.769	-5.170	-5.152	-7.537	-5.881	-5.146	-5.136	-7.273	-5.616	-4.882	-4.871	-7.411	-5.755	-5.020	-5.010
Delta	4.836	1.133	0.321	0.297	4.761	1.204	0.515	0.512	4.761	1.204	0.515	0.512	4.761	1.204	0.515	0.512
Rank	1	2	3	4	1	2	3	4	1	2	3	4	1	2	3	4
Profile 5				Profile 6			Profile 7			Profile 8						
Level	$t$	$V_f$	$m_a$	$P$	$t$	$V_f$	$m_a$	$P$	$t$	$V_f$	$m_a$	$P$	$t$	$V_f$	$m_a$	$P$
1	-3.434	-5.465	-6.319	-6.276	-3.241	-5.271	-6.125	-6.083	-2.989	-5.019	-5.873	-5.831	-2.264	-4.295	-5.149	-5.107
2	-6.679	-6.322	-6.067	-6.128	-6.486	-6.129	-5.874	-5.935	-6.234	-5.876	-5.622	-5.682	-5.510	-5.152	-4.897	-4.958
3	-8.270	-6.597	-5.998	-5.979	-8.077	-6.404	-5.805	-5.786	-7.825	-6.152	-5.552	-5.534	-7.101	-5.427	-4.828	-4.810
Delta	4.836	1.133	0.321	0.297	4.836	1.133	0.321	0.297	4.836	1.133	0.321	0.297	4.836	1.133	0.321	0.297
Rank	1	2	3	4	1	2	3	4	1	2	3	4	1	2	3	4
Profile 9				Profile 10			Profile 11			Profile 12						
Level	$t$	$V_f$	$m_a$	$P$	$t$	$V_f$	$m_a$	$P$	$t$	$V_f$	$m_a$	$P$	$t$	$V_f$	$m_a$	$P$
1	-2.519	-4.550	-5.404	-5.361	-2.264	-4.295	-5.149	-5.107	-2.177	-4.208	-5.062	-5.019	-2.279	-4.309	-5.164	-5.121
2	-5.764	-5.407	-5.152	-5.213	-5.510	-5.152	-4.897	-4.958	-5.422	-5.065	-4.810	-4.871	-5.524	-5.167	-4.912	-4.973
3	-7.355	-5.682	-5.083	-5.064	-7.101	-5.427	-4.828	-4.810	-7.013	-5.340	-4.741	-4.722	-7.115	-5.442	-4.843	-4.824
Delta	4.836	1.133	0.321	0.297	4.836	1.133	0.321	0.297	4.836	1.133	0.321	0.297	4.836	1.133	0.321	0.297
Rank	1	2	3	4	1	2	3	4	1	2	3	4	1	2	3	4

Table B4. Average response table for signal to noise ratios for material removal rate (larger is better).

Profile 1		Profile 2			Profile 3			Profile 4								
Level	$t$	$V_f$	$m_a$	$P$	$t$	$V_f$	$m_a$	$P$	$t$	$V_f$	$m_a$	$P$	$t$	$V_f$	$m_a$	$P$
1	50.10	50.46	53.16	52.44	50.05	50.50	52.76	52.28	49.53	49.90	52.59	51.87	50.09	50.38	52.99	52.42
2	53.87	53.64	53.22	53.04	53.66	53.36	53.02	52.66	53.30	53.07	52.66	52.47	53.77	53.53	53.18	52.95
3	55.68	55.55	53.26	54.17	55.37	55.21	53.30	54.14	55.11	54.98	52.69	53.61	55.50	55.44	53.18	53.98
Delta	5.58	5.08	0.10	1.74	5.32	4.71	0.54	1.86	5.58	5.08	0.10	1.74	5.41	5.06	0.20	1.55
Rank	1	2	4	3	1	2	4	3	1	2	4	3	1	2	4	3
Profile 5				Profile 6			Profile 7			Profile 8						
Level	$t$	$V_f$	$m_a$	$P$	$t$	$V_f$	$m_a$	$P$	$t$	$V_f$	$m_a$	$P$	$t$	$V_f$	$m_a$	$P$
1	49.92	50.37	52.63	52.18	50.41	50.85	53.18	52.64	50.23	50.68	53.01	52.52	50.65	51.09	53.45	52.94
2	53.53	53.23	52.89	52.56	53.96	53.67	53.28	53.12	53.79	53.49	53.11	53.00	54.20	53.91	53.53	53.42
3	55.24	55.08	53.17	53.95	55.69	55.54	53.59	54.30	55.51	55.37	53.42	54.01	55.96	55.81	53.83	54.44
Delta	5.32	4.71	0.54	1.77	5.28	4.69	0.41	1.67	5.28	4.69	0.41	1.49	5.30	4.72	0.38	1.50
Rank	1	2	4	3	1	2	4	3	1	2	4	3	1	2	4	3
Profile 9				Profile 10			Profile 11			Profile 12						
Level	$t$	$V_f$	$m_a$	$P$	$t$	$V_f$	$m_a$	$P$	$t$	$V_f$	$m_a$	$P$	$t$	$V_f$	$m_a$	$P$
1	50.11	50.56	52.91	52.41	49.45	49.81	52.51	51.78	49.88	50.32	52.65	52.17	49.70	50.14	52.47	51.98
2	53.67	53.37	52.99	52.89	53.22	52.98	52.57	52.38	53.43	53.13	52.75	52.65	53.25	52.95	52.57	52.46
3	55.42	55.27	53.30	53.91	55.02	54.89	52.61	53.52	55.16	55.01	53.06	53.65	54.97	54.83	52.88	53.47
Delta	5.30	4.72	0.38	1.50	5.58	5.08	0.10	1.74	5.28	4.69	0.41	1.49	5.28	4.69	0.41	1.49
Rank	1	2	4	3	1	2	4	3	1	2	4	3	1	2	4	3



## APPENDIX C Data for multi-objective optimisation of AWJ contour cutting process parameters

Table C1. ANOVA of  $R_a$  for  $t = 4$  mm

Source	$R_a$ 1		$R_a$ 2		$R_a$ 3	
	Contribution %	p-Value	Contribution %	p-Value	Contribution %	p-Value
$X_1$	59.90	0.001	69.43	0.000	69.39	0.000
$X_2$	5.16	0.067	3.49	0.068	3.77	0.017
$X_3$	30.19	0.002	23.86	0.002	24.09	0.001
Error	4.74		3.23		2.74	
Total	100.00		100		100	

Table C2. ANOVA of  $R_a$  for  $t = 8$  mm

Source	$R_a$ 1		$R_a$ 2		$R_a$ 3	
	Contribution %	p-Value	Contribution %	p-Value	Contribution %	p-Value
$X_1$	72.21	0.000	71.07	0.000	64.06	0.000
$X_2$	7.96	0.007	11.57	0.003	3.94	0.013
$X_3$	17.84	0.001	15.52	0.001	30.64	0.001
Error	1.99		1.84		1.36	
Total	100.00		100.00		100.00	

Table C3. ANOVA of  $R_a$  for  $t = 12$  mm

Source	$R_a$ 1		$R_a$ 2		$R_a$ 3	
	Contribution %	p-Value	Contribution %	p-Value	Contribution %	p-Value
$X_1$	57.23	0.000	58.85	0.000	57.21	0.001
$X_2$	3.44	0.026	5.31	0.002	17.66	0.011
$X_3$	34.59	0.000	33.1	0.000	19.47	0.009
Error	4.74		2.74		3.23	3.23
Total	100.00		100.00		100.00	

Table C4. ANOVA of MRR for  $t = 4$  mm

Source	MRR 1		MRR 2		MRR 3	
	Contribution %	p-Value	Contribution %	p-Value	Contribution %	p-Value
$X_1$	71.14	0.000	70.98	0	75.503	0
$X_2$	4.35	0.023	2.65	0.067	3.345	0.048
$X_3$	22.42	0.002	23.93	0.001	18.688	0.002
Error	2.08		2.44		2.464	
Total	100.00		100.00		100.00	

Table C5. ANOVA of MRR for  $t = 8$  mm

Source	MRR 1		MRR 2		MRR 3	
	Contribution %	p-Value	Contribution %	p-Value	Contribution %	p-Value
$X_1$	76.69	0.000	76.12	0.000	70.51	0.000
$X_2$	7.13	0.002	3.62	0.038	0.12	0.751
$X_3$	15.05	0.000	17.98	0.002	24.09	0.005
Error	1.14		2.29		5.27	
Total	100.00		100.00		100.00	

Table C6. ANOVA of MRR for t = 12 mm

Source	MRR 1		MRR 2		MRR 3	
	Contribution %	p-Value	Contribution %	p-Value	Contribution %	p-Value
$X_1$	77.55	0.000	78.94	0.000	73.29	0.000
$X_2$	9.03	0.002	4.13	0.04	4.15	0.028
$X_3$	12.11	0.001	13.3	0.001	20.35	0.001
Error	1.31		3.63		2.21	
Total	100.00		100.00		100.00	

Table C7. ANOVA of KTA for t = 4 mm

Source	KTA 1		KTA 2		KTA 3	
	Contribution %	p-Value	Contribution %	p-Value	Contribution %	p-Value
$X_1$	64.21	0.000	58.7	0.000	56.74	0.000
$X_2$	6.75	0.014	6.77	0.017	5.27	0.075
$X_3$	26.6	0.001	31.78	0.001	32.74	0.001
Error	2.45		2.74		5.26	
Total	100.00		100.00		100.00	

Table C8. ANOVA of KTA for t = 8 mm

Source	KTA 1		KTA 2		KTA 3	
	Contribution %	p-Value	Contribution %	p-Value	Contribution %	p-Value
$X_1$	59.49	0.001	67.49	0.000	60.95	0.000
$X_2$	11.84	0.015	5.63	0.013	4.42	0.047
$X_3$	26.69	0.002	21.65	0.001	31.42	0.001
Error	1.98		5.24		3.21	
Total	100.00		100.00		100.00	

Table C9. ANOVA of KTA for t = 12 mm

Source	KTA 1		KTA 2		KTA 3	
	Contribution %	p-Value	Contribution %	p-Value	Contribution %	p-Value
$X_1$	53.33	0.000	70.59	0.000	55.67	0.000
$X_2$	12.65	0.055	0.22	0.245	5.24	0.033
$X_3$	31.40	0.001	25.50	0.000	36.04	0.001
Error	0.63		3.70		3.05	
Total	100.00		100.00		100.00	

## BIBLIOGRAPHY

1. Rajurkar, K.; Hadidi, H.; Pariti, J.; Reddy, G. Review of sustainability issues in non-traditional machining processes. *Procedia Manufacturing* 2017, 7, 714-720.
2. Liu, X.; Liang, Z.; Wen, G.; Yuan, X. Waterjet machining and research developments: a review. *The International Journal of Advanced Manufacturing Technology* 2019, 102, 1257-1335.
3. Rajurkar, K.P.; Hadidi, H.; Pariti, J.; Reddy, G.C. Review of Sustainability Issues in Non-traditional Machining Processes. *International Conference on Sustainable Materials Processing and Manufacturing (Smpm 2017)* 2016, 7, 714-720, doi:10.1016/j.promfg.2016.12.106.
4. Ahn, Y.; Lee, S.H. Classification and prediction of burr formation in micro drilling of ductile metals. *Int J Prod Res* 2017, 55, 4833-4846.
5. Kowsari, K.; Nouraei, H.; James, D.; Spelt, J.; Papini, M. Abrasive slurry jet micro-machining of holes in brittle and ductile materials. *Journal of Materials Processing Technology* 2014, 214, 1909-1920.
6. Yuvaraj, N.; Kumar, M.P. Surface integrity studies on abrasive water jet cutting of AISI D2 steel. *Materials and Manufacturing Processes* 2017, 32, 162-170.
7. Kaladhar, M.; Subbaiah, K.V.; Rao, C.S. Machining of austenitic stainless steels—a review. *International Journal of Machining and Machinability of Materials* 2012, 12, 178-192.
8. Mardi, K.B.; Dixit, A.; Mallick, A. Studies on non-traditional machining of metal matrix composites. *Materials Today: Proceedings* 2017, 4, 8226-8239.
9. Alsoufi, M.S. State-of-the-Art in Abrasive Water Jet Cutting Technology and the Promise for Micro-and Nano-Machining. *International Journal of Mechanical Engineering and Applications* 2017, 5, 1.
10. Gupta, K. Introduction to Abrasive Water Jet Machining. In *Abrasive Water Jet Machining of Engineering Materials*, Springer: 2020; pp. 1-11.
11. Natarajan, Y.; Murugesan, P.K.; Mohan, M.; Khan, S.A.L.A. Abrasive Water Jet Machining process: A state of art of review. *Journal of Manufacturing Processes* 2020, 49, 271-322.
12. Liu, H. “7M” Advantage of Abrasive Waterjet for Machining Advanced Materials. *Journal of Manufacturing and Materials Processing* 2017, 1.
13. Saravanan, S.; Vijayan, V.; Suthahar, S.T.J.; Balan, A.V.; Sankar, S.; Ravichandran, M. A review on recent progresses in machining methods based on abrasive water jet machining. *Mater Today-Proc* 2020, 21, 116-122, doi:10.1016/j.matpr.2019.05.373.
14. Liu, H.; Schubert, E. Micro abrasive-waterjet technology. *Micromachining techniques for fabrication of micro and nano structures* 2012, 205-233.
15. Singh, P.; Pramanik, A.; Basak, A.; Prakash, C.; Mishra, V. Developments of non-conventional drilling methods—a review. *The International Journal of Advanced Manufacturing Technology* 2020, 106, 2133-2166.
16. Sureban, R.; Kulkarni, V.N.; Gaitonde, V. Modern Optimization Techniques for Advanced Machining Processes—A Review. *Materials Today: Proceedings* 2019, 18, 3034-3042.
17. Nguyen, T.; Wang, J. A review on the erosion mechanisms in abrasive waterjet micromachining of brittle materials. *International Journal of Extreme Manufacturing* 2019, 1, 012006.
18. Mieszala, M.; Torrubia, P.L.; Axinte, D.A.; Schwiedrzik, J.J.; Guo, Y.; Mischler, S.; Michler, J.; Philippe, L. Erosion mechanisms during abrasive waterjet machining: Model microstructures and single particle experiments. *Journal of Materials Processing Technology* 2017, 247, 92-102, doi:10.1016/j.jmatprotec.2017.04.003.

19. Hlaváčová, I.M.; Sadílek, M.; Váňová, P.; Szumilo, Š.; Tyč, M. Influence of steel structure on machinability by abrasive water jet. *Materials* 2020, *13*, 4424.
20. Ruiz-Garcia, R.; Ares, P.F.M.; Vazquez-Martinez, J.M.; Gomez, J.S. Influence of Abrasive Waterjet Parameters on the Cutting and Drilling of CFRP/UNS A97075 and UNS A97075/CFRP Stacks. *Materials* 2019, *12*, doi:ARTN 10710.3390/ma12010107.
21. Supriya, S.; Srinivas, S. Machinability studies on stainless steel by abrasive water jet-Review. *Materials Today: Proceedings* 2018, *5*, 2871-2876.
22. Rajurkar, K.P.; Sundaram, M.M.; Malshe, A.P. Review of Electrochemical and Electrodischarge Machining. *Proceedings of the Seventeenth Cirp Conference on Electro Physical and Chemical Machining (Isem)* 2013, *6*, 13-26, doi:10.1016/j.procir.2013.03.002.
23. Akkurt, A. Surface properties of the cut face obtained by different cutting methods from AISI 304 stainless steel materials. 2009.
24. Krajcarz, D. Comparison Metal Water Jet Cutting with Laser and Plasma Cutting. *24th Daaam International Symposium on Intelligent Manufacturing and Automation, 2013* 2014, *69*, 838-843, doi:10.1016/j.proeng.2014.03.061.
25. Chaturvedi, C.; Rao, P.S. Some Technical Issues and Critical Assessment of Abrasive Water Jet Machining (AWJM) Process.
26. Rakshit, R.; Das, A.K. A review on cutting of industrial ceramic materials. *Precis Eng* 2019, *59*, 90-109, doi:10.1016/j.precisioneng.2019.05.009.
27. Kovacevic, R.; Mohan, R.; Beardsley, H. Monitoring of thermal energy distribution in abrasive waterjet cutting using infrared thermography. 1996.
28. Babu, M.K.; Chetty, O.K. A study on recycling of abrasives in abrasive water jet machining. *Wear* 2003, *254*, 763-773.
29. Schramm, A.; Morczinek, F.; Götze, U.; Putz, M. Technical-economic evaluation of abrasive recycling in the suspension fine jet process chain. *The International Journal of Advanced Manufacturing Technology* 2020, *106*, 981-992.
30. Maneiah, D.; Shunmugasundaram, M.; Reddy, A.R.; Begum, Z. Optimization of machining parameters for surface roughness during abrasive water jet machining of aluminium/magnesium hybrid metal matrix composites. *Materials Today: Proceedings* 2020.
31. Tripathi, D.R.; Vachhani, K.H.; Kumari, S.; Abhishek, K. Experimental investigation on material removal rate during abrasive water jet machining of GFRP composites. *Materials Today: Proceedings* 2020.
32. Mogul, Y.I.; Nasir, I.; Myler, P. Investigation and optimization for depth of cut and surface roughness for control depth milling in Titanium Ti6AL4V with abrasive water jet cutting. *Materials Today: Proceedings* 2020.
33. Naik, M.B.; Srikanth, D.; Rao, M.S. Abrasive Jet Machining on Soda lime Glass- An experimental investigation. *Abrasive Jet Machining on Soda lime Glass-An experimental investigation* 2020, *44*, 11-11.
34. Jeykrishnan, J.; Ramnath, B.V.; Vignesh, S.S.; Sridharan, P.; Saravanan, B. Optimization of process parameters in abrasive water jet machining/cutting (AWJM) of nickel alloy using traditional analysis to minimize kerf taper angle. *Materials Today: Proceedings* 2019, *16*, 392-397.
35. Marichamy, S.; Ravichandran, M.; Stalin, B.; Babu, S.B. Optimization of abrasive water jet machining parameters for  $\alpha$ - $\beta$  brass using Taguchi methodology. *FME Transactions* 2019, *47*, 116-121.
36. Kumar, P.; Tank, B.; Kant, R. EXPERIMENTAL INVESTIGATION ON ABRASIVE WATERJET MACHINING OF FIBRE VINYL ESTER COMPOSITE. *Journal of Manufacturing Engineering* 2019, *14*, 134-138.

37. Srikanth, D.V.; Rao, M.S. Application of Taguchi & Response surface methodology in Optimization for machining of ceramics with abrasive jet machining. *Mater Today-Proc* 2015, *2*, 3308-3317, doi:10.1016/j.matpr.2015.07.149.
38. Niranjan, C.; Srinivas, S.; Ramachandra, M. An experimental study on depth of cut of AZ91 Magnesium Alloy in abrasive water jet cutting. *Materials Today: Proceedings* 2018, *5*, 2884-2890.
39. Rajamanickam, S.; Manjunathan, R.; Mariyappan, K.; Aravindh, S. COMPARATIVE ANALYSIS OF MRR ON ABRASIVE WATER JET MACHINING PARAMETERS OVER AEROSPACE ALLOYS: INCONEL 825 & Ti-6Al-4V. *International Journal of Pure and Applied Mathematics* 2018, *118*, 727-733.
40. Yuvaraj, N.; Kumar, M.P. Optimisation of abrasive water jet cutting process parameters for AA5083-H32 aluminium alloy using fuzzy TOPSIS method. *International Journal of Machining and Machinability of Materials* 2018, *20*, 118-140.
41. Kmec, J.; Gombár, M.; Harničárová, M.; Valíček, J.; Kušnerová, M.; Kříž, J.; Kadnár, M.; Karková, M.; Vagaská, A. The Predictive Model of Surface Texture Generated by Abrasive Water Jet for Austenitic Steels. *Applied Sciences* 2020, *10*, 3159.
42. Samson, R.M.; Rajak, S.; Kannan, T.D.B.; Sampreet, K. Optimization of Process Parameters in Abrasive Water Jet Machining of Inconel 718 Using VIKOR Method. *Journal of The Institution of Engineers (India): Series C* 2020, 1-7.
43. Senthilkumar, T.; Muralikannan, R.; Kumar, S.S. Surface morphology and parametric optimization of AWJM parameters using GRA on aluminum HMMC. *Materials Today: Proceedings* 2020, *22*, 410-415.
44. Madara, S.R.; Pillai, S.R. Modelling of surface roughness in abrasive waterjet cutting of Kevlar 49 composite using artificial neural network. *Materials Today: Proceedings* 2020.
45. Jagadish; Bhowmik, S.; Ray, A. Prediction of surface roughness quality of green abrasive water jet machining: a soft computing approach. *Journal of Intelligent Manufacturing* 2019, *30*, 2965-2979, doi:10.1007/s10845-015-1169-7.
46. BRUCELY, Y.; AULTRIN, K.; JAISON, M.D. USING GENETIC ALGORITHM OPTIMIZING THE CUTTING PARAMETERS OF AWJM PROCESS FOR ALUMINIUM 6061 ALLOY.
47. Kumar, A.; Singh, H.; Kumar, V. Study the parametric effect of abrasive water jet machining on surface roughness of Inconel 718 using RSM-BBD techniques. *Mater Manuf Process* 2018, *33*, 1483-1490.
48. Manoj, M.; Jinu, G.R.; Muthuramalingam, T. Multi Response Optimization of AWJM Process Parameters on Machining TiB2 Particles Reinforced Al7075 Composite Using Taguchi-DEAR Methodology. *Silicon* 2018, *10*, 2287-2293, doi:10.1007/s12633-018-9763-x.
49. Pawar, P.J.; Vidhate, U.S.; Khalkar, M.Y. Improving the quality characteristics of abrasive water jet machining of marble material using multi-objective artificial bee colony algorithm. *J Comput Des Eng* 2018, *5*, 319-328, doi:10.1016/j.jcde.2017.12.002.
50. Rao, R.V.; Rai, D.P.; Balic, J. Multi-objective optimization of abrasive waterjet machining process using Jaya algorithm and PROMETHEE Method. *Journal of Intelligent Manufacturing* 2019, *30*, 2101-2127, doi:10.1007/s10845-017-1373-8.
51. Nair, A.; Kumanan, S. Optimization of size and form characteristics using multi-objective grey analysis in abrasive water jet drilling of Inconel 617. *J Braz Soc Mech Sci* 2018, *40*, 121.

52. Chakraborty, S.; Mitra, A. Parametric optimization of abrasive water-jet machining processes using grey wolf optimizer. *Mater Manuf Process* 2018, *33*, 1471-1482, doi:10.1080/10426914.2018.1453158.
53. Johari, N.F.; Zain, A.M.; Mustaffa, N.H.; Udin, A. Machining parameters optimization using hybrid firefly algorithm and particle swarm optimization. In *Proceedings of Journal of Physics: Conference Series*; p. 012005.
54. Liu, S.; Zhou, F.; Li, H.; Chen, Y.; Wang, F.; Guo, C. Experimental Investigation of Hard Rock Breaking Using a Conical Pick Assisted by Abrasive Water Jet. *Rock Mechanics and Rock Engineering* 2020, 1-10.
55. Madara, S.R.; Selvan, C.P.; Sampath, S.; Pillai, S.R. Impact of process parameters on surface roughness of hastelloy using abrasive waterjet machining technology. *Int. J. Recent Technol. Eng.* 2019, *7*, 419-425.
56. Balamurugan, K.; Uthayakumar, M.; Sankar, S.; Hareesh, U.; Warriar, K. Effect of abrasive waterjet machining on LaPO<sub>4</sub>/Y<sub>2</sub>O<sub>3</sub> ceramic matrix composite. *Journal of the Australian Ceramic Society* 2018, *54*, 205-214.
57. Krajcarz, D.; Bankowski, D.; Mlynarczyk, P. The effect of traverse speed on kerf width in AWJ cutting of ceramic tiles. *12th International Scientific Conference of Young Scientists on Sustainable, Modern and Safe Transport* 2017, *192*, 469-473, doi:10.1016/j.proeng.2017.06.081.
58. e Lima, C.E.d.A.; Lebrón, R.; de Souza, A.J.; Ferreira, N.F.; Neis, P.D. Study of influence of traverse speed and abrasive mass flowrate in abrasive water jet machining of gemstones. *The International Journal of Advanced Manufacturing Technology* 2016, *83*, 77-87.
59. Kumar, R.S.; Gajendran, S.; Kesavan, R. Evaluation of Optimum Machining Parameters by AWJM for Granite through Multi Response Methods. *Materials Today: Proceedings* 2020, *22*, 3056-3066.
60. Kalusuraman, G.; Kumaran, S.T.; Siva, I.; Kumar, S.A. Cutting performance of luffa cylindrica fiber-reinforced composite by abrasive water jet. *Journal of Testing and Evaluation* 2020, *48*.
61. Kumar, R.S.; Gajendran, S.; Kesavan, R. Estimation of Optimal Process Parameters for Abrasive Water Jet Machining Of Marble Using Multi Response Techniques. *Mater Today-Proc* 2018, *5*, 11208-11218, doi:10.1016/j.matpr.2018.01.145.
62. Yu, Y.; Sun, T.X.; Yuan, Y.M.; Gao, H.; Wang, X.P. Experimental investigation into the effect of abrasive process parameters on the cutting performance for abrasive waterjet technology: a case study. *Int J Adv Manuf Tech* 2020, *107*, 2757-2765, doi:10.1007/s00170-020-05183-3.
63. Shibin, R.; Anandakrishnan, V.; Sathish, S.; Sujana, V.M. Investigation on the abrasive water jet machinability of AA2014 using SiC as abrasive. *Mater Today-Proc* 2020, *21*, 519-522, doi:10.1016/j.matpr.2019.06.659.
64. Yogeswaran, R.; Pitchipoo, P. Characterization and machining analysis of AA3003 honeycomb sandwich. *Materials Today: Proceedings* 2020.
65. Shukla, R.; Singh, D. Experimentation investigation of abrasive water jet machining parameters using Taguchi and Evolutionary optimization techniques. *Swarm and Evolutionary Computation* 2017, *32*, 167-183, doi:10.1016/j.swevo.2016.07.002.
66. Wang, S.; Zhang, S.; Wu, Y.; Yang, F. Exploring kerf cut by abrasive waterjet. *The International Journal of Advanced Manufacturing Technology* 2017, *93*, 2013-2020.
67. Mohamad, W.; Kasim, M.; Norazlina, M.; Hafiz, M.; Izamshah, R.; Mohamed, S. Effect of standoff distance on the kerf characteristic during abrasive water jet machining. *Results in Engineering* 2020, *6*, 100101.



68. El-Hofy, M.; Helmy, M.; Escobar-Palafox, G.; Kerrigan, K.; Scaife, R.; El-Hofy, H. Abrasive water jet machining of multidirectional CFRP laminates. *Procedia Cirp* 2018, *68*, 535-540.
69. Perec, A. Experimental research into alternative abrasive material for the abrasive water-jet cutting of titanium. *The International Journal of Advanced Manufacturing Technology* 2018, *97*, 1529-1540.
70. Li, M.; Huang, M.; Chen, Y.; Kai, W.; Yang, X. Experimental study on hole characteristics and surface integrity following abrasive waterjet drilling of Ti6Al4V/CFRP hybrid stacks. *Int J Adv Manuf Tech* 2019, *104*, 4779-4789, doi:10.1007/s00170-019-04334-5.
71. Tiwari, T.; Sourabh, S.; Nag, A.; Dixit, A.R.; Mandal, A.; Das, A.K.; Mandal, N.; Srivastava, A.K. Parametric investigation on abrasive waterjet machining of alumina ceramic using response surface methodology. In Proceedings of IOP Conf. Series: Materials Science and Engineering.
72. Hashish, M. A modeling study of metal cutting with abrasive waterjets. 1984.
73. Liu, H.-T.P. Advanced waterjet technology for machining curved and layered structures. *Curved and Layered Structures* 2019, *6*, 41-56.
74. Saraçyakupoğlu, T. Abrasive Water Jet (AWJ) Applications in the Aviation Industry. 2019.
75. Aurich, J.C.; Kirsch, B.; Setti, D.; Axinte, D.; Beaucamp, A.; Butler-Smith, P.; Yamaguchi, H. Abrasive processes for micro parts and structures. *CIRP Annals* 2019, *68*, 653-676.
76. Selvan, M.C.P.; Midhunchakkaravarthy, D.; Senanayake, R.; Pillai, S.R.; Madara, S.R. A mathematical modelling of Abrasive Waterjet Machining on Ti-6Al-4V using Artificial Neural Network. *Materials Today: Proceedings* 2020.
77. Pahuja, R.; Ramulu, M. Machinability of randomly chopped discontinuous fiber composites: a comparative assessment of conventional and abrasive waterjet. In Proceedings of The 23rd int conf on water jetting. Seattle, USA; pp. 127-148.
78. Chen, M.; Zhang, S.; Zeng, J.; Chen, B.; Xue, J.; Ji, L. Correcting shape error on external corners caused by the cut-in/cut-out process in abrasive water jet cutting. *The International Journal of Advanced Manufacturing Technology* 2019, *103*, 849-859.
79. Miao, X.; Qiang, Z.; Wu, M.; Song, L.; Ye, F. Research on quality improvement of the cross section cut by abrasive water jet based on secondary cutting. *The International Journal of Advanced Manufacturing Technology* 2018, *97*, 71-80.
80. Miao, X.; Ye, F.; Wu, M.; Song, L.; Qiang, Z. The method of 3D nozzle tilt cutting of abrasive water jet. *The International Journal of Advanced Manufacturing Technology* 2019, *103*, 3109-3114.
81. Gnanavelbabu, A.; Saravanan, P.; Rajkumar, K.; Karthikeyan, S. Experimental investigations on multiple responses in abrasive waterjet machining of Ti-6Al-4V alloy. *Materials Today: Proceedings* 2018, *5*, 13413-13421.
82. Uthayakumar, M.; Khan, M.A.; Kumaran, S.T.; Slota, A.; Zajac, J. Machinability of nickel-based superalloy by abrasive water jet machining. *Mater Manuf Process* 2016, *31*, 1733-1739.
83. Khan, M.A.; Gupta, K. Machinability Studies on Abrasive Water Jet Machining of Low Alloy Steel for Different Thickness. In Proceedings of IOP Conference Series: Materials Science and Engineering; p. 044099.
84. Liu, X.C.; Liang, Z.W.; Wen, G.L.; Yuan, X.F. Waterjet machining and research developments: a review (vol 102, pg 1257, 2019). *Int J Adv Manuf Tech* 2019, *102*, 1337-1338, doi:10.1007/s00170-019-03556-x.

85. Kechagias, J.; Petropoulos, G.; Vaxevanidis, N. Application of Taguchi design for quality characterization of abrasive water jet machining of TRIP sheet steels. *The International Journal of Advanced Manufacturing Technology* 2012, *62*, 635-643.
86. Naresh Babu, M.; Muthukrishnan, N. Investigation on surface roughness in abrasive water-jet machining by the response surface method. *Materials and Manufacturing Processes* 2014, *29*, 1422-1428.
87. Akkurt, A.; Kulekci, M.K.; Seker, U.; Ercan, F. Effect of feed rate on surface roughness in abrasive waterjet cutting applications. *Journal of Materials Processing Technology* 2004, *147*, 389-396.
88. Liu, H.; Schubert, E.; McNeil, D.; Soo, K. Applications of abrasive-fluidjets for precision machining of composites. In Proceedings of International SAMPE Symposium and Exhibition (Proceedings); pp. 17-20.
89. Pashmforoush, F.; Hassanpour Babajan, A.; Beyraghi Baranlou, R. Experimental Study of Geometric Tolerances and Surface Roughness in Abrasive Water Jet Machining Process of Hardox 400 Steel. *Modares Mechanical Engineering* 2020, *20*, 0-0.
90. Perec, A.; Pude, F.; Grigoryev, A.; Kaufeld, M.; Wegener, K. A study of wear on focusing tubes exposed to corundum-based abrasives in the waterjet cutting process. *Int J Adv Manuf Tech* 2019, *104*, 2415-2427, doi:10.1007/s00170-019-03971-0.
91. Liu, H.-T. Waterjet technology for machining fine features pertaining to micromachining. *J Manuf Process* 2010, *12*, 8-18.
92. Dong, Y.Z.; Liu, W.W.; Zhang, H.; Zhang, H.C. On-line recycling of abrasives in abrasive water jet cleaning. *21st Cirp Conference on Life Cycle Engineering* 2014, *15*, 278-282, doi:10.1016/j.procir.2014.06.045.
93. Hlavacova, I.; Geryk, V. Abrasives for water-jet cutting of high-strength and thick hard materials. *The International Journal of Advanced Manufacturing Technology* 2017, *90*, 1217-1224.
94. Perec, A.; Pude, F.; Stirnimann, J.; Wegener, K. Feasibility Study on the Use of Fractal Analysis for Evaluating the Surface Quality Generated by Waterjet. *Teh Vjesn* 2015, *22*, 879-883, doi:Doi 10.17559/Tv-20140128231244.
95. Melentiev, R.; Fang, F. Recent advances and challenges of abrasive jet machining. *CIRP Journal of Manufacturing Science and technology* 2018, *22*, 1-20.
96. Hashish, M. Optimization Factors in Abrasive-Waterjet Machining. *J Eng Ind-T Asme* 1991, *113*, 29-37, doi:Doi 10.1115/1.2899619.
97. Thamizhvalavan, P.; Arivazhagan, S.; Yuvaraj, N.; Ramesh, B. Machinability study of abrasive aqua jet parameters on hybrid metal matrix composite. *Mater Manuf Process* 2019, *34*, 321-344.
98. Babu, M.N.; Muthukrishnan, N. Exploration on Kerf-angle and surface roughness in abrasive waterjet machining using response surface method. *Journal of The Institution of Engineers (India): Series C* 2018, *99*, 645-656.
99. Hashish, M. A Model for Abrasive-Waterjet (Awj) Machining. *J Eng Mater-T Asme* 1989, *111*, 154-162, doi:Doi 10.1115/1.3226448.
100. Radovanovic, M. Multi-Objective Optimization of Abrasive Water Jet Cutting Using MOGA. *Procedia Manufacturing* 2020, *47*, 781-787.
101. Nandakumar, N.; Sasikumar, K.; Sambathkumar, M.; Saravanan, N. Investigations on AWJ cutting process of hybrid aluminium 7075 metal matrix composites using nozzle oscillation technique. *Materials Today: Proceedings* 2020.
102. Sasikumar, K.; Arulshri, K.; Ponappa, K.; Uthayakumar, M. A study on kerf characteristics of hybrid aluminium 7075 metal matrix composites machined using abrasive water jet machining technology. *Proceedings of the Institution of*

- Mechanical Engineers, Part B: Journal of Engineering Manufacture* 2018, *232*, 690-704.
103. Ishfaq, K.; Ahmad Mufti, N.; Ahmed, N.; Pervaiz, S. Abrasive waterjet cutting of clad material: kerf taper and MRR analysis. *Mater Manuf Process* 2019, *34*, 544-553.
  104. Karmiris-Obratański, P.; Karkalos, N.E.; Kudelski, R.; Papazoglou, E.L.; Markopoulos, A.P. On the Effect of Multiple Passes on Kerf Characteristics and Efficiency of Abrasive Waterjet Cutting. *Metals* 2021, *11*, 74.
  105. Yuvaraj, N.; Kumar, M.P. Cutting of aluminium alloy with abrasive water jet and cryogenic assisted abrasive water jet: A comparative study of the surface integrity approach. *Wear* 2016, *362*, 18-32.
  106. Srinivas, S.; Babu, N.R. Penetration Ability of Abrasive Waterjets in Cutting of Aluminum-Silicon Carbide Particulate Metal Matrix Composites. *Mach Sci Technol* 2012, *16*, 337-354, doi:10.1080/10910344.2012.698935.
  107. Gostimirovic, M.; Pucovsky, V.; Sekulic, M.; Rodic, D.; Pejic, V. Evolutionary optimization of jet lag in the abrasive water jet machining. *The International Journal of Advanced Manufacturing Technology* 2019, *101*, 3131-3141.
  108. Hanif, M.I.; Aamir, M.; Ahmed, N.; Maqsood, S.; Muhammad, R.; Akhtar, R.; Hussain, I. Optimization of facing process by indigenously developed force dynamometer. *The International Journal of Advanced Manufacturing Technology* 2019, *100*, 1893-1905.
  109. Kumar, P.; Kant, R. Development of a predictive model for kerf taper angle in AWJM of Kevlar epoxy composite. *Materials Today: Proceedings* 2020, *28*, 1164-1169.
  110. Nair, A.; Kumanan, S. Multi-performance optimization of abrasive water jet machining of Inconel 617 using WPCA. *Mater Manuf Process* 2017, *32*, 693-699, doi:10.1080/10426914.2016.1244844.
  111. Otto, K.N.; Antonsson, E.K. Extensions to the Taguchi method of product design. 1993.
  112. Aamir, M.; Tu, S.S.; Tolouei-Rad, M.; Giasin, K.; Vafadar, A. Optimization and Modeling of Process Parameters in Multi-Hole Simultaneous Drilling Using Taguchi Method and Fuzzy Logic Approach. *Materials* 2020, *13*, doi:ARTN 680 10.3390/ma13030680.
  113. Rao, R.V.; Rai, D.P.; Balic, J. Optimization of Abrasive Waterjet Machining Process using Multi-objective Jaya Algorithm. *Mater Today-Proc* 2018, *5*, 4930-4938, doi:10.1016/j.matpr.2017.12.070.
  114. Opricovic, S.; Tzeng, G.H. Extended VIKOR method in comparison with outranking methods. *Eur J Oper Res* 2007, *178*, 514-529, doi:10.1016/j.ejor.2006.01.020.
  115. Rao, R. Jaya: A simple and new optimization algorithm for solving constrained and unconstrained optimization problems. *Int J Ind Eng Comp* 2016, *7*, 19-34.
  116. Fan, Z.; Liu, E.; Xu, B. Weighted principal component analysis. In Proceedings of International Conference on Artificial Intelligence and Computational Intelligence; pp. 569-574.
  117. Supriya, S.B.; Srinivas, S. Machinability Studies on Stainless steel by abrasive water jet - Review. *Mater Today-Proc* 2018, *5*, 2871-2876.
  118. Aydin, G.; Kaya, S.; Karakurt, I. Effect of abrasive type on marble cutting performance of abrasive waterjet. *Arabian Journal of Geosciences* 2019, *12*, 1-8.
  119. Saravanan, S.; Vijayan, V.; Suthahar, S.J.; Balan, A.; Sankar, S.; Ravichandran, M. A review on recent progresses in machining methods based on abrasive water jet machining. *Materials Today: Proceedings* 2020, *21*, 116-122.

120. Kavya, J.; Keshavamurthy, R.; Kumar, G.P. Studies on parametric optimization for abrasive water jet machining of Al7075-TiB2 in-situ composite. In Proceedings of IOP Conference Series: Materials Science and Engineering; p. 012024.
121. Thakkar, P.; Prajapati, P.; Thakkar, S.A. A machinability study of mild steel using abrasive water jet machining technology. *Int. J. Eng. Res. Appl* 2013, *3*, 1063-1066.
122. Sanghani, C.; Korat, M. Performance analysis of abrasive water jet machining process for AISI 304 stainless steel. *Journal of Experimental & Applied Mechanics* 2018, *8*, 53-55.
123. Kumar, K.R.; Sreebalaji, V.S.; Pridhar, T. Characterization and optimization of Abrasive Water Jet Machining parameters of aluminium/tungsten carbide composites. *Measurement* 2018, *117*, 57-66, doi:10.1016/j.measurement.2017.11.059.
124. Kumbhar, M.A.D.; Chatterjee, M.; Student, M. OPTIMIZATION OF ABRASIVE WATER JET MACHINING PROCESS PARAMETERS USING RESPONSE SURFACE METHOD ON INCONEL-188.
125. Llanto, J.M.; Tolouei-Rad, M.; Vafadar, A.; Aamir, M. Recent Progress Trend on Abrasive Waterjet Cutting of Metallic Materials: A Review. *Applied Sciences* 2021, *11*, 3344.
126. Wang, J.; Liu, H. Profile cutting on alumina ceramics by abrasive waterjet. Part 1: experimental investigation. *P I Mech Eng C-J Mec* 2006, *220*, 703-714, doi:10.1243/09544062jmes207a.
127. Hlavac, L.M.; Hlavacova, I.M.; Geryk, V.; Plancar, S. Investigation of the taper of kerfs cut in steels by AWJ. *Int J Adv Manuf Tech* 2015, *77*, 1811-1818, doi:10.1007/s00170-014-6578-9.
128. El-Domiaty, A.; Shabara, M.; Abdel-Rahman, A.; Al-Sabeeh, A. On the modelling of abrasive waterjet cutting. *The International Journal of Advanced Manufacturing Technology* 1996, *12*, 255-265.
129. Radovanović, M. Multi-objective Optimization of Process Performances when Cutting Carbon Steel with Abrasive Water Jet. *Tribology in Industry* 2016, *38*.
130. Wang, S.; Zhang, S.; Wu, Y.; Yang, F. A key parameter to characterize the kerf profile error generated by abrasive water-jet. *The International Journal of Advanced Manufacturing Technology* 2017, *90*, 1265-1275.
131. Hlavac, L.M.; Hlavacova, I.M.; Arleo, F.; Vigano, F.; Annoni, M.P.G.; Geryk, V. Shape distortion reduction method for abrasive water jet (AWJ) cutting. *Precis Eng* 2018, *53*, 194-202, doi:10.1016/j.precisioneng.2018.04.003.
132. Kumar, R.; Chattopadhyaya, S.; Dixit, A.R.; Bora, B.; Zelenak, M.; Foldyna, J.; Hloch, S.; Hlavacek, P.; Scucka, J.; Klich, J. Surface integrity analysis of abrasive water jet-cut surfaces of friction stir welded joints. *The International Journal of Advanced Manufacturing Technology* 2017, *88*, 1687-1701.
133. Gnanavelbabu, A.; Saravanan, P.; Rajkumar, K.; Karthikeyan, S. Experimental Investigations on Multiple Responses in Abrasive Waterjet Machining of Ti-6Al-4V Alloy. *Mater Today-Proc* 2018, *5*, 13413-13421, doi:DOI 10.1016/j.matpr.2018.02.335.
134. Li, M.; Huang, M.; Chen, Y.; Gong, P.; Yang, X. Effects of processing parameters on kerf characteristics and surface integrity following abrasive waterjet slotting of Ti6Al4V/CFRP stacks. *J Manuf Process* 2019, *42*, 82-95.
135. Aamir, M.; Tolouei-Rad, M.; Giasin, K.; Vafadar, A. Machinability of Al2024, Al6061, and Al5083 alloys using multi-hole simultaneous drilling approach. *Journal of Materials Research and Technology* 2020, *9*, 10991-11002.
136. Aamir, M.; Tolouei-Rad, M.; Giasin, K.; Vafadar, A. Feasibility of tool configuration and the effect of tool material, and tool geometry in multi-hole simultaneous

- drilling of Al2024. *The International Journal of Advanced Manufacturing Technology* 2020, *111*, 861-879.
137. Aamir, M.; Tu, S.; Giasin, K.; Tolouei-Rad, M. Multi-hole simultaneous drilling of aluminium alloy: A preliminary study and evaluation against one-shot drilling process. *Journal of Materials Research and Technology* 2020, *9*, 3994-4006.
  138. Aamir, M.; Tu, S.; Tolouei-Rad, M.; Giasin, K.; Vafadar, A. Optimization and modeling of process parameters in multi-hole simultaneous drilling using taguchi method and fuzzy logic approach. *Materials* 2020, *13*, 680.
  139. Pahuja, R.; Ramulu, M. Abrasive water jet machining of Titanium (Ti6Al4V)-CFRP stacks - A semi-analytical modeling approach in the prediction of kerf geometry. *J Manuf Process* 2019, *39*, 327-337, doi:10.1016/j.jmapro.2019.01.041.
  140. Miao, X.; Wu, M.; Qiang, Z.; Wang, Q.; Miao, X. Study on optimization of a simulation method for abrasive water jet machining. *The International Journal of Advanced Manufacturing Technology* 2017, *93*, 587-593.
  141. Veerappan, G.; Ravichandran, M. Experimental investigations on abrasive water jet machining of nickel-based superalloy. *Journal of the Brazilian Society of Mechanical Sciences and Engineering* 2019, *41*, 1-12.
  142. Begic-Hajdarevic, D.; Cekic, A.; Mehmedovic, M.; Djelmic, A. Experimental study on surface roughness in abrasive water jet cutting. *Procedia Engineering* 2015, *100*, 394-399.
  143. Bhandarkar, V.; Singh, V.; Gupta, T. Experimental analysis and characterization of abrasive water jet machining of Inconel 718. *Materials Today: Proceedings* 2020, *23*, 647-650.
  144. Lehocka, D.; Botko, F.; Klich, J.; Sitek, L.; Hvizdos, P.; Fides, M.; Cep, R. Effect of pulsating water jet disintegration on hardness and elasticity modulus of austenitic stainless steel AISI 304L. *The International Journal of Advanced Manufacturing Technology* 2020, 1-12.
  145. Desu, R.K.; Krishnamurthy, H.N.; Balu, A.; Gupta, A.K.; Singh, S.K. Mechanical properties of Austenitic Stainless Steel 304L and 316L at elevated temperatures. *Journal of Materials Research and Technology* 2016, *5*, 13-20.
  146. Barabas, S.A.; Florescu, A. Optimization Method of Abrasive Water Jet Cutting of Welded Overlay Materials. *Metals* 2019, *9*, 1046.
  147. Kuntoğlu, M.; Acar, O.; Gupta, M.K.; Sağlam, H.; Sarikaya, M.; Giasin, K.; Pimenov, D.Y. Parametric Optimization for Cutting Forces and Material Removal Rate in the Turning of AISI 5140. *Machines* 2021, *9*, 90.
  148. Kuntoğlu, M.; Aslan, A.; Pimenov, D.Y.; Giasin, K.; Mikolajczyk, T.; Sharma, S. Modeling of cutting parameters and tool geometry for multi-criteria optimization of surface roughness and vibration via response surface methodology in turning of AISI 5140 steel. *Materials* 2020, *13*, 4242.
  149. Aamir, M.; Giasin, K.; Tolouei-Rad, M.; Vafadar, A. A review: Drilling performance and hole quality of aluminium alloys for aerospace applications. *Journal of Materials Research and Technology* 2020, *9*, 12484-12500.
  150. Sutowska, M.; Kapłonek, W.; Pimenov, D.Y.; Gupta, M.K.; Mia, M.; Sharma, S. Influence of variable radius of cutting head trajectory on quality of cutting kerf in the abrasive water jet process for soda–lime glass. *Materials* 2020, *13*, 4277.
  151. Singh, D.; Chaturvedi, V. Investigation of optimal processing condition for abrasive water jet machining for stainless steel AISI 304 using grey relational analysis coupled with S/N ratio. In Proceedings of Applied Mechanics and Materials; pp. 438-443.
  152. Löschner, P.; Jarosz, K.; Niesłony, P. Investigation of the effect of cutting speed on surface quality in abrasive water jet cutting of 316L stainless steel. *Procedia Engineering* 2016, *149*, 276-282.

153. Karthik, K.; Sundarsingh, D.S.; Harivignesh, M.; Karthick, R.G.; Praveen, M. Optimization of machining parameters in abrasive water jet cutting of stainless steel 304. *Materials Today: Proceedings* 2021.
154. Hlaváč, L.M.; Hlaváčová, I.M.; Geryk, V.; Plančár, Š. Investigation of the taper of kerfs cut in steels by AWJ. *The International Journal of Advanced Manufacturing Technology* 2015, *77*, 1811-1818.
155. Lin, C. Use of the Taguchi method and grey relational analysis to optimize turning operations with multiple performance characteristics. *Materials and manufacturing processes* 2004, *19*, 209-220.
156. Sharma, M.K.; Chaudhary, H.; Kumar, A. Optimization of abrasive waterjet machining process parameters on aluminium AL-6061. *International Journal of Science and Research* 2017, *6*, 869-874.
157. Jiang, W.; Cao, Y.; Jiang, Y.; Liu, Y.; Mao, Q.; Zhou, H.; Liao, X.; Zhao, Y. Effects of nanostructural hierarchy on the hardness and thermal stability of an austenitic stainless steel. *Journal of Materials Research and Technology* 2021, *12*, 376-384.
158. Ramana, M.V.; Kumar, B.R.; Krishna, M.; Rao, M.V.; Kumar, V. Optimization and influence of process parameters of dissimilar SS304L–SS430 joints produced by Robotic TIG welding. *Materials Today: Proceedings* 2020, *23*, 479-482.
159. Wang, S.; Zhang, S.; Wu, Y.; Yang, F. A key parameter to characterize the kerf profile error generated by abrasive water-jet. *The International Journal of Advanced Manufacturing Technology* 2017, *90*, 1265-1275.
160. Barad, M. Taguchi Experimental-Design Techniques - Revisited. *Transformation of Science and Technology into Productive Power, Supplement* 1991, 1101-1104.
161. Patel Gowdru Chandrashekarappa, M.; Kumar, S.; Pimenov, D.Y.; Giasin, K. Experimental Analysis and Optimization of EDM Parameters on HcHcr Steel in Context with Different Electrodes and Dielectric Fluids Using Hybrid Taguchi-Based PCA-Utility and CRITIC-Utility Approaches. *Metals* 2021, *11*, 419.
162. Aamir, M.; Giasin, K.; Tolouei-Rad, M.; Ud Din, I.; Hanif, M.I.; Kuklu, U.; Pimenov, D.Y.; Ikhlaiq, M. Effect of Cutting Parameters and Tool Geometry on the Performance Analysis of One-Shot Drilling Process of AA2024-T3. *Metals* 2021, *11*, 854.
163. Yu, Y.; Sun, T.; Yuan, Y.; Gao, H.; Wang, X. Experimental investigation into the effect of abrasive process parameters on the cutting performance for abrasive waterjet technology: a case study. *International Journal of Advanced Manufacturing Technology* 2020, *107*.
164. Selvan, M.C.P.; Raju, N.M.S.; Sachidananda, H. Effects of process parameters on surface roughness in abrasive waterjet cutting of aluminium. *Frontiers of Mechanical Engineering* 2012, *7*, 439-444.
165. Trivedi, P.; Dhanawade, A.; Kumar, S. An experimental investigation on cutting performance of abrasive water jet machining of austenite steel (AISI 316L). *Advances in Materials and Processing Technologies* 2015, *1*, 263-274.
166. Singh, D.; Shukla, R.S. Investigation of kerf Characteristics in Abrasive Water Jet Machining of Inconel 600 using Response Surface Methodology. *Defence Science Journal* 2020, *70*.
167. Madankar, A.; Dumbhare, P.; Deshpande, Y.V.; Andhare, A.B.; Barve, P.S. Estimation and control of surface quality and traverse speed in abrasive water jet machining of AISI 1030 steel using different work-piece thicknesses by RSM. *Australian Journal of Mechanical Engineering* 2021, 1-8.
168. Pérez, L.; Carmelo, J. On the Application of a Design of Experiments along with an ANFIS and a Desirability Function to Model Response Variables. *Symmetry* 2021, *13*, 897.



169. Luis Pérez, C. A Proposal of an Adaptive Neuro-Fuzzy Inference System for Modeling Experimental Data in Manufacturing Engineering. *Mathematics* 2020, *8*, 1390.
170. Maneiah, D.; Shunmugasundaram, M.; Reddy, A.R.; Begum, Z. Optimization of machining parameters for surface roughness during abrasive water jet machining of aluminium/magnesium hybrid metal matrix composites. *Materials Today: Proceedings* 2020, *27*, 1293-1298.
171. Rajamanickam, S.; Manjunathan, R.; Mariyappan, K.; Aravindh, S. Comparative analysis of MRR on abrasive water jet machining parameters over aerospace alloys: Inconel 825 & Ti-6Al-4V. *Int. J. Pure Appl. Math* 2018, *118*, 727-733.
172. Hlaváč, L.M.; Hlaváčová, I.M.; Arleo, F.; Viganò, F.; Annoni, M.P.G.; Geryk, V. Shape distortion reduction method for abrasive water jet (AWJ) cutting. *Precision Engineering* 2018, *53*, 194-202.
173. Msomi, V.; Mabuwa, S. Analysis of material positioning towards microstructure of the friction stir processed AA1050/AA6082 dissimilar joint. *Advances in Industrial and Manufacturing Engineering* 2020, *1*, 100002.
174. Nagaraj, Y.; Jagannatha, N.; Sathisha, N.; Niranjana, S. Prediction of material removal rate and surface roughness in hot air assisted hybrid machining on soda-lime-silica glass using regression analysis and artificial neural network. *Silicon* 2020, 1-13.
175. Aydin, G.; Karakurt, I.; Hamzacebi, C. Artificial neural network and regression models for performance prediction of abrasive waterjet in rock cutting. *The International Journal of Advanced Manufacturing Technology* 2014, *75*, 1321-1330.
176. Cetin, M.H.; Ozcelik, B.; Kuram, E.; Demirbas, E. Evaluation of vegetable based cutting fluids with extreme pressure and cutting parameters in turning of AISI 304L by Taguchi method. *Journal of Cleaner Production* 2011, *19*, 2049-2056.
177. Llanto, J.M.; Vafadar, A.; Aamir, M.; Tolouei-Rad, M. Analysis and Optimization of Process Parameters in Abrasive Waterjet Contour Cutting of AISI 304L. *Metals* 2021, *11*, 1362.
178. Llanto, J.M.; Tolouei-Rad, M.; Vafadar, A.; Aamir, M. Impacts of Traverse Speed and Material Thickness on Abrasive Waterjet Contour Cutting of Austenitic Stainless Steel AISI 304L. *Applied Sciences* 2021, *11*, 4925.
179. Koli, Y.; Yuvaraj, N.; Aravindan, S. Multi-response mathematical model for optimization of process parameters in CMT welding of dissimilar thickness AA6061-T6 and AA6082-T6 alloys using RSM-GRA coupled with PCA. *Advances in Industrial and Manufacturing Engineering* 2021, *2*, 100050.
180. Kumar, K.R.; Sreebalaji, V.; Pridhar, T. Characterization and optimization of abrasive water jet machining parameters of aluminium/tungsten carbide composites. *Measurement* 2018, *117*, 57-66.
181. Chabbi, A.; Yallese, M.A.; Meddour, I.; Nouioua, M.; Mabrouki, T.; Girardin, F. Predictive modeling and multi-response optimization of technological parameters in turning of Polyoxymethylene polymer (POM C) using RSM and desirability function. *Measurement* 2017, *95*, 99-115.
182. Chate, G.R.; Patel, G.M.; Kulkarni, R.M.; Vernekar, P.; Deshpande, A.S.; Parappagoudar, M.B. Study of the effect of nano-silica particles on resin-bonded moulding sand properties and quality of casting. *Silicon* 2018, *10*, 1921-1936.
183. Javed, S.A.; Mahmoudi, A.; Khan, A.M.; Javed, S.; Liu, S. A critical review: shape optimization of welded plate heat exchangers based on grey correlation theory. *Applied Thermal Engineering* 2018, *144*, 593-599.
184. Ratner, B. The correlation coefficient: Its values range between+ 1/– 1, or do they? *Journal of targeting, measurement and analysis for marketing* 2009, *17*, 139-142.

185. Deshpande, Y.; Andhare, A.; Sahu, N.K. Estimation of surface roughness using cutting parameters, force, sound, and vibration in turning of Inconel 718. *Journal of the Brazilian Society of Mechanical Sciences and Engineering* 2017, *39*, 5087-5096.
186. Galpin, J.S.; Hawkins, D.M. The use of recursive residuals in checking model fit in linear regression. *The American Statistician* 1984, *38*, 94-105.
187. Andrzej, P. Experimental research into alternative abrasive material for the abrasive water-jet cutting of titanium. *The International Journal of Advanced Manufacturing Technology* 2018, *97*, 1529-1540.